Supplementary Information

Design of hyperporous graphene networks and their application in solid-amine based carbon capture systems

Srinivas Gadipelli[a]*, Yue Lu[a], Neal Skipper[b], Taner Yildirim[c] and Zhengxiao Guo[a]*

[a]Department of Chemistry, University College London, 20 Gordon Street, London, WC1H 0AJ, UK

[b]Department of Physics & Astronomy, University College London, Gower Street, London, WC1E 6BT, UK

[c]NIST Centre for Neutron Research, National Institute of Standards and Technology, Gaithersburg, Maryland, 20899, USA

Email. gsrinivasphys@gmail.com; s.gadipelli@ucl.ac.uk & z.x.guo@ucl.ac.uk

Synthesis of GO-A by Hummer's method

1. Graphite powder, 10 g was stirred with cold concentrated H_2SO_4 (230 ml at 0 °C).
2. Then $KMnO_4$ (30 g) was added to the suspension slowly to prevent a rapid rise in the temperature (less than 20 °C). The solution underwent a colour change at this point from black to a very dark green.
3. After removal of the ice-bath the mixture was stirred at room temperature for another 2 h.
4. DI water (230 ml) was slowly added to the reaction vessel to keep the temperature under 98 °C.
5. The diluted suspension was stirred for an additional 15 min and further diluted with DI water (1.4 l) before adding H_2O_2 (100 ml). Upon addition vigorous foaming occurred and the solution turned to brown.
6. The mixture stirred for 2 h at room temperature and left overnight.
7. Product settled at bottom was separated from the excess liquid by decantation followed by centrifugation.
8. The product was washed by centrifugation until the pH reached neutral.
9. Freeze dried to obtain a final product, **called GO-A**.

Synthesis of GO-B by Hummer's method

1. Graphite powder, 2.0 g was stirred with cold (0 °C) concentrated H_2SO_4 (24 ml).

2. To this, $KMnO_4$ (6.0 g) was added, ensuring that the temperature of the solution did not exceed 20°C. The solution underwent a colour change at this point from black to a very dark green.
3. The reaction vessel was removed from the ice bath and stirred at room temperature for 1.5 h, and then it was covered and left overnight.
4. Next day the solution was brought up to 80 °C and DI water (46 ml) was added dropwise to make sure that the temperature of the solution did not exceed 98 °C. At this point the solution turned brown.
5. Solution was stirred for an additional 15 minutes before adding more DI water (280 ml). After which H_2O_2 (20 ml) was added slowly. Upon addition vigorous foaming occurred and the solution turned green-yellow. The solution was then stirred for 30 minutes and then left at a warm phase (30 °C) for an additional 30 minutes.
6. After being left overnight the GO particles which had settled at the bottom were separated from the excess liquid by decantation followed by centrifugation.
7. The solution was further washed by centrifugation in DI water (4 l).
8. After the pH of the washings was neutral, the sample was freeze dried, **called GO-B**.

Synthesis of GO-C by modified Hummer's method

GO-C was synthesized by firstly pre-oxidizing the graphite powder.

1. Concentrated H_2SO_4 (8.0 ml) was heated to 80 °C (oil bath) to which a mixture of $K_2S_2O_8$ (1.7 g) and P_2O_5 (1.7 g) was added and stirred until fully dissolved.
2. Graphite powder (2.0 g) was added to the reactants and then stirred at 80 °C for overnight.
3. The mixture was cooled to room temperature (17 °C) and diluted with DI water (2 l). This solution was then filtered using filter paper under vacuum and washed with further DI water. The pre-oxidized graphite powder (PG) was left to dry in air.

From now we used modified Hummer's method using PG:

4. $NaNO_3$ (1.5 g) was added to cold (0 °C) concentrated H_2SO_4 (72 ml) and stirred until completely dissolved.
5. PG (1.5 g) was added under vigorous stirring. To the solution $KMnO_4$ (9.0 g) was added taking care to keep the reaction temperature under 15 °C. Upon addition of the $KMnO_4$, the solution turned a very dark green. The solution was brought to 35 °C and left stirring for 3 h.
6. H_2O_2 was added slowly, the colour turned from dark green to green-yellow. The solution was left to stir at 35 °C for 1 h.
7. The GO solid was separated & washed in dilute (3.4%) HCl acid (1 l) to remove any remaining salts, followed by further washing in DI water (≈ 2.25 l) until the washings were pH neutral.
8. The sample was then freeze-dried, **called GO-C**.

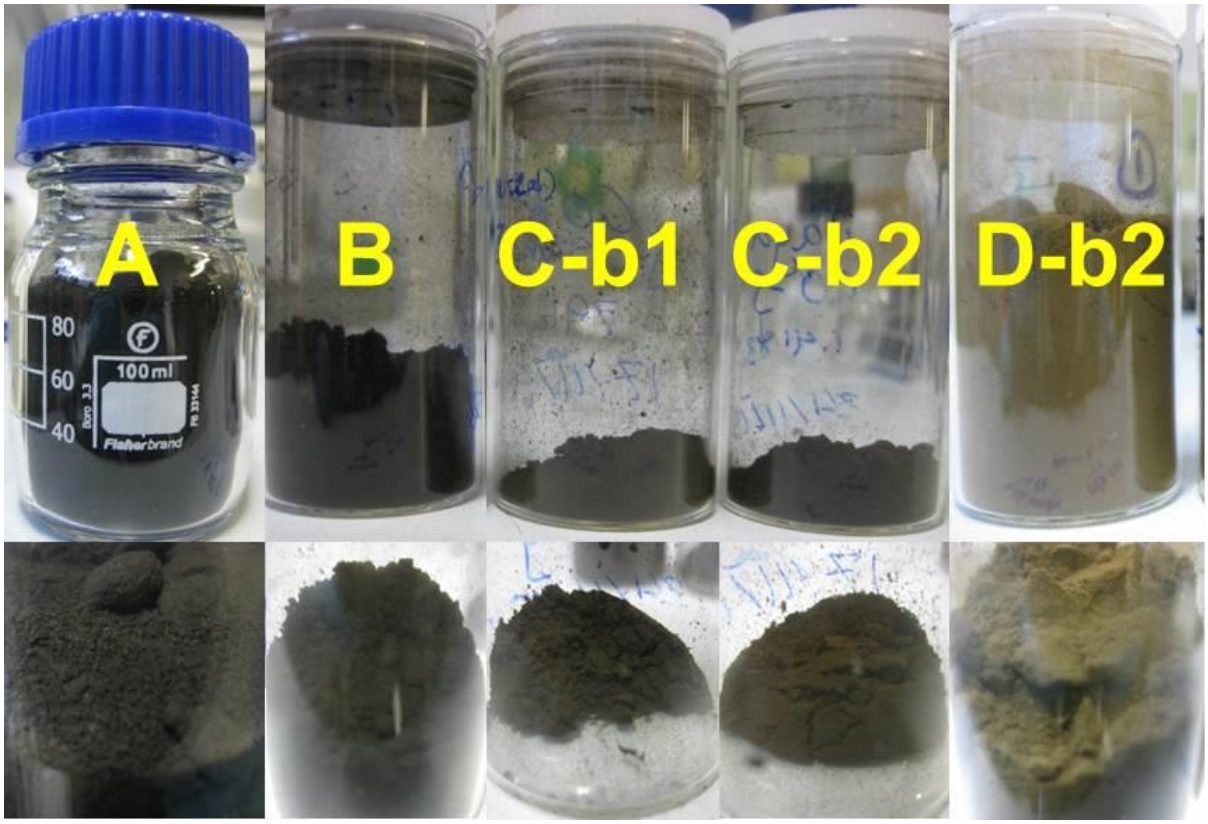

Figure S1. Digital photographs of the as-synthesized GO samples of different degree of oxidation. GO-A was produced from 10 g graphite, whereas all other samples were obtained from 2 g graphite in each batch. Photographs at bottom panel to show clear sample colour.

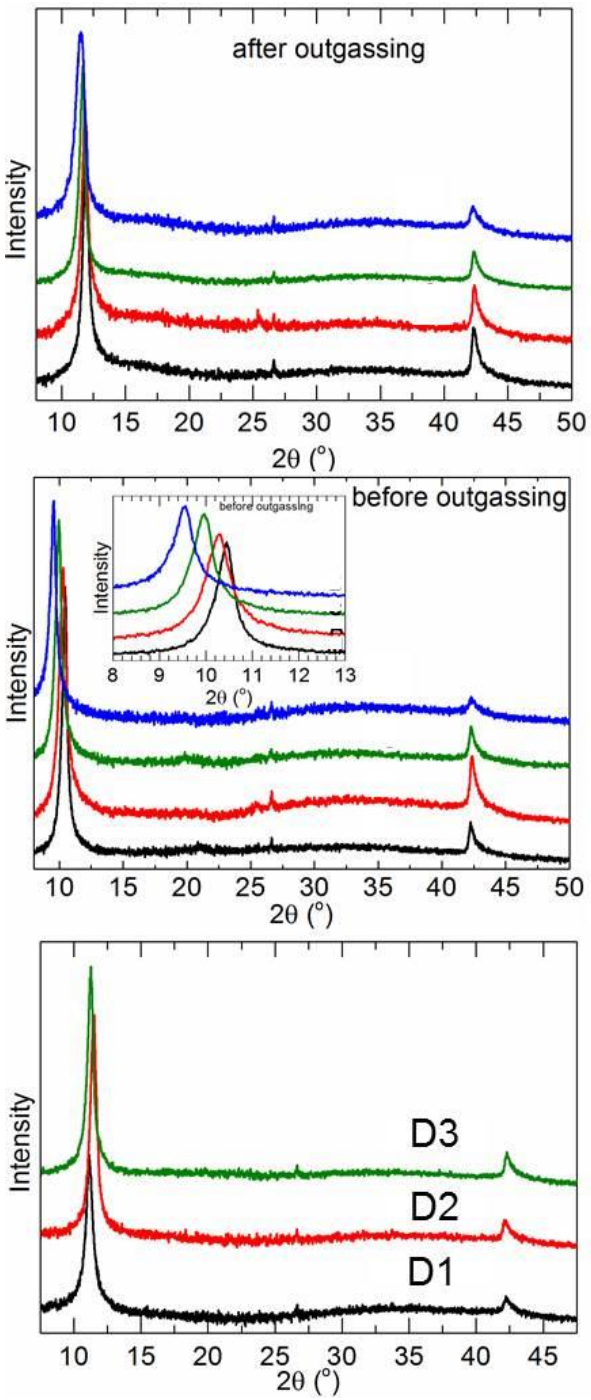

	2θ (°)	d-spacing (nm)
GO-D	11.510	0.768
GO-C	11.660	0.758
GO-B	11.825	0.748
GO-A	11.915	0.742

GO-D	9.560	0.924
GO-C	9.965	0.887
GO-B	10.295	0.859
GO-A	10.445	0.846

Figure S2. PXRD patterns of the GO (top - outgassed GO under rotary vacuum of 1 x 10^{-3} mbar at room temperature for overnight & middle - as synthesized) and GO-D batches (bottom) synthesized at different times. The interlayer distance between GO-sheets is represented by d-spacing, calculated from the 2θ position of (001) peak, positioned around (9-12)°.

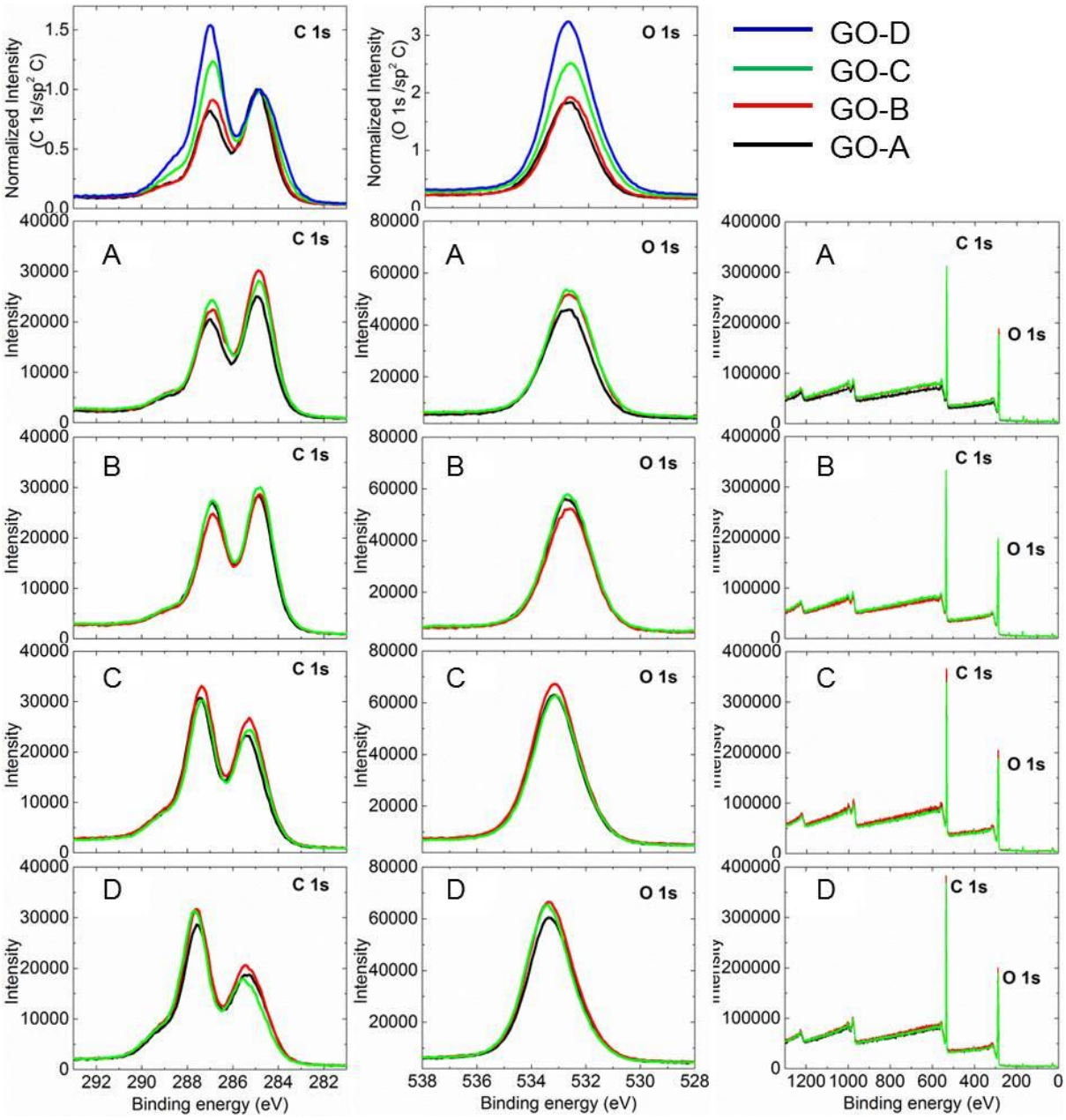

Figure S3. XPS spectra; C 1s (left panel), O 1s (middle panel) and Survey (right panel) of GO samples. Top two panels represent the comparative C 1s and O 1s spectra with the intensity normalized to a sp^2 carbon peak to show the clearer increase of the oxidation when going from sample GO-A to GO-D. Bottom nine panels showing the XPS spectra taken at three different spots for each sample, exhibit good homogeneity of the samples.

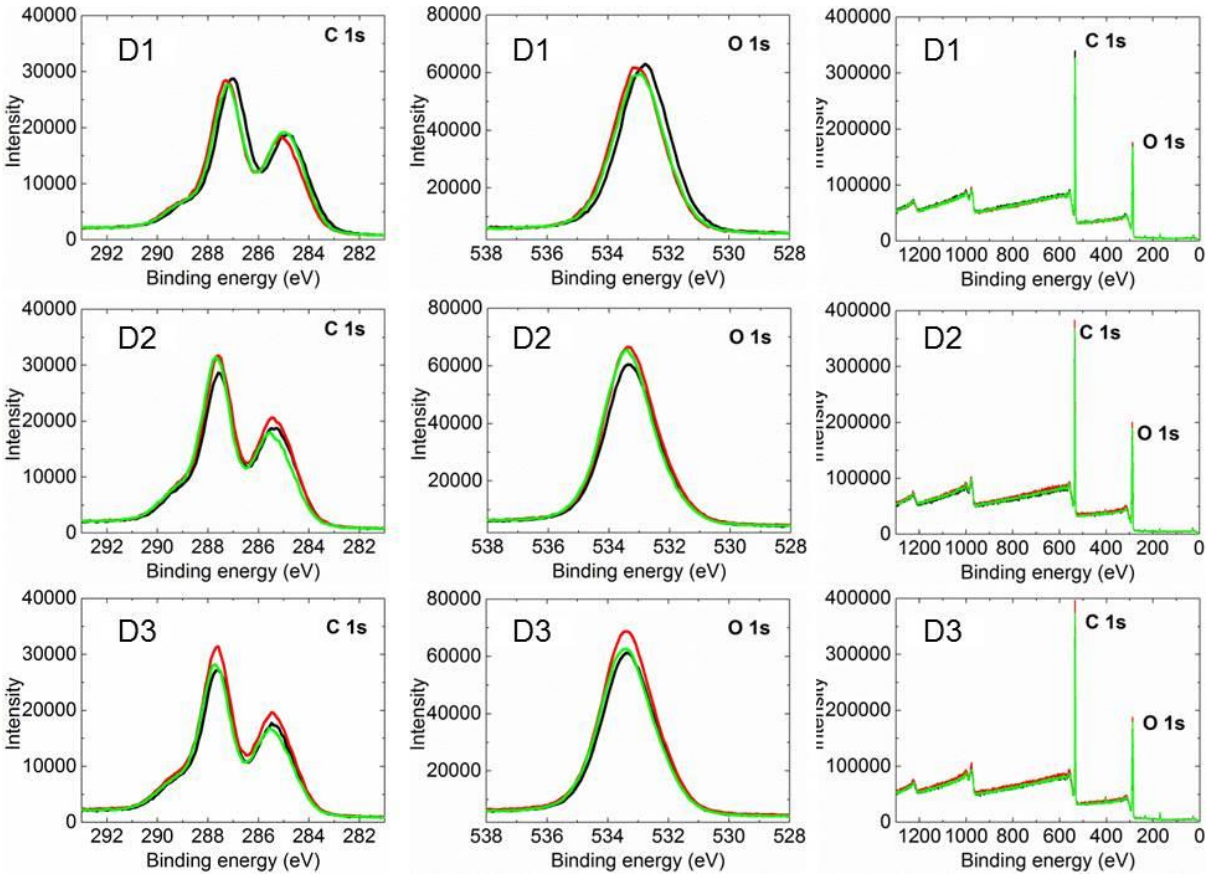

Figure S4. XPS spectra of GO-D batch samples synthesized at different times. The spectra recorded at 3 different spots on each of the sample confirming the good homogeneity of the samples.

Table S1. XPS elemental analysis of GO samples, the spectra was recorded at multiple spots on each sample. The atomic percentage for C and O were estimated from the C 1s and O 1s peaks in the Survey spectra. The percentage of oxidation is estimated by deconvolution of the C 1s peak into three peaks, representing the C=C/C–C, C–O/C–OH and C=O/COO. Clearly, the increased oxidation degree of GO samples from -A to -D is understood from the relative increase of the C–O/C–OH & C=O/COO atomic percentage at the expense of graphitic C=C/C–C, atomic percentage (at%).

S/N	Sample	C (at%)	O (at%)	% of oxidation – deconvoluted C 1s peak		
				C=C/C–C (284.7-285.5) eV	C–O/C–OH (287-287.7) eV	C=O/COO (288.5-289) eV
1	GO-A	71.3	28.7	53.9	39.0	7.1
		71.5	28.5	55.8	36.5	7.7
		71.4	28.6	52.6	39.1	8.4
2	GO-B	71.5	28.5	55.0	38.0	7.0
		71.5	28.5	54.0	38.0	8.0
		72.3	27.7	55.8	35.8	8.4
3	GO-C	71.0	29.0	49.7	40.1	10.2
		71.9	28.1	53.1	37.4	9.6
		71.3	28.7	51.5	40.0	8.5
4	GO-Db1	68.1	31.9	44.0	41.0	15.0
		69.1	30.9	46.0	41.0	13.0
		68.9	31.1	46.0	41.0	13.0
5	GO-Db2	67.5	32.5	42.8	43.2	14.0
		67.7	32.3	42.2	44.8	13.0
		68.2	31.8	44.7	44.0	11.3
6	GO-Db3	66.4	33.2	41.0	42.0	16.5
		67.8	32.2	43.5	40.8	15.9
		68.2	31.8	44.3	40.8	14.9

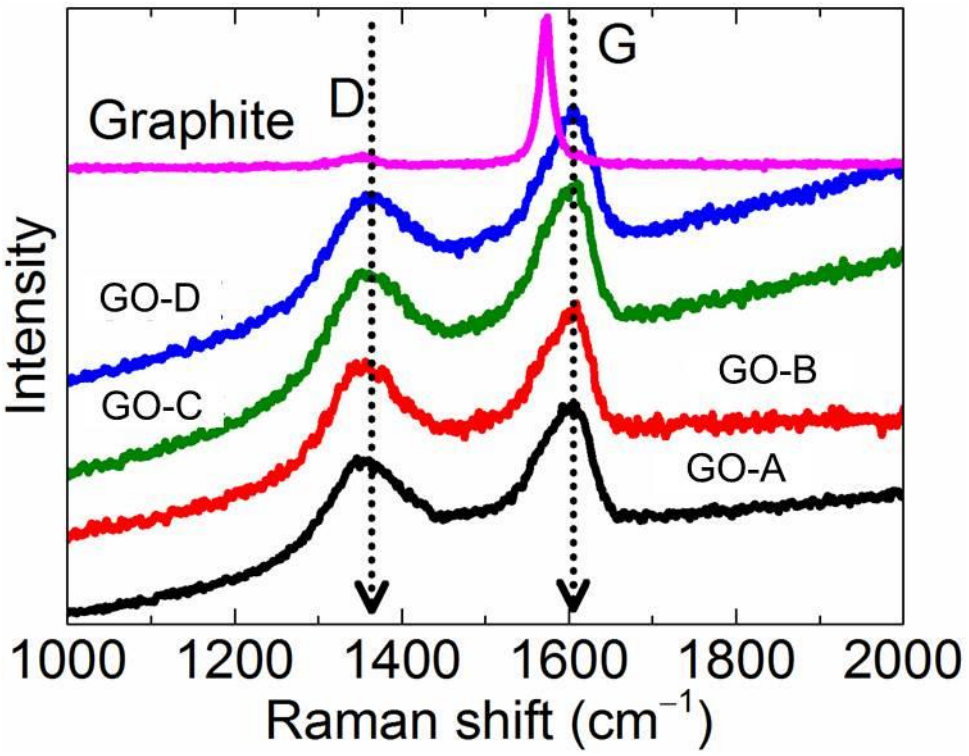

Figure S5. Raman spectra of GO samples. The shift of the G-band with respect to the graphite suggesting the chemical modification.

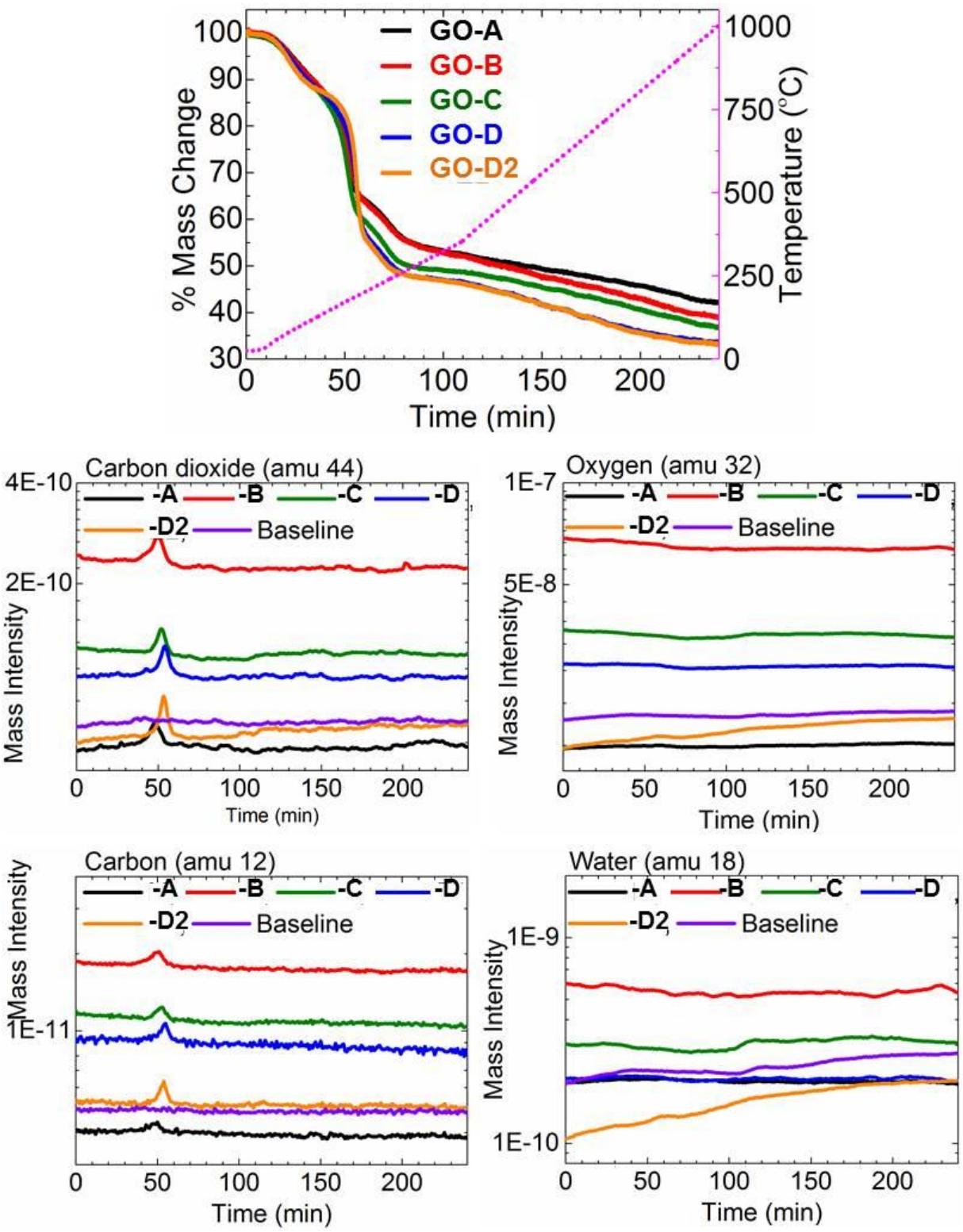

Figure S6. TG (top) and MS (bottom four) curves of GO samples with a controlled heating rate, initially at 3 °C per minute and 5 °C per minute after reaching the decomposition point. The TG signals show that about 50% mass loss at the decomposition point; more in highly oxidized GO-D than mildly oxidized GO-A. MS signals attribute this mass-loss to mainly the release of CO_2.

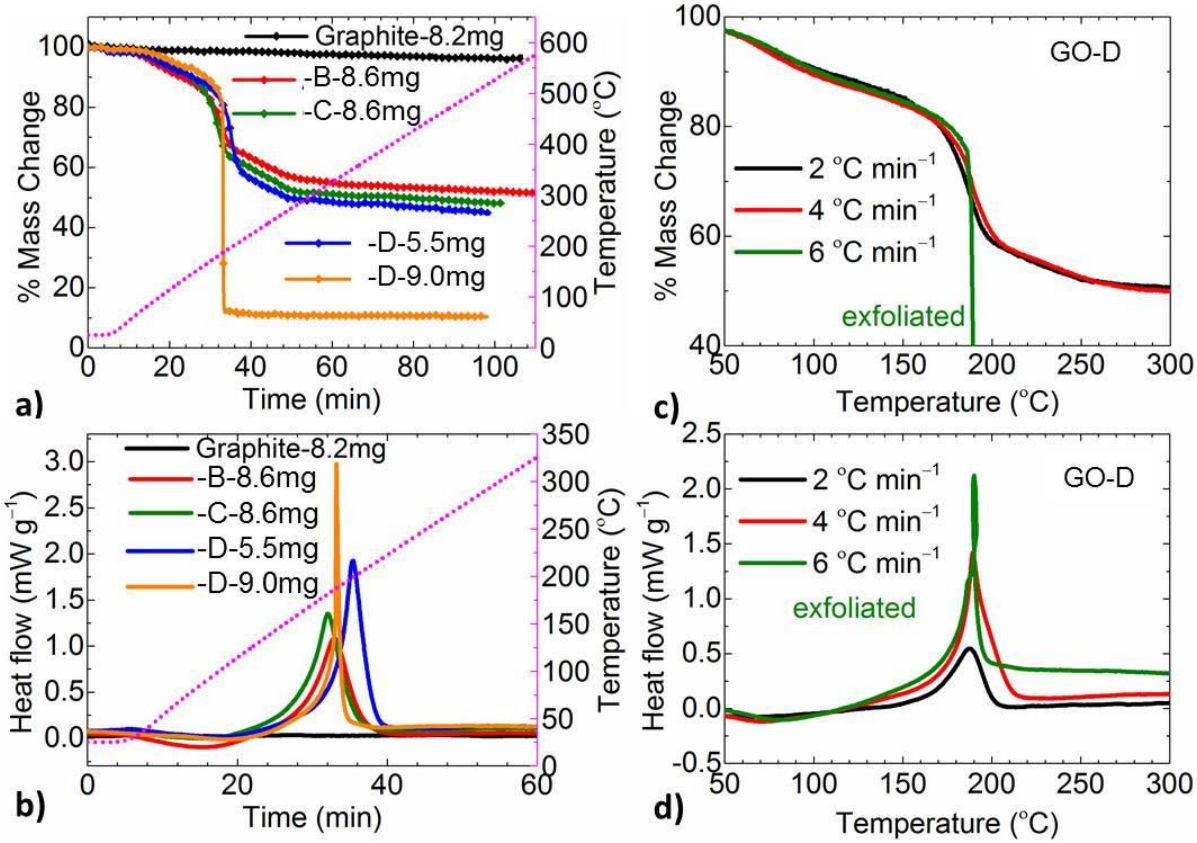

Figure S7. a-b) TG-DSC curves of GO samples at a heating rate of 5 °C per minute. See that the highly oxidized GO-D sample exfoliates when used sample mass of 9.0 mg packed in a TG crucible of 70 µl volume. This is not the case when the same sample of 5.5 mg loosely put in the crucible. The other samples of similar mass of >8.0 mg do not exfoliate, suggesting a highly oxidized nature of GO-D. The differential scanning calorimetry curves show that the decomposition of GO is exothermic. This exothermic heat is further enhanced with increased degree of oxidation of GO. This highly exothermic nature of the highly oxidized GO leads to the explosive nature of decomposition in GO-D sample. c-d) TG-DSC curves of GO-D measured at different heating rates of (2, 4 & 6) °C per minute. The sample exfoliates at a heating rate of ≥6 °C per minute.

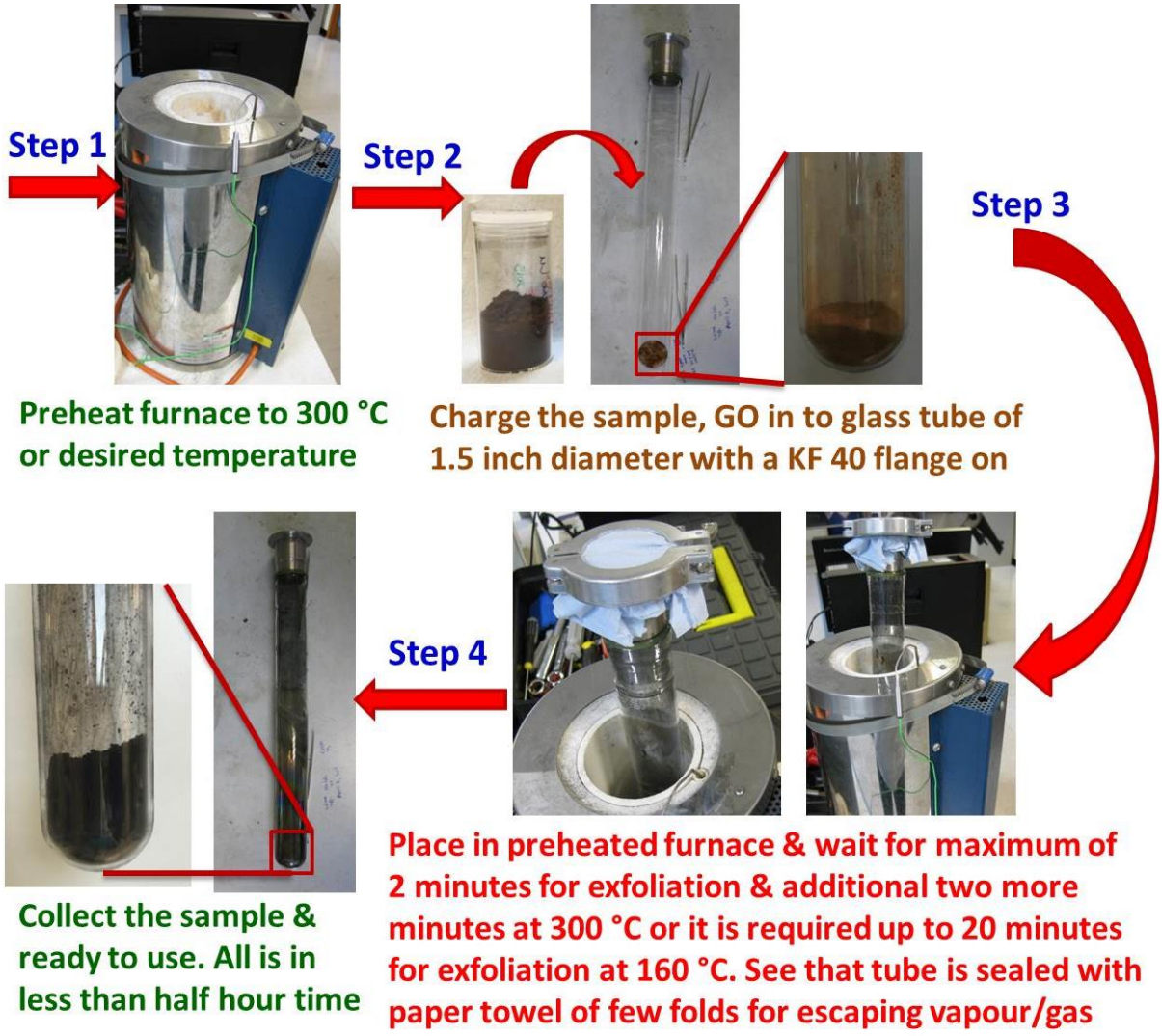

Figure S8. Four steps to exfoliation process at 300 °C, all in less than a half-hour time. Important to note that a care should be taken with respect to the amount of GO sample put into the glass tube, excessive amount of GO sample can lead the exfoliation to be more violent and dangerously explosive.

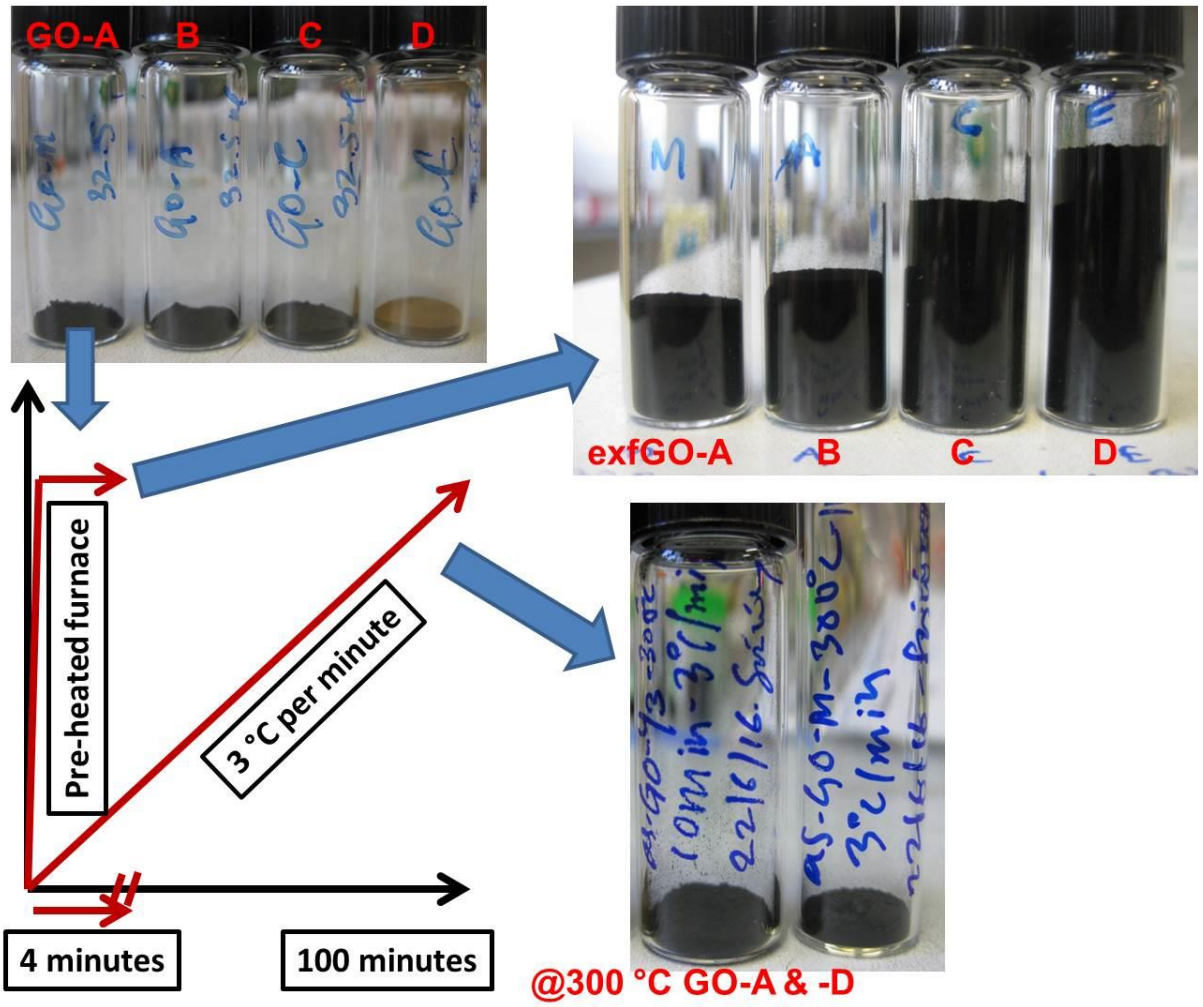

Figure S9. Experimental procedure diagram for exfoliation and slow heating. From top-left and in clockwise: digital photographs of the GO (-A, -B, -C, -D), after exfoliation at 300 °C & the samples after slow heating to same temperature of 300 °C. All the samples are in a 4 ml vials with an equal mass of 32.5 mg in each case.

Sample volume in a 4 ml vial (in cm^3) for the given sample mass of 32.5 mg

exfGO-A = ~1.60 cc, equivalent density = ~0.0203 g cm^{-3}

exfGO-B = ~2.00 cc, equivalent density = ~0.0162 g cm^{-3}

exfGO-C = ~2.90 cc, equivalent density = ~0.0112 g cm^{-3}

exfGO-D = ~3.80 cc, equivalent density = ~0.0086 g cm^{-3}

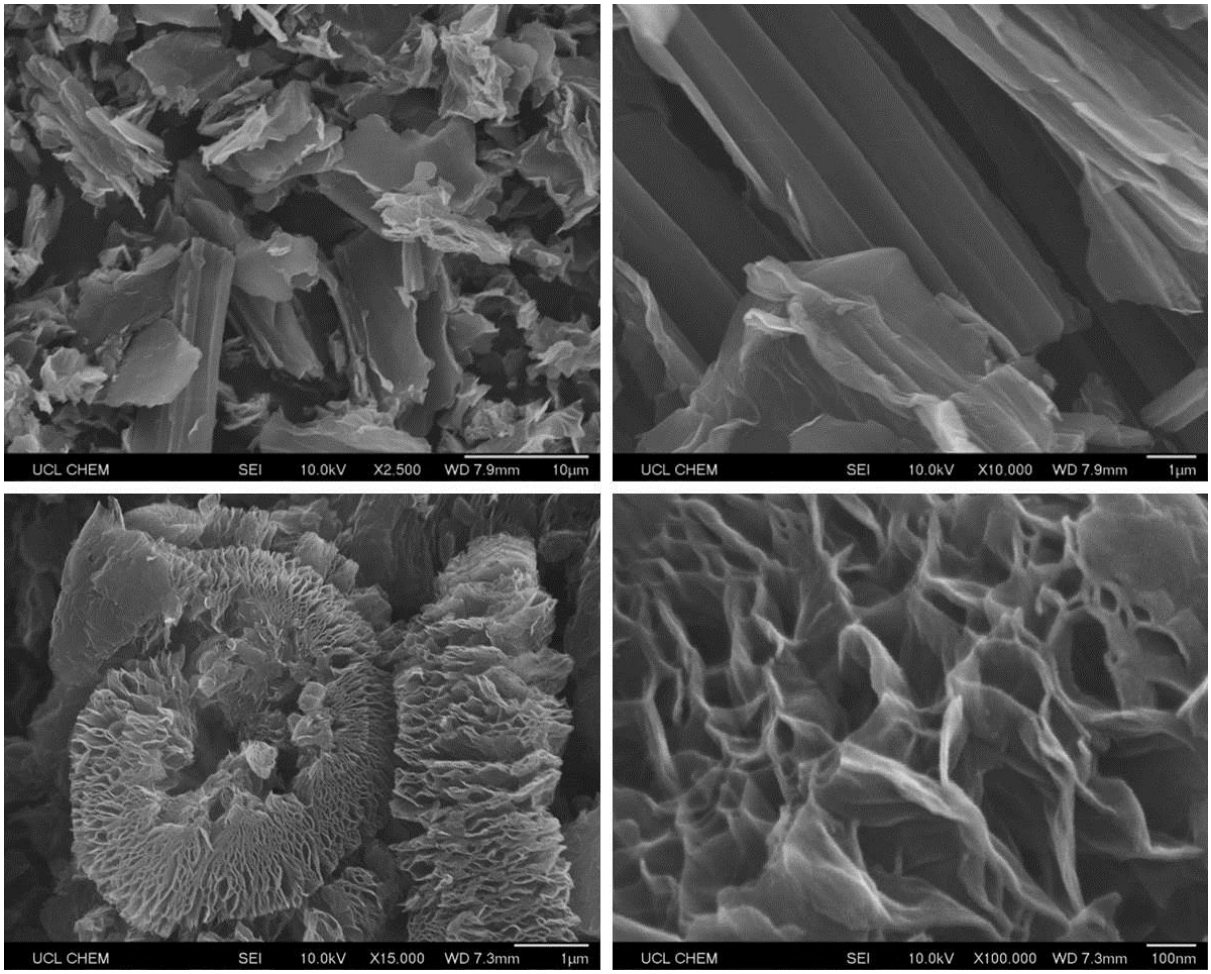

Figure S10. SEM micrographs of GO-D sample after subjecting at slow heating (3 °C per minute) to 300 °C (top two) and directly placed at 300 °C preheated furnace (bottom two).

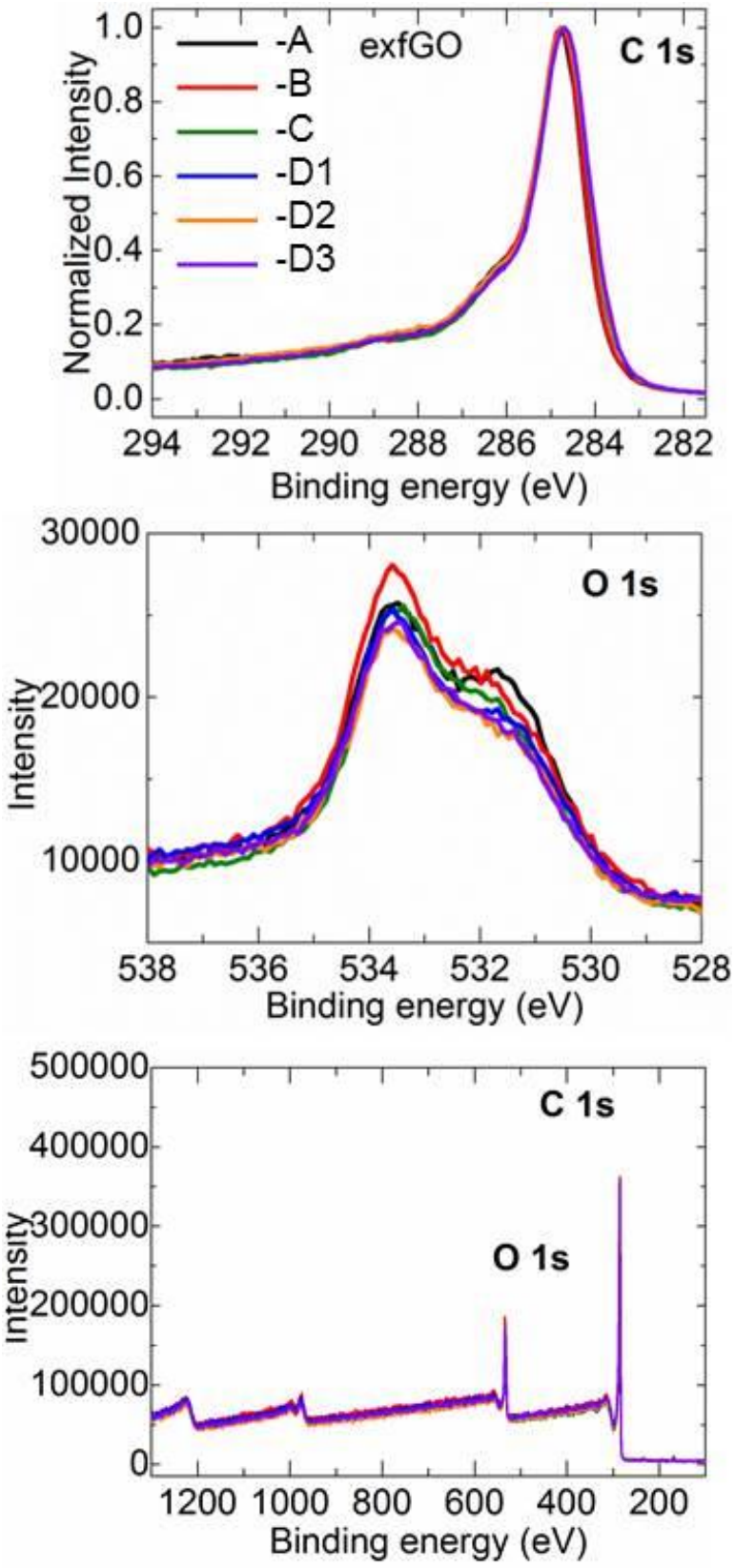

Figure S11. XPS spectra; C 1s, O 1s and Survey of exfGO samples. Top: Comparative C 1s spectra with the intensity normalized to a sp^2 carbon peak, show similar reduction (also see O 1s spectra - middle). Bottom: XPS Survey spectra, consisting of only two peaks corresponding to C 1s and O 1s.

Table S2. XPS elemental analysis of exfGO samples, the spectra was recorded at multiple spots on each sample. The atomic percentage for C and O were estimated from the C 1s and O 1s peaks in the Survey spectra. More reduction is seen for exfGO-D samples compared to the exfGO-A sample, could be due to the trapped molecules in the narrow slit-pores in the exfGO-A.

S/No	Sample	As exfoliated	
		C (at%)	O (at%)
1	exfGO-A	85.7	14.3
		86.0	14.0
2	exfGO-B	86.4	13.3
		87.3	12.7
3	exfGO-Cb2	86.7	13.3
		86.2	13.8
		87.0	13.0
4	exfGO-Db1	87.4	12.6
		87.7	12.3
		88.0	12.0
5	exfGO-Db2	87.7	12.3
		87.2	12.8
6	exfGO-Db3	87.4	12.6
		87.4	12.6
7	exfGO-Db4	87.4	12.6
		87.7	12.3

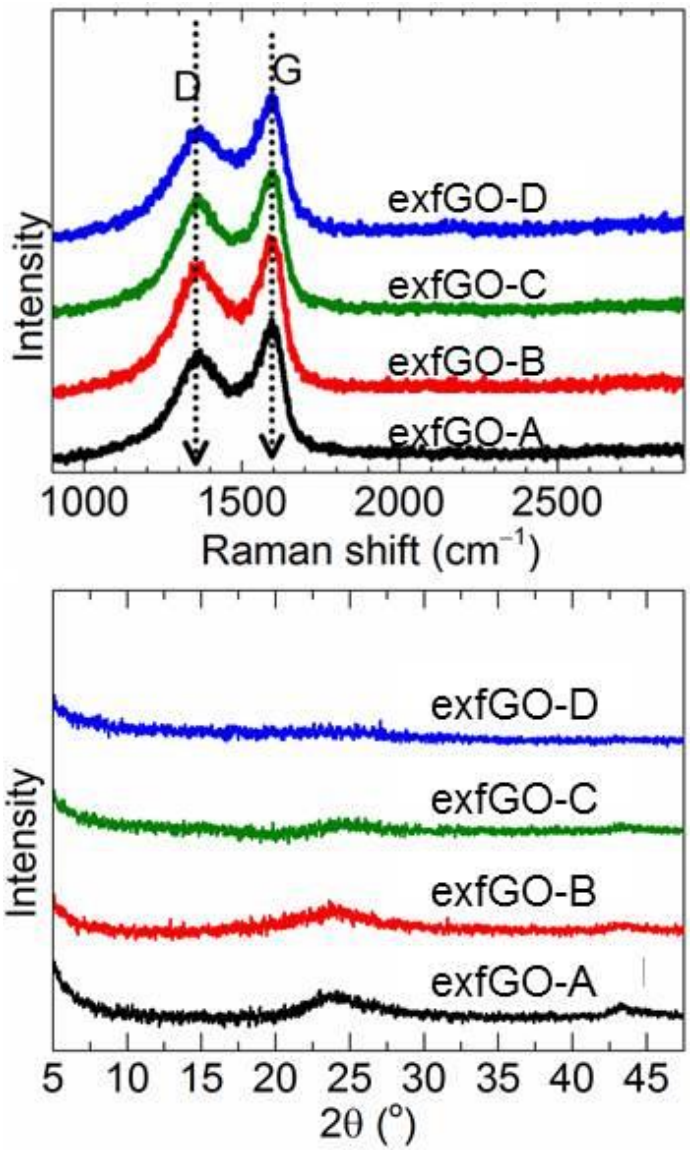

Figure S12. Raman spectra (top) and PXRD patterns (bottom) of exfGO samples represent a highly disorder state of the samples. See that there is hardly any signature of structure order Raman mode, 2D at around 2700 cm^{-1} as well characteristic PXRD (001) peak of GO or (002) peak of graphite.

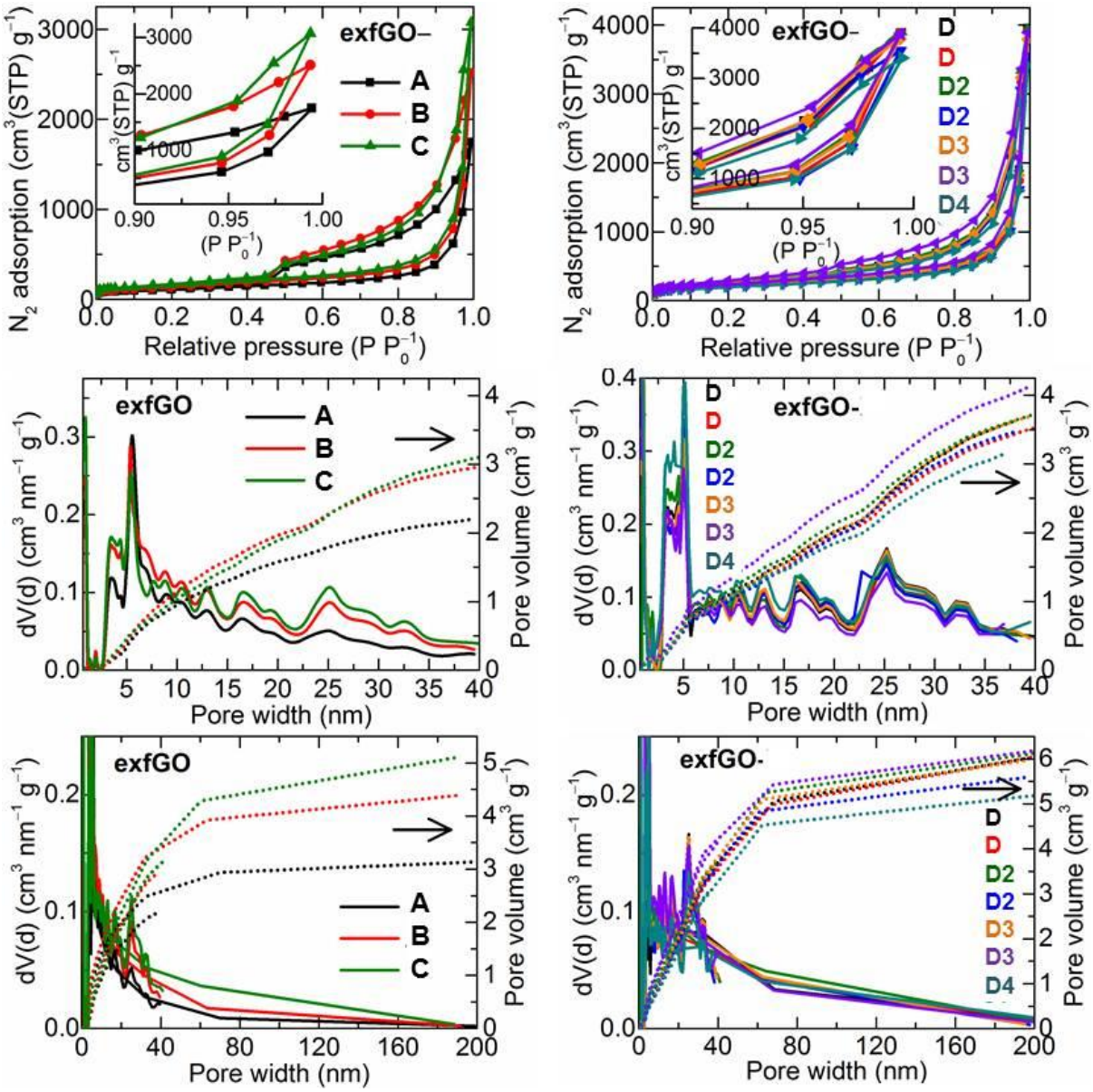

Figure S13. Porosity characteristics of as exfoliated GO samples: 77 K N_2 adsorption-desorption isotherms (top) and QSDFT (for micro- to meso- porous region) (middle) and DH (meso- to macro- porous region) (bottom) model fittings derived pore size distribution (line data on left Y-axis) and pore volume (dotted data on right Y-axis) curves. The hysteresis between adsorption and desorption (type H3) is assigned to the plate-like geometry of the macro-pores.

Note that for GO-D sample, the different batch samples (D, D2, D2, D3, & D4) and repeated measurements have been carried out & they are indeed in good agreement in both the uptake, and pore size distribution and pore volume. See **Table S3** for the calculated SSA and pore volume of the samples.

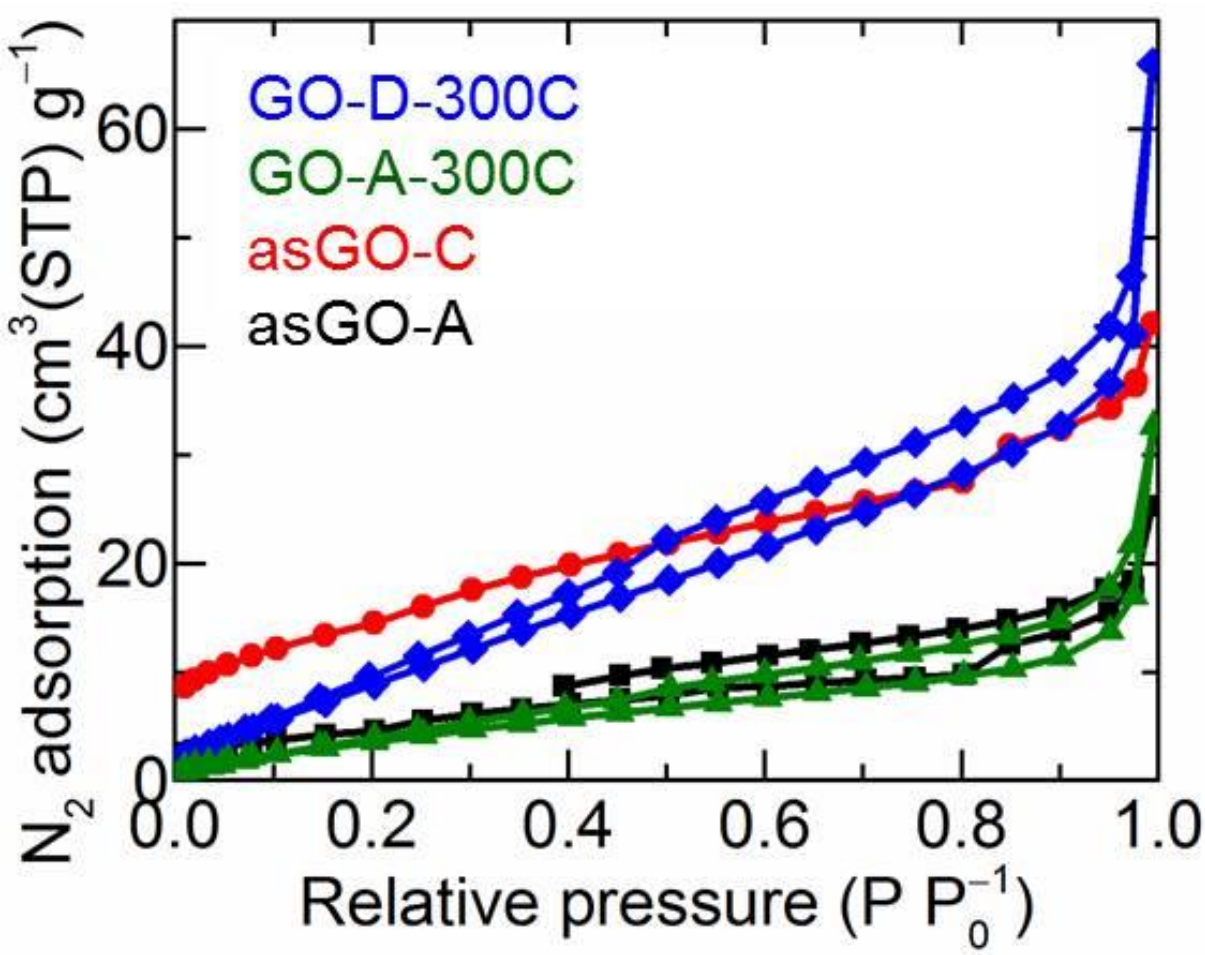

Figure S14. N_2 adsorption-desorption isotherms (at 77 K) of as-synthesized GO (-A & -C) and non-exfoliated GO (-A & -D) with a slow heating rate at 3 °C min^{-1}) to 300 °C. All samples show negligible uptake thus show negligible porosity. See **Table S3** for the calculated SSA and pore volume of the samples.

Table S3. Porosity; BET SSA, QSDFT & DH model fittings derived pore volumes of the as-exfoliated GO and as-synthesized GO samples. Samples synthesized by a slow heating (without exfoliation) is also measured.

Sample	**BET SSA ($m^2 g^{-1}$)**	**QSDFT Micropore Volume (at 2.0 nm) ($cm^3 g^{-1}$)**	**DH Mesopore Volume (at 50.0 nm) ($cm^3 g^{-1}$)**	**N_2 uptake at P P_o^{-1} of ≤0.994 ($cm^3 g^{-1}$)**	**Total pore volume at P P_o^{-1} of ≤0.994 ($cm^3 g^{-1}$)**
asGO-A	15	-	-	25.0	0.039
asGO-C	50	-	-	42.0	0.065
GO-A-300C	10	-	-	32.6	0.051
GO-D-300C	25	-	-	66.0	0.102
exfGO-A	360	0.069	2.60	1748.0	2.71
exfGO-B	480	0.069	3.60	2515.0	3.89
exfGO-B(J3)	460			2495.0	3.86
exfGO-C	570	0.094	3.86	3075.0	4.77
exfGO-Cb2(J1)	696			3407.0	5.28
exfGO-Dr1	780	0.152	4.19	3953.0	6.13
exfGO-D2r1(E-OG6h)	770	0.150	4.11	3919.0	6.08
exfGO-D2r2(E-OG24h)	814	0.146	4.40	3935.0	6.09
exfGO-D2(E2)	735	0.143	4.22	3549.0	5.50
exfGO-D3(Y2)	805	0.168	4.37	3793.0	5.88
exfGO-D4(Y3)	830	0.176	4.65	3891.0	6.03

*OG6h & OG24h stands for the sample out gassed for 6 h and 24 h, respectively.

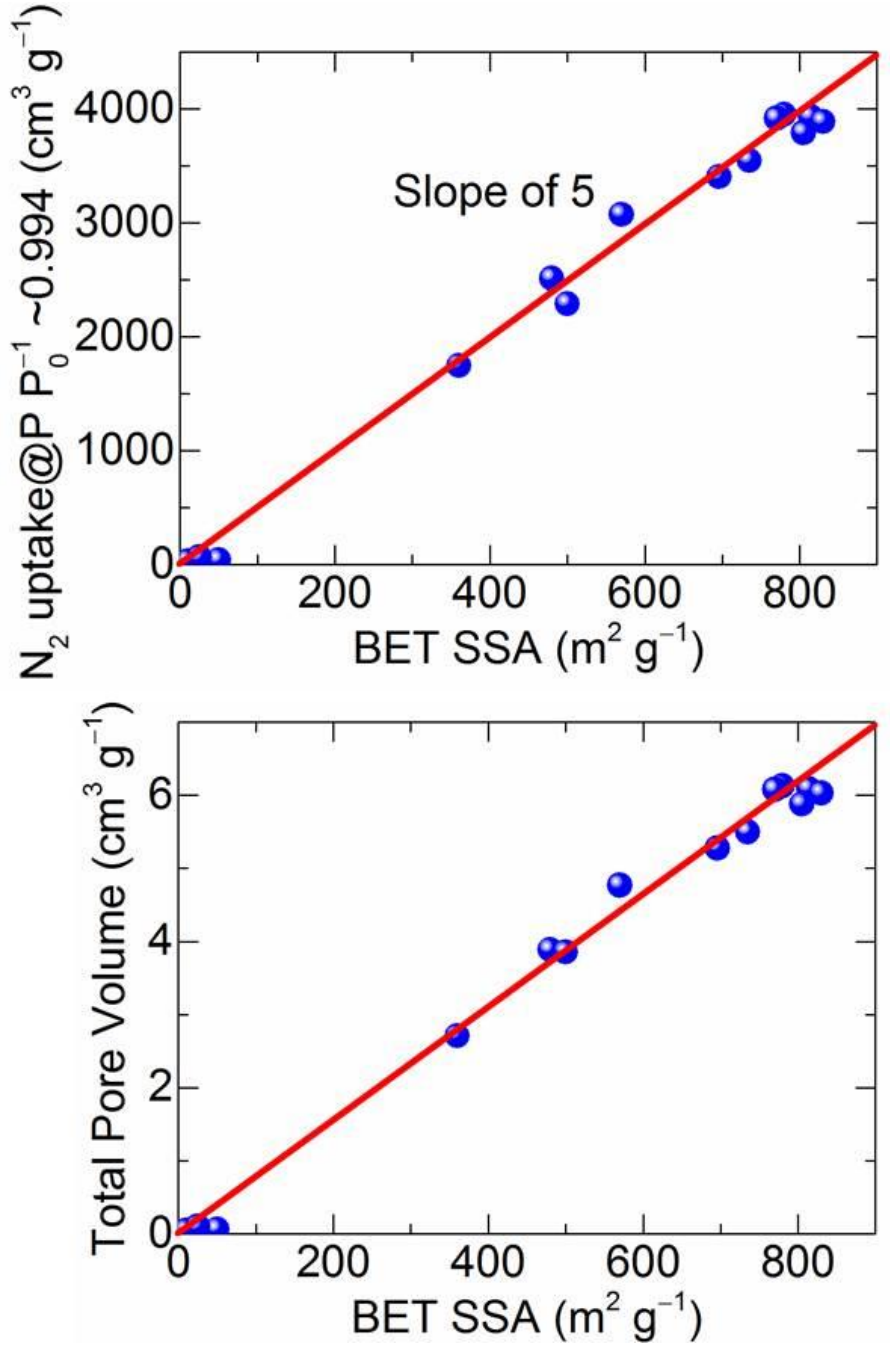

Figure S15. A relation between SSA and total pore volume in the exfGO samples shows a simultaneous enhancement in both the SSA and pore volume.

Table S4-1 Literature porosities, BET SSA ($m^2\ g^{-1}$, specific surface area) and V_t ($cm^3\ g^{-1}$, total pore volume) of the porous graphene-based materials synthesized by chemical reduction, thermal & microwave exfoliation & reduction, hydro-/solvo-thermal reduction/modification, hydrogels, aerogels and xerogels, pillared or cross-linked layers, templated & CVD. A summary of synthesis methods is also included with corresponding references.

S/N	Material	SSA	V_t	Summary of synthesis conditions	Ref.
1	exfGO film	404	2.85	10 °C per min heating to 250 °C	[1]
2	exfGO cake	300	2.26	10 °C per min heating to 250 °C	[2]
3	exfGO	600-750	-	1050 °C (pre-heated) for 30 s	[3]
4	exfGO	480	2.00	150 °C for 45 min under vacuum	[4]
5	exfGO	547	2.47	100 °C for 1 h under CO_2 pressure of 20 bar & rapid release	[5]
6	T-rGO	377	1.14	1000 °C for 30 min	[6]
7	H-rGO	310	0.50	Hydrothermal at 180 °C for 6h → immerse in $FeCl_3$ → Freeze dry → Pyrolyze at 850 °C for 2 h → acid etching of Fe_2O_3	[7]
8	H-rGO-N-doped	362	0.44	GO + Pyrrole → ,,	
9	H-rGO-S-doped	280	0.41	GO → Hydrothermal at 180 °C for 6 h → immerse in $FeCl_3$ → Freeze dry → Sulphur powder → Pyrolyze at 850 °C for 2 h → acid etching of Fe_2O_3	
10	H-rGO-N-,S-doped	405	0.60	GO + Pyrrole → Hydrothermal at 180 °C for 6 h → Immerse in $FeCl_3$ → Freeze dry → Sulphur powder → Pyrolyze at 850 °C for 2 h → Acid etching of Fe_2O_3	
11	H-rGO	151	0.24	GO → Hydrothermal at 180 °C for 6 h → Freeze dry → Pyrolyze at 850 °C for 2 h	
12	H-rGO-N-doped	186	0.39	GO + Pyrrole → Hydrothermal at 180 °C for 6 h → Freeze dry → Pyrolyze at 850 °C for 2 h	
13	H-rGO-S-doped	164	0.20	GO → Hydrothermal at 180 °C for 6 h → Freeze dry → Sulphur → Pyrolyze at 850 °C for 2 h	
14	H-rGO-N, S-doped	207	0.35	GO + Pyrrole → Hydrothermal at 180 °C for 6 h → Freeze dry → Sulphur → Pyrolyze at 850 °C for 2 h	
15	T-rGO (sprayed)	365	2.36	GO dispersion → Spray in to 160 °C of immiscible solvent, octanol + Reducing agent L-ascorbic acid → Heat-treated at 600 °C in Ar gas	[8]
16	rGO (Non-assembled)	425	2.35	GO dispersion → Spray in to 160 °C of miscible solvent, ethylene glycol + Reducing agent L-ascorbic acid → Heat-treated at 600 °C in Ar gas	
17	rGO	40	0.26	GO dispersion → Spray in to 110 °C of immiscible solvent, octanol + Reducing agent L-ascorbic acid → Heat-treated at 600 °C in Ar gas	
18	C-rGO (holey)	430	0.60	Aqueous mixture of GO and H_2O_2 at 100 °C for 4 h under stirring	[9]
19	T-rGO-N-doped (	465	3.42	GO + NH_2CN at 400 °C for 1 h → 900 °C for 2 h	[10]

	crumpled)				
20	C-rGO	409	0.52	GO + $NaBH_4$, stir for 2 h	
21	T-rGO	76	0.05	GO → Anneal at 900C for 2 h	
22	exfGO (sprayed)	650	1.93	GO suspension spay dryer → GO spheres → Microwave oven operated at 1100 W for 40 s	[11]
23	exfGO	493	2.30	1050 °C (pre-heated) for several minutes	[12]
24	C-rGO	320	-	Hydrazine @ GO in a desiccator for 72 h	[13]
25	exfGO	463	-	Microwave oven at 700 W for 1 min	[14]
26	exfGO (sprayed)	567	-	400 °C for 5 min	[15]
27	,,	410	-	400 °C for 5 min → Solution processing	
28	,,	255	-	400 °C for 5 min → Compressed at 55 MPa	
29	T-rGO (sprayed)	344	-	Slow heating to 400 °C for 5 min	
30	exfGO	407	-	400 °C (pre-heated) for 5 min	
31	exfGO-solution processed	226	-	400 °C (pre-heated) for 5 min → Solution processed	
32	exfGO-compressed	66	-	400 °C for 5 min → Compressed at 55 MPa	
33	T-rGO (Non stacked)	671	4.11	GO in ethanol → Anti-solvent directed non-stocked GO → 1000 °C for 1 h	[16]
34	T-rGO (Non stacked)	1435	4.11	GO + Ethanol + Hexane → Vacuum filtrate → Rotary dry → 1000 °C for 1 h	[17]
35	T-rGO film	311	1.33	GO dispersion → Petri dish & dry at room temperature → 1000 °C for 1h	
36	H-rGO	220	0.45	GO dispersion at 180 °C for 12h	[18]
37	rGO-SiO_2	350	0.81	Graphene aerogel + SiO_2	
38	rGO/Carbon (templated)	295	0.62	Graphene aerogel + SiO_2 + Sucrose → Freeze dry → Pyrolyze at 700 °C for 3 h → NaOH treat to remove SiO_2	
39	T-rGO-N-doped	864	1.99	A multi-step heating to 120 °C for 20 min → 800 °C for 2 h	[19]
40	exfGO	328	1.59	250 °C (pre-heated) for 5 min	[20]
41	exfGO	404	1.87	300 °C (pre-heated) for 5 min	
42	exfGO	418	2.16	400 °C (pre-heated) for 5 min	
43	exfGO	125	0.31	1000 °C (pre-heated) for 30 s	[21]
44	exfGO	540	1.46	1000 °C (pre-heated) for 30 s	
45	exfGO	524	1.16	1000 °C (pre-heated) for 30 s	
46	FeOOH/Graphene	333	0.50	rGO + $FeCl_3.6H_2O$ + Ethanol + NH_4HCO_3, stir for 8 h	[22]
47	exfGO	356	1.40	250 °C (pre-heated)	[23]
48	exfGO	156	0.80	1050 °C (pre-heated) for 30 s	[24]
49	C-rGO	466	0.50	Sonicated GO + Hydrazine hydrate stir @ 100 °C for 24 h	[25]
50	exfGO	300	0.50	A rapid heating to expansion	[26]
51	exfGO	477	1.04	150 °C for 45 min under vacuum	[27]
52	C-rGO	1206	3.20	Sonicated GO + Glucose + $NH_2.H_20$ stir @ 95 °C for 120 min	[28]
53	exfGO	443	2.50	200 °C under hydrogen	[29]
54	exfGO	151	0.63	1 °C per min heating to 150 °C under vacuum	[30]
55	exfGO	437	1.72	,, at 200 °C	

56	exfGO	480	1.73	,, at 300 °C	
57	exfGO	245	1.03	, at 400 °C	
58	T-rGO	192	0.69	220 °C	[31]
59	T-rGO	186	0.68	190 °C	
60	T-rGO	183	0.63	170 °C	
61	T-rGO	101	0.11	100 °C	
62	GO-frameworks	470	0.30	GO + Benzene diboronic acid + Methanol → Solvothermal at 100 °C for 24 h	[32]
63	,,	367	0.29	GO + 1,4-Phenyldiboronic acid + Methanol → Solvothermal at 120 °C for 24 h	
64	,,	151	0.13	GO + 1,4-Phenyldiboronic acid + Methanol → Solvothermal at 150 °C for 24 h	
65	,,	342	0.25	GO + 1-Phenylboronic acid + Methanol → Solvothermal at 80 °C for 24 h	
66	,,	442	0.25	GO + 1-Phenylboronic acid + Methanol → Solvothermal at 100 °C for 24 h	
67	,,	426	0.25	GO + 1-Phenylboronic acid + Methanol → Solvothermal at 120 °C for 24 h	
68	,,	78	0.11	GO + 1-Phenylboronic acid + Methanol → Solvothermal at 150 °C for 24 h	
69	,,	280	0.21	GO + 4,4-Biphenyldiboronic acid + Methanol → Solvothermal at 100 °C for 24 h	
70	S-rGO	54	0.09	Methanol solvothermal at 150 °C	
71	Electrochem exf-graphite	470	2.85	Graphite rod electrode + LiCl salt + moist Ar → 800 °C & 33.0 A for 60 min → 1450 °C for 30 min	[33]
72	exfGO	528	2.71	1000 °C (pre-heated) for 60 s	[34]
73	exfGO/CNT	175	1.00	GO → 1000 C (pre-heated) for 60 s + Ferrocene + Ethylene diamine → CVD at 700 °C → Acid wash	
74	T-rGO	450	1.82	Pre-oxydized graphite → GO at 300 °C for 5 min	[35]
75	H-rGO (holey)	830	0.82	GO + H_2O_2 → Hydrothermal at 180 °C for 6 h → Sodium ascorbate at 100 °C for 2 h → Freeze dry	[36]
76	H-rGO	260	0.45	GO → Hydrothermal → Freeze dry	
77	exfGO	368	-	GO → Vacuum exfoliation at 200 °C & left at for 5 h	[37]
78	exfGO	370	-	GO → Vacuum exfoliation at 300 °C & left at for 5 h	
79	exfGO	382	-	GO → Vacuum exfoliation at 400 °C & left at for 5 h	
80	exfGO	350		GO → 1000 °C	
81	H-rGO (aerogel)	473	0.25	GO + Urea → Hydrothermal → 160 °C for 12 h → Freeze dry → 800 °C for 1.5 h	[38]
82	C-rGO	6	0.03	GO + Sodium dodecylbenzenesulfonate + NaOH + Hydrazine hydrate at 90 °C for 24 h	[39]
83	C-rGO-daizonium linked	296	0.59	rGO + Benzedine + CH_2Cl_2 + Boron trifluoride etherate + Isoamyl nitrite, stir for a day	
84	exfGO	343	1.70	300 °C for 10 min	[40]

85	H-rGO	344	0.39	160 °C for 16 h	[41]
86	T-rGO (spheres; templated)	1159	0.94	Aminated silica + GO solution → Pyrolyze at 550 °C for 2 h → HF etching of silica	[42]
87	S-rGO	272	1.77	GO + Ethylene glycol at 180 °C for 10 h	[43]
88	S-rGO-NH_2	346	2.88	GO + Ammonia + Ethylene glycol at 180 °C for 10 h	
89	T-rGO (aerogel)	671	0.54	GO gelation → Pyrolyze at 800 °C	[44]
90	T-rGO paper	275	1.10	GO → Vacuum filtrate → Put on lighter flame for 5 s	[45]
91	H-rGO	1377		GO → Hydrothermal at 160 °C for 3 h	[46]
92	H-rGO	482		Microwave hydrothermal at 190 °C for 10 min	[47]
93	H-rGO-N-doped	355		GO + Urea → Microwave hydrothermal at 190 °C for 10 min	
94	H-rGO	265	0.22	180 °C for 6 h	[48]
95	H-rGO-N-doped	479	0.31	GO + Ammonia → Hydrothermal 180 °C for 6 h	
96	exfGO-N-doped	237		GO at 800 °C → Hexamethylenetetramine → Hydrothermal at 180 °C for 12 h	[49]
97	H-rGO-N-doped	141		GO + Hexamethylenetetramine → Hydrothermal at 180 °C for 12 h	
98	H-rGO-N-, B-doped	249	0.54	Flake GO + NH_3BF_3 → Hydrothermal at 180 °C for 12 h	[50]
99	H-rGO	642	0.34	Flake GO Hydrothermal at 180 °C for 4 h	[51]
100	C-rGO-etched	1374	1.16	GO + $KMnO_4$ → Microwave heating for 5 min → Hydrazine reduction at 100 °C for 24 h	[52]
101	exfGO	520	2.17	Exfoliate at 900 °C for 10 s → Freeze in liquid nitrogen	[53]
102	exfGO	380	1.58	Exfoliate at 900 °C for 10 s	
103	T-rGO (freeze dried)	445	3.25	Solution freeze dry → Pyrolyze at 700 °C for 3 h	[54]
104	H-rGO	370	0.16	GO → Amine/Ammonia → Hydrothermal at 150 °C for 6 h	[55]
105	H-rGO	370		GO → Hydrothermal at 150 °C for 6 h → Vacuum dry	
106	H-rGO	720	0.46	GO → Hydrothermal at 150 °C for 6 h → Freeze dry	
107	H-rGO	450		GO → Hydrothermal at 150 °C for 6 h → Vacuum dry → Pyrolyze at 800 °C for 3 h	
108	C-rGO films	19		Hydrazine reduction at 95 °C for 1 h → Vacuum filtration	[56]
109	C-rGO films (templated)	194		Hydrazine reduction at 95 °C for 1 h → Polystyrene particles → Vacuum filtration → Remove Polystyrene	
110	C-rGO	801	0.9	Hydrazine reduction	[57]
111	C-rGO	512	2.48	GO + L-ascorbic acid, stir at 40 °C for 16 h → Freeze dry → Supercritical CO_2 dry	[58]
112	H-rGO	964	0.40	GO → Hydrothermal at 180 °C for 12 h	[59]
113	H & C-rGO	951	0.42	GO → Hydrothermal at 180 °C for 12 h → Hydrazine monohydrate reduced at 100 °C for 8 h	
114	H & C-rGO	911	0.42	GO → Hydrothermal at 180 °C for 12 h → Hydroiodic acid reduced at 100 °C for 3 h	
115	C-rGO	705		GO + Hydrazine monohydrate → Stir at 100 °C for 24 h	[60]
116	H-rGO	1018		GO → Hydrothermal → Supercritical dry → Pyrolyze at 1050	[61]

				°C for 3 h	
117	GO/RF aerogel	739		GO + RF + Fumed silica → 3D print → Cure at 85 °C → Supercritical CO_2 dry → Pyrolyse at 1050 °C for 3 h → HF treat for 2 days	[62]
118	H-rGO	245	2.50	Hydrothermal	[63]
119	C-rGO/C-S,N-doped	681	0.45	GO + Sodium dodecylbenzenesulfonate + $N_2H_4.H_2O$ at 100 °C for 8 h → Diazonium salt → DMF + 1,3,5-triethynylbenzene + 2,5-dibromothiazole, stir at 80 °C for 72 h → Soxhlet extraction for 48 h & dry → Pyrolyze @ 800 °C for 2 h	[64]
120	C-rGO/C-S-doped	618	0.58	GO + Sodium dodecylbenzenesulfonate + $N_2H_4.H_2O$ at 100 °C for 8 h → Diazonium salt → DMF + 1,3,5-triethynylbenzene + 2,5-dibromothiophene, stir at 80 °C for 72 h → Soxhlet extraction for 48h & dry → Pyrolyze @ 800 °C for 2 h	
121	C-rGO/C-N-doped	560	0.38	GO + Sodium dodecylbenzenesulfonate + $N_2H_4.H_2O$ at 100 °C for 8 h→ Diazonium salt → DMF + 1,3,5-triethynylbenzene + 2,6-dibromopyridine, stir at 80 °C for 72 h → Soxhlet extraction for 48 h & dry → Pyrolyze @ 800 °C for 2 h	
122	C-rGO	640		Hydrazine reduced GO	[65]
123	S-rGO-frameworks	74	0.08	GO + 1,4-Phenyldiboronic acid + Methanol → Solvothermal at 120 °C for 12 h	[66]
124	,,	138	0.15	,,	
125	,,	280	0.22	,,	
126	,,	470	0.30	,,	
127	,,	275	0.19	,,	
128	,,	465	0.40	,,	[67]
129	,,	363	0.17	GO + Diboronic acid → Solvothermal at 90 °C for 4 h	[68]
130	,,	1028	0.42	,, 24 h	
131	,,	658	0.36	,, 48 h	
132	,,	264		,,	
133	,,	313		,,	
134	,,	128		,,	
135	,,	56		,,	
136	,,	430		,,	
137	,,	490		,,	
138	,,	458		,,	
139	,,	495		,,	
140	,,	397		,,	
141	exfGO	561	3.25	300 °C for 10 min	[69]
142	S-rGO	211	0.89	GO + NMP at 180 °C for 10 h	[70]
143	H-rGO	437	1.82	GO dispersion → 180 °C for 12 h → Freeze dry	[71]
144	H-rGO	599	2.13	GO dispersion → 180 °C for 12 h → Freeze dry → 800 °C for 1 h	
145	C-rGO-templated	927	3.29	GO suspension + Hydrazine, stir for 12 h + F127 + HCl, stir for	[72]

	(MPG)			24 h→ Vacuum filtrate → Sinter at 350 °C for 5 h & Pyrolyze at 900 °C for 5 h	
146	MPG by hydrothermal	930	3.89	GO suspension + Hydrazine, stir for 12 h + F127 + HCl, stir for 24 h→ Hydrothermal at 120 °C for 24 h → Sinter at 350 °C for 5 h & Pyrolyze at 900 °C for 5 h	
147	MPG-N-doped	916	3.37	MPG + Cyanamide, ground → Sinter at 800 °C for 3 h	
148	C-rGO	127	0.22	Hydrazine reduced GO → 900 °C for 5 h	
149	C-rGO-N-doped	173	0.21	rGO + Cyanamide → 800 °C for 3 h	
150	T-rGO-templated	246	0.66		
151	C-rGO-templated	513	0.62	GO suspension + Hydrazine + F127 +C_{16}TAB, stir for 24 h → Vacuum filtrate → Sinter at 350 °C for 5 h & Pyrolyze at 900 °C for 5 h	
152	T-rGO-templated	851	4.28	GO + Hollow silica spheres suspension → Sinter at 900 °C for 5 h → HF etching of silica	[73]
153	,,	354	2.21	GO + 60 nm silica spheres → Sinter at 900 °C for 5 h → HF etching of silica	
154	,,	401	4.31	,, with 120 nm silica spheres	
155	,,	238	0.47		
156	T-rGO	363	2.01	GO → 900 °C	
157	C-rGO/CNT foam	272	0.88	GO + CNT aqueous dispersion → pore in to mould → Freeze dry → Hydrazine vapour reduction at 90 °C for 24 h	[74]
158	H-rGO/C-N-doped	280	1.1	GO + Pyrrole aqueous dispersion → Hydrothermal at 180 °C for 12 h → Freeze dry → Graphitize at 1050 °C for 3 h	[75]
159	T-rGO/C-N-doped	900	1.52	GO dispersion + Aniline + Phytic acid, stir cold to gel formation for 24 h → Pyrolyze at 850 °C for 2 h	[76]
160	H-rGO	364		2 mg/ml GO dispersion → Hydrothermal at 180 °C for 12 h	[77]
161	H-rGO-N-,S-doped	315		GO + Thiourea → Hydrothermal	
162	H-rGO (holey)	271		GH → Treated with H_2O_2 at 100 °C for 3 h	
163	H-rGO (holey)-N-, S-doped	153		HG + Thiourea → Hydrothermal	
164	H-rGO	325	0.33	GO dispersion → Hydrothermal at 180 °C for 12 h → Freeze dry	[78]
165	exfGO	925	-	1050 °C under Ar	[79]
166	S-rGO-iron oxide monolith	901	0.60	Flake GO dispersion + $Fe(acac)_3$ + DMF → Solvothermal at 200 °C for 20 h	[80]
167	,,	769	0.43	,,	
168	,,	635	0.42	,,	
169	,,	503	0.36	,,	
170	,,	418	0.33	,,	
171	C-rGO-polyoxometalate (GPOM)	680	0.57	Flake GO suspension + Phosphomolybdic acid + Hydrazine hydrate at 40 °C	[81]
172	oGPOM	580	0.48	GPOM + H_2O_2, stir & left overnight	
173	exfGO	550		1000 °C under H_2/Ar & anneal for 15 min	[82]

174	exfGO-diazonium linked	440		exfGO + Chlorosulfonic acid + 4, 4'-methylenedianiline + 4-Chloroaniline + sodium nitrate + 2, 2'-Azobis(2-methylpropionitrile) → stir at 80 °C for 6 h	
175	C-rGO-terpyridine linked	440	0.34	Alkynyl GO + DMF + (Azido-terpyridine)2Fe(II), stir at 80 °C for 2 h	[83]
176	T-rGO-silsesquioxane pillared	562	0.29	GO + n-butylamine + Toluene + Silylating reagent → stand for 2 days at 60 °C → thermal reduction at (500-600) °C under vacuum	[84]
177	,,	591	0.27	,,	
178	,,	839	0.38	,,	
179	,,	942	0.42	,,	
180	,,	562	0.26	,,	
181	,,	675	0.22	,,	
182	GO-PEI network	476	1.30	Flake GO dispersion + NaOH + PEI solution → store at 25 °C for 24 h → Freeze dry	[85]
183	H-rGO	876	-	180 °C for 12 h	
184	Pd@rGO	230	0.36	GO dispersion + bis(ethylenediamine)$PdCl_2$ → $NaBH_4$ reduction → Pyrolyze at 800 °C for 2 h	[86]
185	exfGO	755	3.36	1050 °C for 30 s	[87]
186	exfGO-HNO_3 treated	465	1.74	exfGO + HNO_3 at 70 °C for 1 h	
187	Pt@exfGO	478	1.61	GO-HNO_3 + $HPtCl_6$ + Eethylene glycol, at 100 °C for 6 h	
188	Pd@exfGO	544	1.66	,, with $PdCl_2$ at 70 °C for 5 min	
189	T-rGO	300	0.64	300 °C with a heating rate of 1 °C/min for 1 min	[88]
190	exfGO	477	1.04	150 °C under vacuum for 45 min	[89]
191	T-rGO-silica templated	278	0.58	GO + TEOS + CTAB, stir at 40 °C for 20 h → Pyrolyze at 350 °C for 30 min	[90]
192	,,	408	0.80	,,	
193	,,	866	0.73	,,	
194	GO-silica	1051	1.39	GO + TEOS + CTAB, ultrasoniate & stir at 40 °C for 12 h	[91]
195	T-rGO-silica templated & NH_3 treated	816	1.78	GO-Silica → Heat treat under NH_3 between (600-1000) °C → HF etching of silica	
196	C-rGO-N-doped	553	1.10	GO dispersion + Ammonia + Hydrazine → 95 °C for 1 h → Filtrate & freeze dry → Anneal at 900 °C for 1 h under NH_3 at 100 sccm	[92]
197	,,	1014	2.05	,, for 2h	
198	,,	738	2.78	,, for 3h	
199	,,	1200	1.30	,, for 4h	
200	Plasma-rGO	313	0.22	GO → H_2 plasma at 80 V & 1.6 A for 3 min	[93]
201	,,	391	2.00	GO → H_2 plasma at 50 V & 1.2 A for 2 min	[94]
202	,,	375	2.00	GO → CO_2 plasma at 50 V & 1.2 A for 2 min	
203	,,	420	2.00	GO → Ar plasma at 50 V & 1.2 A for 2 min	

204	CVD Graphene	1654	2.35	MgO template → CVD of CH_4 at 900 °C → HCl wash	[95]
205	C-rGO-B-doped	466		GO + Borane + THF, reflux at 100 °C	[96]
206	,,	91	0.26	GO suspension + H_3BO_3 → Freeze dry → Pyrolyze at 900 °C for 3 h	[97]
207	C-rGO balls	83	0.21	GO suspension → Droplets into liquid nitrogen → Freeze dry → Hydrazine reduction	[98]
208	H-rGO	388	0.31	GO suspension → Hydrothermal for 10 h	
209	T-rGO	520		GO at 300 °C with a slow heating of 1 °C per minute	[99]
210	exfGO	592	3.48	GO at 300 °C pre-heated	
211	T-rGO-templated	196	0.20	GO dispersion + $Zn(NO_3)_2.6H_2O$ + NH_4HCO_3 → Stir for 12 h → 350 °C for 4 h → HCl wash → Freeze dry	[100]
212	T-rGO-templated	540	1.56	Spherical $CaCO_3$ template + GO slurry → Pyrolyze at 900 °C for 5 h → HCl wash	[101]
213	,,	277	0.76	,,	
214	H-rGO (holey)	445	1.70	GO dispersion + H_2O_2 → Hydrothermal at 180 °C for 12 h	[102]
215	,,	247	0.54	GO dispersion → Hydrothermal at 180 °C for 12 h	
216	T-rGO	262	1.05	At 800 °C for 1 h	[103]
217	C-rGO	339		Hydrazine reduction at 98 °C for 30 min	[104]
218	T-rGO	72		At 200 °C for 2 h, heating rate at 5 °C per minute	[105]
219	,,	97		At 300 °C, ,,	
220	,,	181		At 400 °C, ,,	
221	,,	227		At 500 °C, ,,	
222	exfGO (annealed)	309	3.58	Exfoliate at 250 °C and anneal for 20 min	[106]
223	,,	293	2.91	At 600 °C, ,,	
224	,,	302	3.19	At 800 °C, ,,	
225	,,	434	3.14	At 100 °C, ,,	
226	C-rGO	82	0.11	Ethanol treated GO → Hydrazine reduction at 95 °C for 1 h	[107]

Table S4-2. Literature porosities, BET SSA ($m^2\ g^{-1}$, specific surface area) and V_t ($cm^3\ g^{-1}$, total pore volume) of the porous graphene-based materials synthesized by chemical activation with $KOH/ZnCl_2$ or CO_2 and further thermal annealing & CVD. A summary of synthesis methods is also included with corresponding references.

S/N	Material	SSA	Vt	Summary of synthesis conditions	Ref.
227	exfGO followed by annealing	1305	6.96	150 °C for 45 min under vacuum → Anneal at 600 °C for 6 h	[4]
228	KOH activated GO	3290	2.32	Exfoliated GO infiltrate with 3.5M KOH under vacuum directed flow drying → Activation at 800 °C for 1 h → Acetic acid wash to remove salts → Heat to 800 °C for 1 h	[11]
229	KOH activated nonstacked reduced GO	1000	5.03	GO in ethanol → Anti-solvent directed non-stocked GO → Thermal reduction at 1000 °C for 1 h → Immerse in 7M KOH solution for 24 h → Activate at 800 °C for 1 h → wash → Heat to 800 °C for 2 h	[16]
230	exfGO followed by annealing	574	2.44	300 °C (pre-heated) for 5 min → 700 °C for 3 h at 2 °C per min	[20]
231	exfGO followed by annealing	737	3.63	300 °C (pre-heated) for 5 min → 900 °C for 3 h at 2 °C per min	
232	exfGO followed by annealing (FGS)	758	3.26	300 °C (pre-heated) for min → 900 °C for 3 h at 2 °C per min	[22]
233	exfGO followed by KOH activation	619	0.36	exfGO + KOH (1:9 by wt) ground → 600 °C for1 h	[23]
234	,,	916	0.48	exfGO + KOH (1:4 by wt) ground → 600 °C for1 h	
235	,,	1096	0.56	exfGO + KOH (1:4 by wt) ground → 700 °C for1 h	
236	,,	1272	0.99	exfGO + KOH (7M solution)-dry → 900 °C for1 h	
237	,,	1276	0.72	exfGO + KOH (1:4 by wt) ground → 800 °C for1 h	
238	,,	1326	1.10	exfGO + KOH (1:9 by wt) ground →700 °C for1 h	
239	,,	1704	1.65	exfGO + KOH (1:9 by wt) ground → 800 °C for1 h	
240	,,	1894	1.60	exfGO + KOH (7M solution)-dry → 800 °C for1 h	
241	,,	930	0.68	exfGO + KOH (1:4 by wt) ground → 900 °C for1 h	
242	,,	940	1.08	exfGO + KOH (1:9 by wt) ground → 900 °C for1 h	
243	Activated rGO	677	0.39	rGO + KOH (1:4 by wt) ground → 800 °C for1 h	
244	,,	762	0.57	rGO + KOH (1:6 by wt) ground → 800 °C for1 h	
245	,,	923	0.88	rGO + KOH (1:9 by wt) ground → 800 °C for1 h	
246	CO_2 activated thermal reduced GO	885	0.71	GO → 250 °C (5 °C per min) for 30 min → 850 °C for 1 h under CO_2 flow of 1000 ml per min	[108]
247	CO_2 activated thermal reduced GO	1144	0.88	GO → 250 °C (5 °C per min) for 30 min → 750 °C for 1 h under CO_2 flow of 1000 ml per min	
248	CO_2 activated thermal reduced GO	1316	1.07	GO → 250 °C (5 °C per min) for 30 min → 950 °C for 1 h under CO_2 flow of 1000 ml per min	

249	CVD graphene foam monolith	1591	2.62	SiO_2 template → 1100 °C → CVD, H_2 + CH_4 for 1 h → HF etching of SiO_2 → Freeze dry	[109]
250	Graphene-activated carbon composite	798	0.42	GO + p-phenylene diamine + DMF, reflux at 90 °C for 24 h → KOH activation at 800 °C for 1 h	[110]
251	Activated Graphene	107	0.12	GO → KOH activation at 800 °C for 1 h	
252	Activated graphene aerogel	1145	0.81	GO + Urea → Hydrothermal → 160 °C for 12 h → Freeze dry → Impregnate with H_3PO_4 → 800 °C for 1.5 h	[38]
253	CVD multilayer graphene carbon film	688	0.26	Nickel foam → 1000 °C → CVD of ethanol vapour for 20 min → Etching of nickel by $FeCl_3$/HCl	[111]
254	Activated GO	1265	1.10	GO + KOH → 800 °C for 1 h	[112]
255	Activated exfGO	2448	1.34	exfGO + 7M KOH, stir & left 20 h, filtrate & dry → 800 °C for 1 h	[69]
256	Activated exfGO	3240	2.23	,,	
257	KOH activated exfGO	555	2.66	Microwave exfoliate GO + KOH → 700 °C for 1 h	[113]
258	KOH activated GO films	500	0.62	GO + KOH suspension → Dry by evaporation at 100 °C → Sticky paste to PTFE membrane → Vacuum filtrate dry → Actyivate at 800 °C for 1 h → Acetic acid wash to remove salts	[114]
259	,,	1700	1.00	,,	
260	,,	2400	1.53	,,	
261	KOH + exfGO	1550	1.35	Microwave exfoliated GO + KOH mix → heat at 550 °C for 10 h	[115]
262	,,	990	0.90	,, for 3 h	
263	,,	940	0.90	,, at 500 °C for 10 h	
264	,,	640	0.82	,, for 3 h	
265	,,	430	0.62	,, at 450 °C for 10 h	
266	,,	370	0.59	,, for 3 h	
267	KOH activated GO aerogel	1810	-	GO dispersion→ Hydrothermal at 180 °C for 12 h → mixed with KOH → activate at 800 °C for 1 h → HCl wash	[116]
268	CO_2 activated rGO	113	0.11	CO_2 activation at 800 °C for 20 min	[117]
269	,,	153	0.12	,,at 850 °C	
270	,,	257	0.23	,, at 875 °C	
271	,,	320	0.29	,, at 850 °C for 60 min	
272	$ZnCl_2$ activated rGO	210	0.62	At 600 °C for 1 h	
273	KOH activated rGO	87	0.20	700 °C for 1 h	
274	,,	100	0.20	750 °C	
275	,,	123	0.20	800 °C	
276	,,	270	0.18	700 °C for 1 h	
277	,,	335	0.20	750 °C	
278	,,	415	0.26	800 °C	
279	,,	1100	0.70	700 °C for 1 h	
280	,,	1450	0.93	750 °C	
281	,,	1765	1.16	800 °C	

282	,,	1160	1.0	700 °C for 1 h	
283	,,	1510	1.3	750 °C	
284	,,	1840	1.93	800 °C	
285	,,	2200	-	800 °C	
286	KOH activated rGO	453	0.30	rGO at 600 °C for 30 s → KOH mix → activation at 850 °C for 2 h → HCl wash	[118]
287	,,	1631	1.33	,,	
288	,,	2406	1.94	,,	
289	KOH activated rGO/pyrrole	193	0.11	GO + Ammonium persulphate + Pyrrole + Hydrazine hydrate, 90 °C for 12 h → KOH → Activation at 400 °C for 1 h → HCl wash	[119]
290	,,	952	0.41	,, at 500 °C	
291	,,	1360	0.59	,, at 600 °C	
292	,,	1588	0.75	,, at 700 °C	
293	KOH activated rGO/aniline	189	0.12	GO + Ammonium persulphate + Aniline + Hydrazine hydrate, 90 °C for 12 h → KOH → Activation at 500 °C for 1 h → HCl wash	[120]
294	,,	207	0.14	,, at 600 °C	
295	,,	980	0.44	,, at 700 °C	
296	,,	1337	0.68	,, at 800 °C	
297	KOH activated GO/thiophene	579	0.35	At 400 °C	[121]
298	,,	802	0.48	At 500 °C	
299	,,	1396	0.82	At 600 °C	
300	,,	1567	0.87	At 700 °C	

Table S5. Literature collection on highest pore volume (≥4.0 cm^3 g^{-1}) of solids includes activated carbons, CVD carbons, templated ordered mesoporous carbons, silicas & MOFs.

Sample	SSA (m^2 g^{-1})	Vt (cm^3 g^{-1})	Conditions	Ref.
KOH activated graphene	1000	5.03	800 °C for 1 h, a cake made from 200 mg of nonstacked reduced GO + 40 mL of 7 M KOH	[16]
Mesostructured Silica	1235	4.50	Templated	[122]
MOF (NU-110)	>7100	4.40	Self-assembled molecular structure	[123]
Silica templated mesoporous carbon	977	4.69	Resorcinol + Formaldehyde → Silica templated, pyrolyzed at 800 °C	[124]
$NaCl/ZnCl_2$ salt templated biomass derived carbon	2540	5.2	Adenine (biomass) + ($NaCl/ZnCl_2$) → 900 °C for 1 h at 2.5 °C per min	[125]
MgO templated carbon nanocages	1912	5.71	$MgCO_3.Mg(OH)_2.5H_2O$ + benzene vapour at 800 °C → HCl stir for 48 h & wash	[126]
Silica templated & activated carbon	1462	4.21	Resol + Cyanamide + SiO_2 → 800 °C for 2h. Step 2, NH_3 activation at 900 °C for 15 min	[127]
Mesocellular silica foam	688	4.17	Templated	[128]
MOF-5 derived carbon	2517	5.53	Direct carbonization at 1000 °C for 6h	[129]
Carbon aerogels	2299	6.40	1 wt% GO solution + Resorcinal + Formaldehyde + $NaCO_3$) → cure at 85 °C for 12-72h → supercritical CO_2 dry → Pyrolyze at 1050 °C for 3 h	[130]
MgO templated carbon	1276	4.18	$MgCO_3.Mg(OH)_2.5H_2O$ + benzene vapour at 800 °C → HCl stir for 48 h & wash	[131]
3D Ordered Mesoporous Carbon	1415	3.91	Furfuryl alcohol + Oxalic acid + Silica → 200 °C for 2 h → 900 °C for 5 h → silica etching in 6 M KOH	[132]
3D Ordered Mesoporous Carbon	1045	3.94	Furfuryl alcohol + Oxalic acid + Silica → 70 °C for 2 days → 200 °C for 3 h → 900 °C for 2 h → silica etching in 6 M KOH at 150 °C for 2 days	[133]

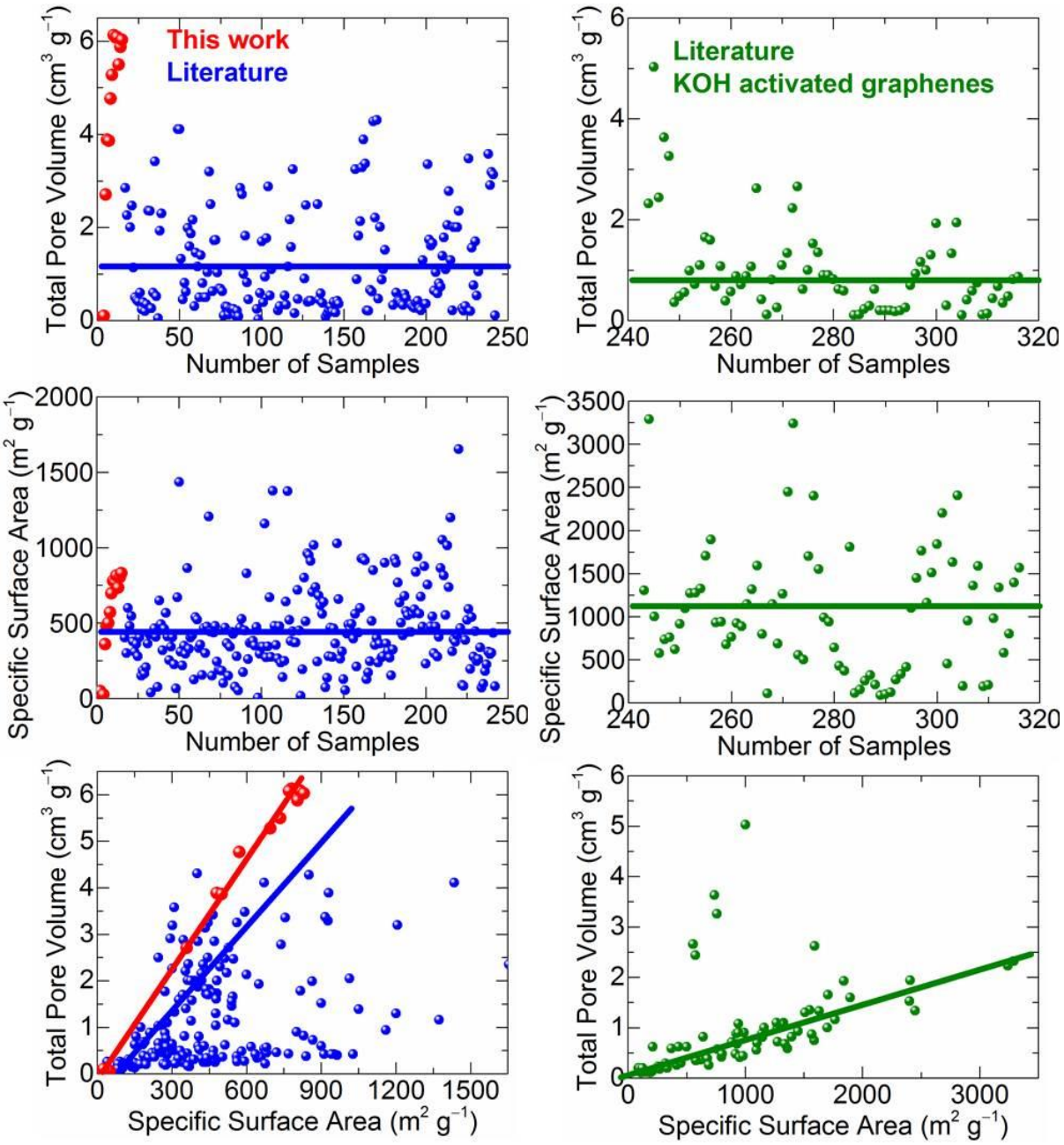

Figure S16. Porosity characteristics of literature graphene samples. Top: Total pore volume against number of samples. Middle: SSA against number of samples. Bottom: A relation between SSA and total pore volume in the literature graphene based materials. Right panel represents the graphene samples after KOH/$ZnCl_2$/CO_2 activation, whereas the left panel represents the graphene samples synthesized by various chemical routes including the thermal/microwave reduction, exfoliation, chemical reduction & pillaring and hydrothermal aerogels, and also further heat treatment at higher temperatures, templated & CVD. The solid lines are the guide-lines to show the trend or an average values. All these data is obtained from the samples listed in **Tables S3-4**.

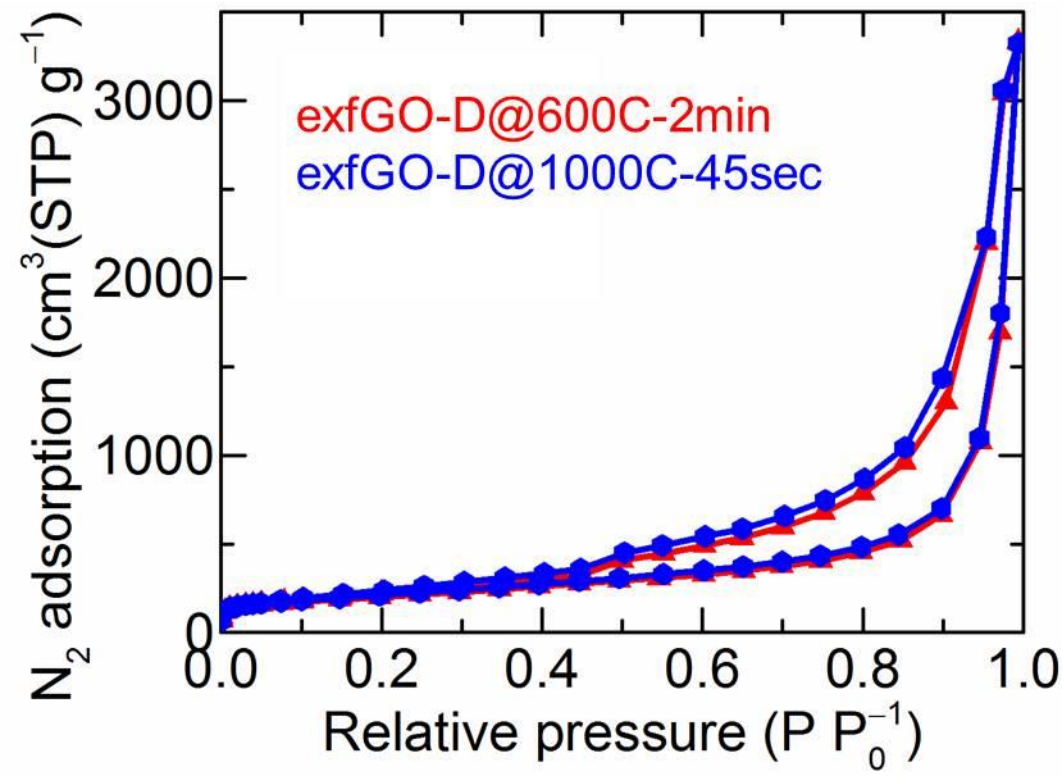

Figure S17. Porosity characteristics (N_2 isotherm at 77 K) of the exfGO-D sample, exfoliated at 600 °C and 1000 °C; shows SSA of (712 and 743) $m^2\ g^{-1}$ and total pore volume of (5.23 & 5.15) $cm^3\ g^{-1}$, respectively. Note that these porosity values are somewhat lower than the sample exfoliated at 300 °C, from the same precursor GO-D.

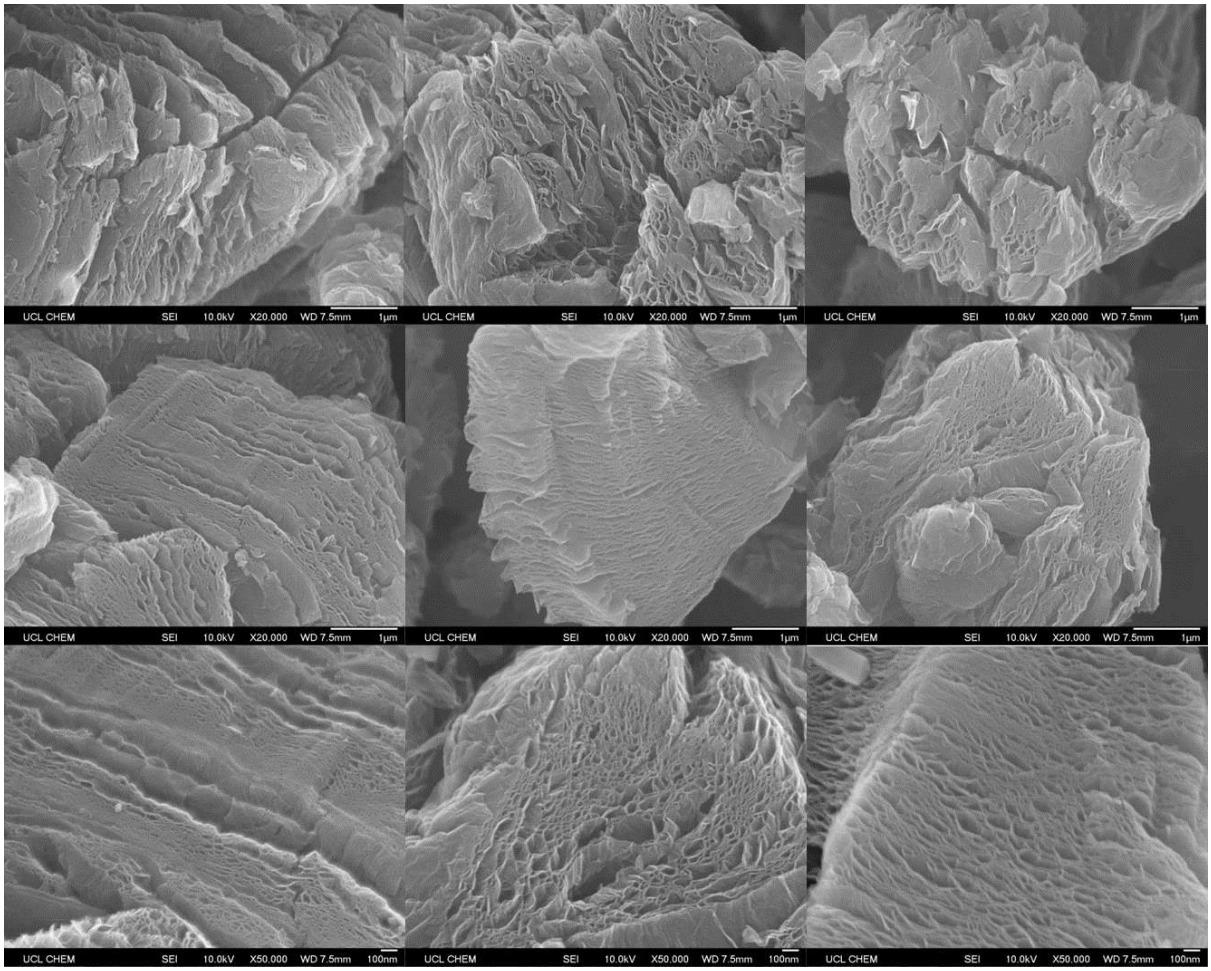

Figure S18. SEM micrographs of exfGO-A, recorded at different magnifications.

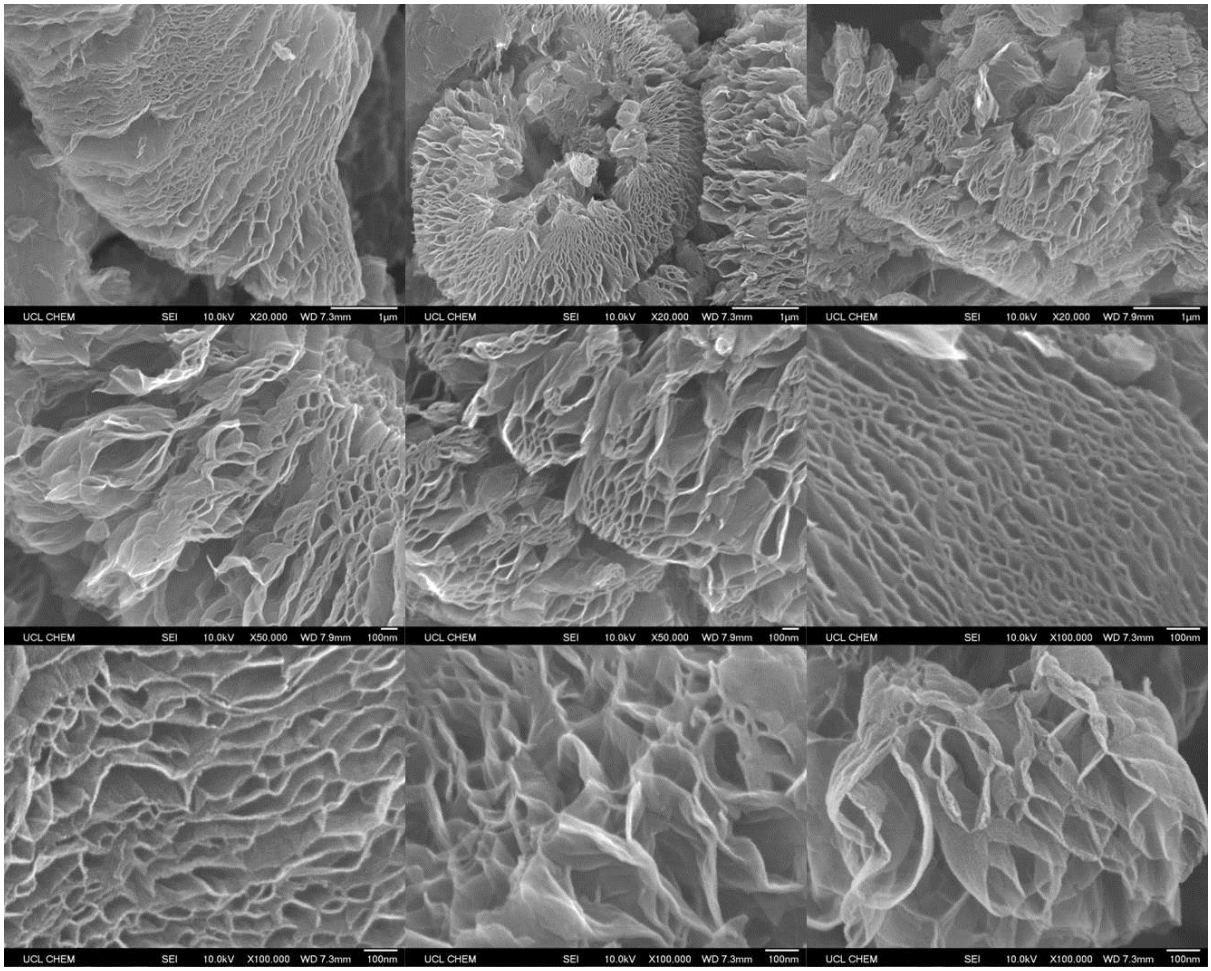

Figure S19. SEM micrographs of exfGO-D, recorded at different magnifications. Showing a high exfoliation compared to exfGO-A (**Figure S18**). Also note that the highly hierarchical pores in a networked graphene structures.

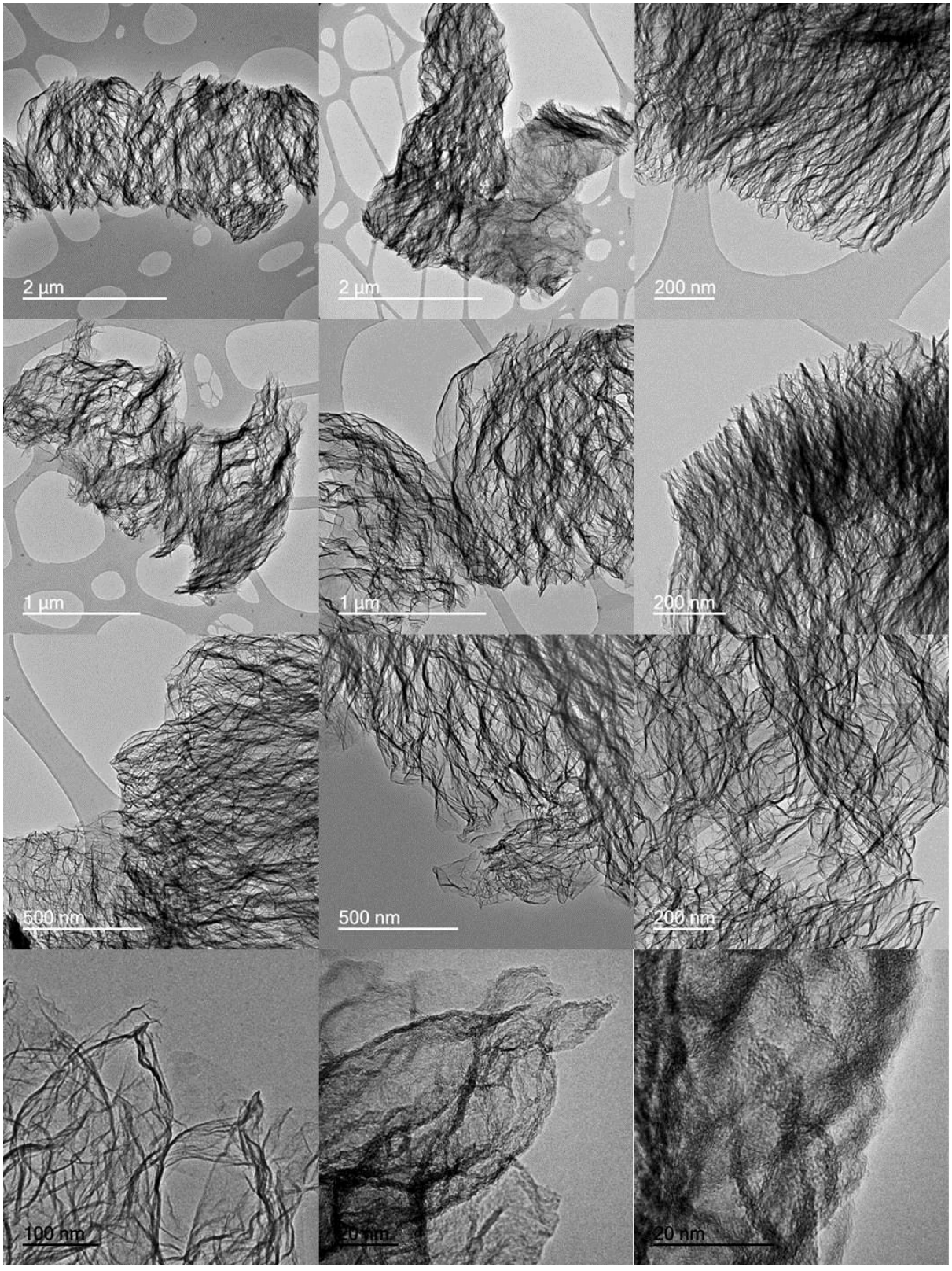

Figure S20. TEM micrographs of exfGO-D, recorded at different magnifications. Showing a high exfoliation & networked graphene structures.

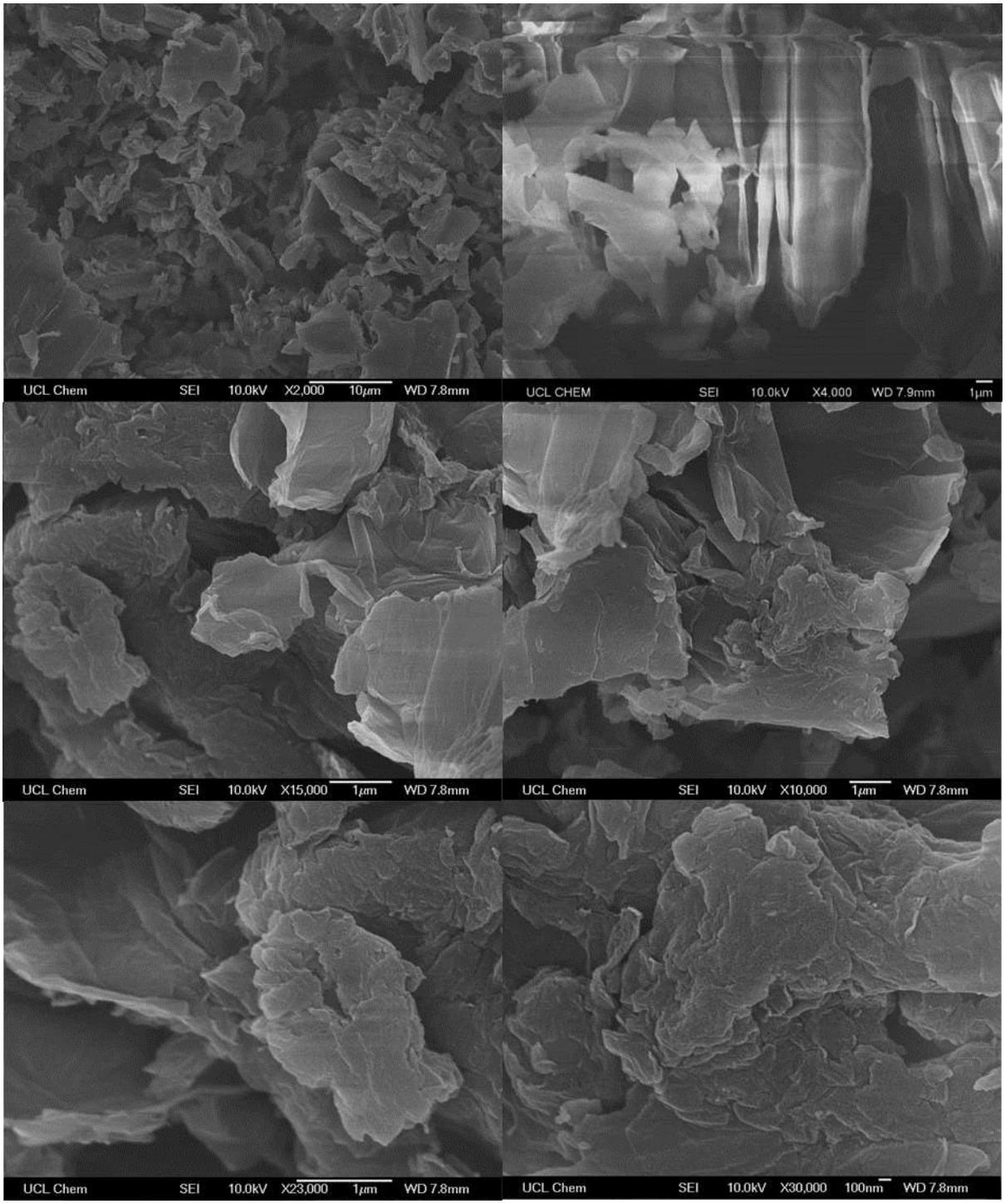

Figure S21. SEM micrographs of asGO-D, showing basically stacks of platelets, very different from their exfoliated samples (**Figure S18-19)**

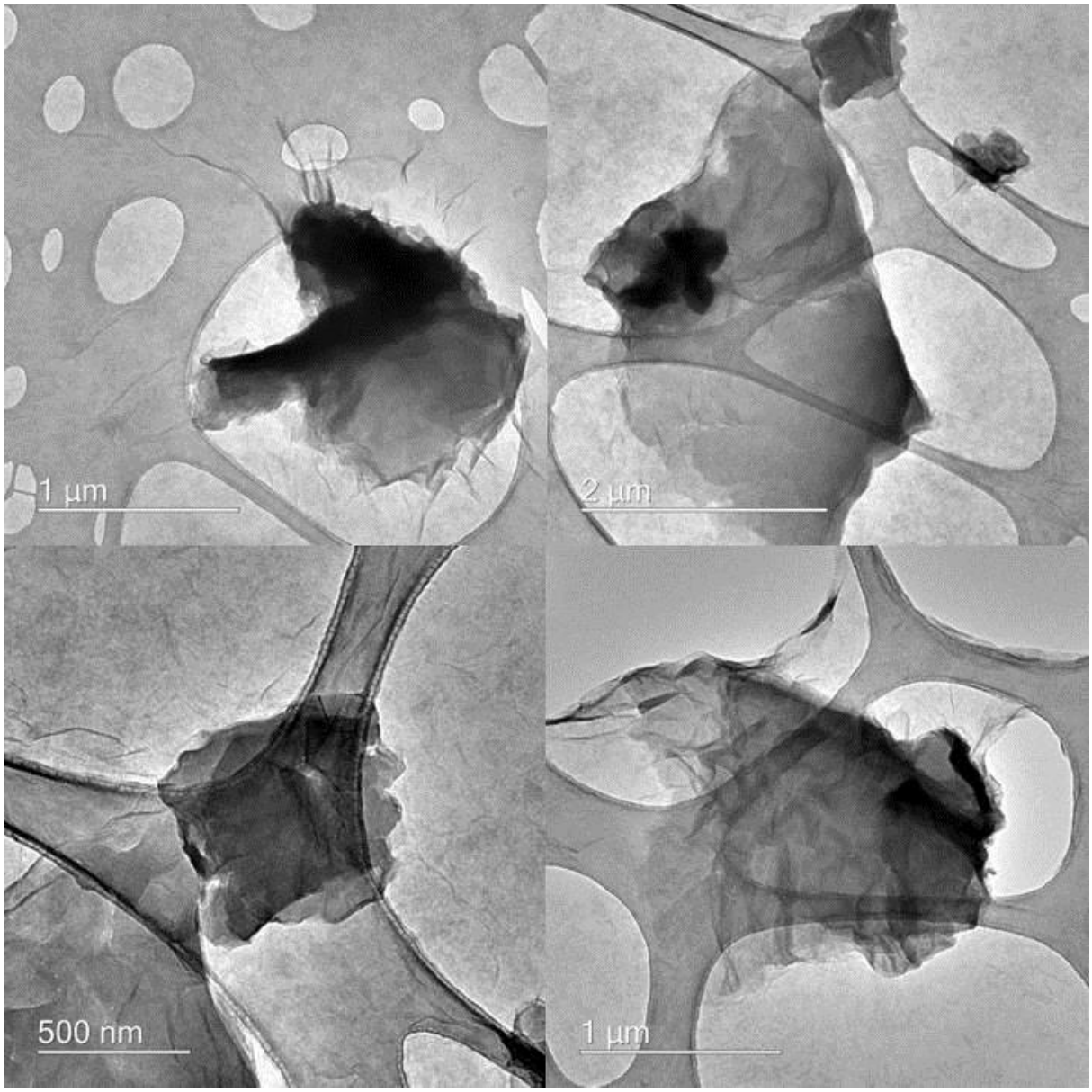

Figure S22. TEM micrographs of asGO-D solution, showing basically stacks of platelets, very different from their exfoliated samples (**Figure S20)**.

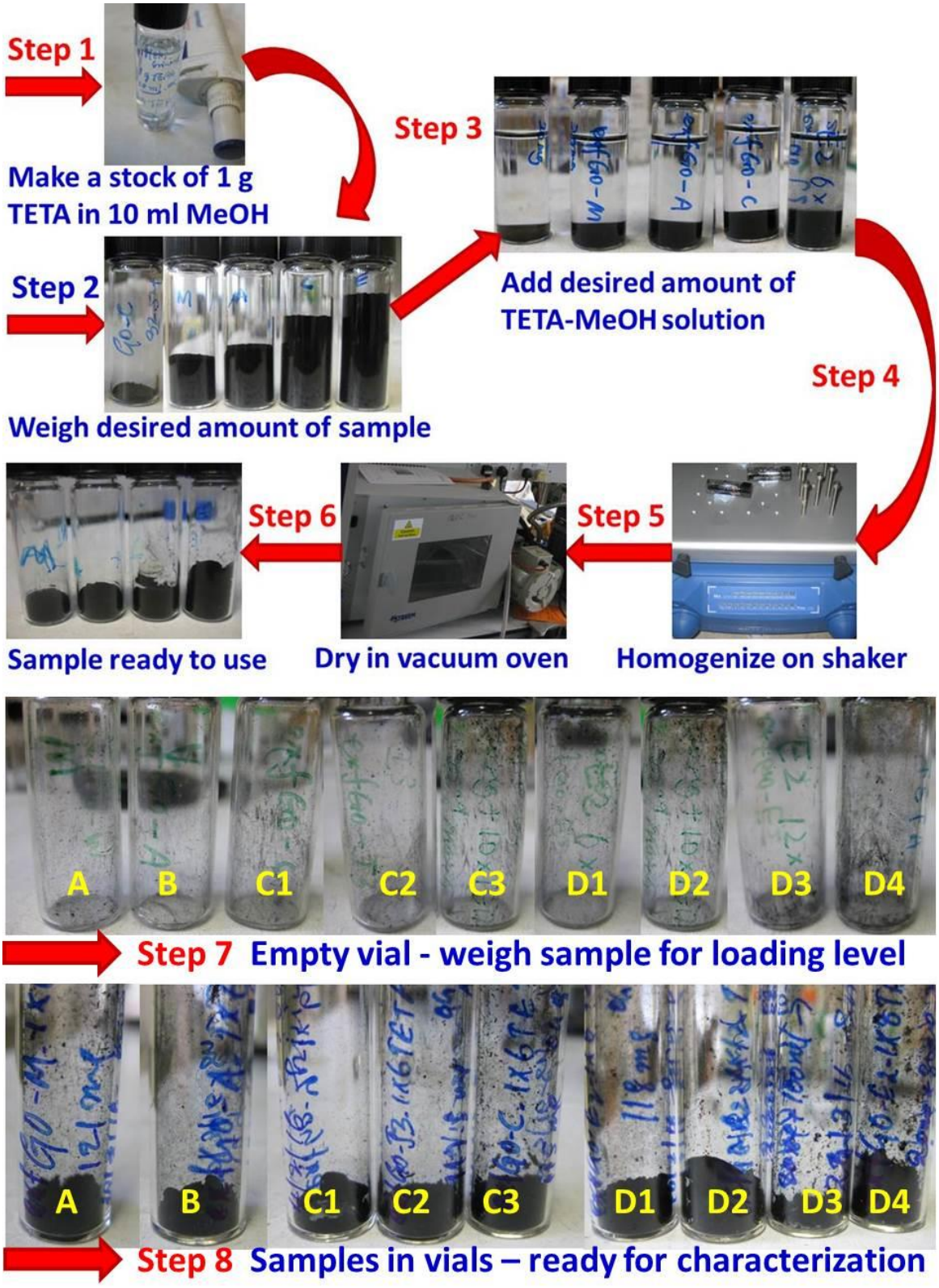

Figure S23. Step-by-step guide for synthesis of amine impregnated samples. Digital photographs of the amine impregnated asGO and exfGO samples. Different amounts of TETA loading is achieved by varying quantity of TETA-methanol to be added to the exfGO samples. We have added (4 to12) gram of TETA equivalent solution to a gram of the exfGO sample.

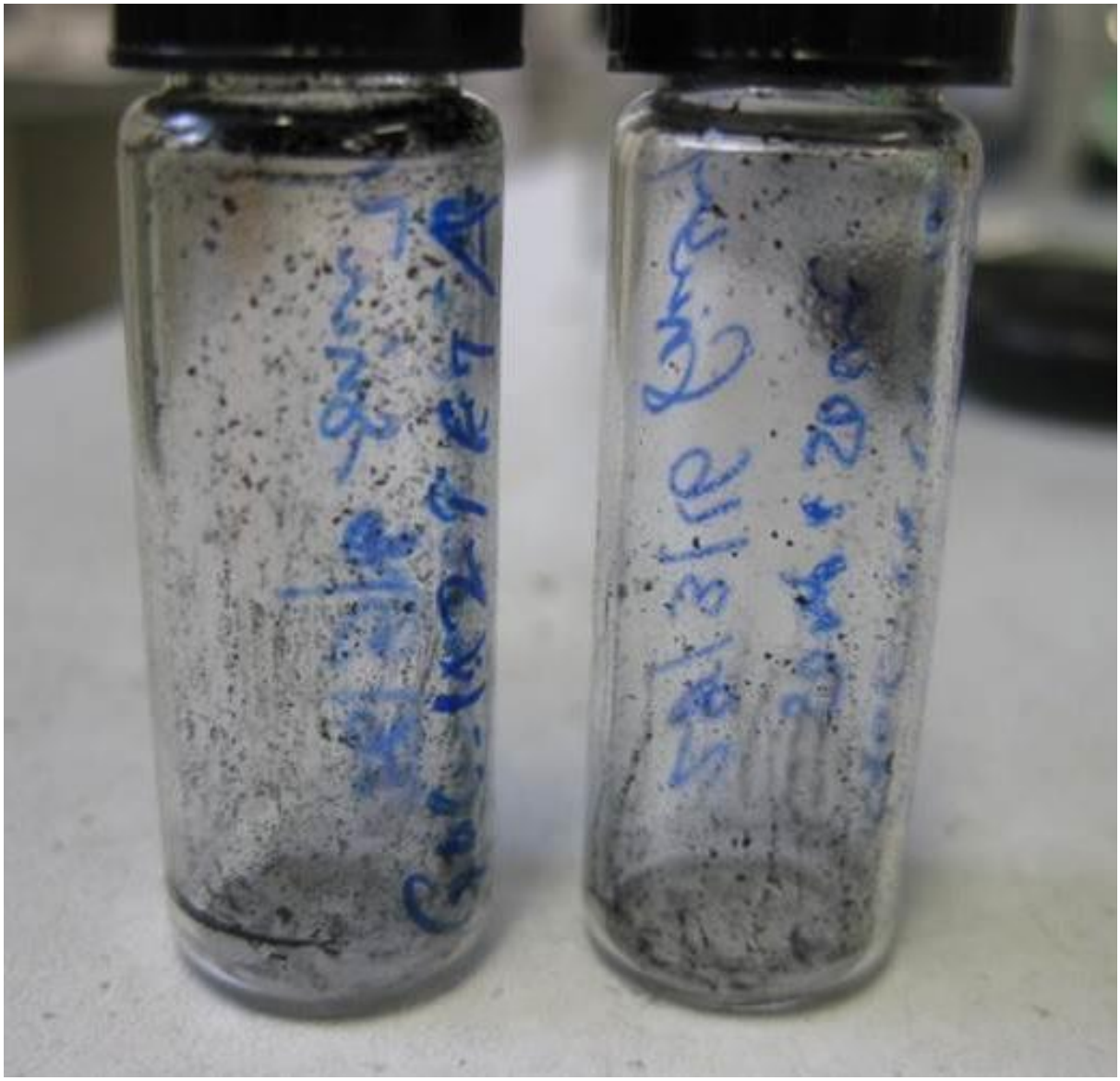

Figure S24. Digital photographs of the asGO × 1.0TETA & asGO × 2.0TETA sample vials, after emptying the sample to show surface wetting of amine.

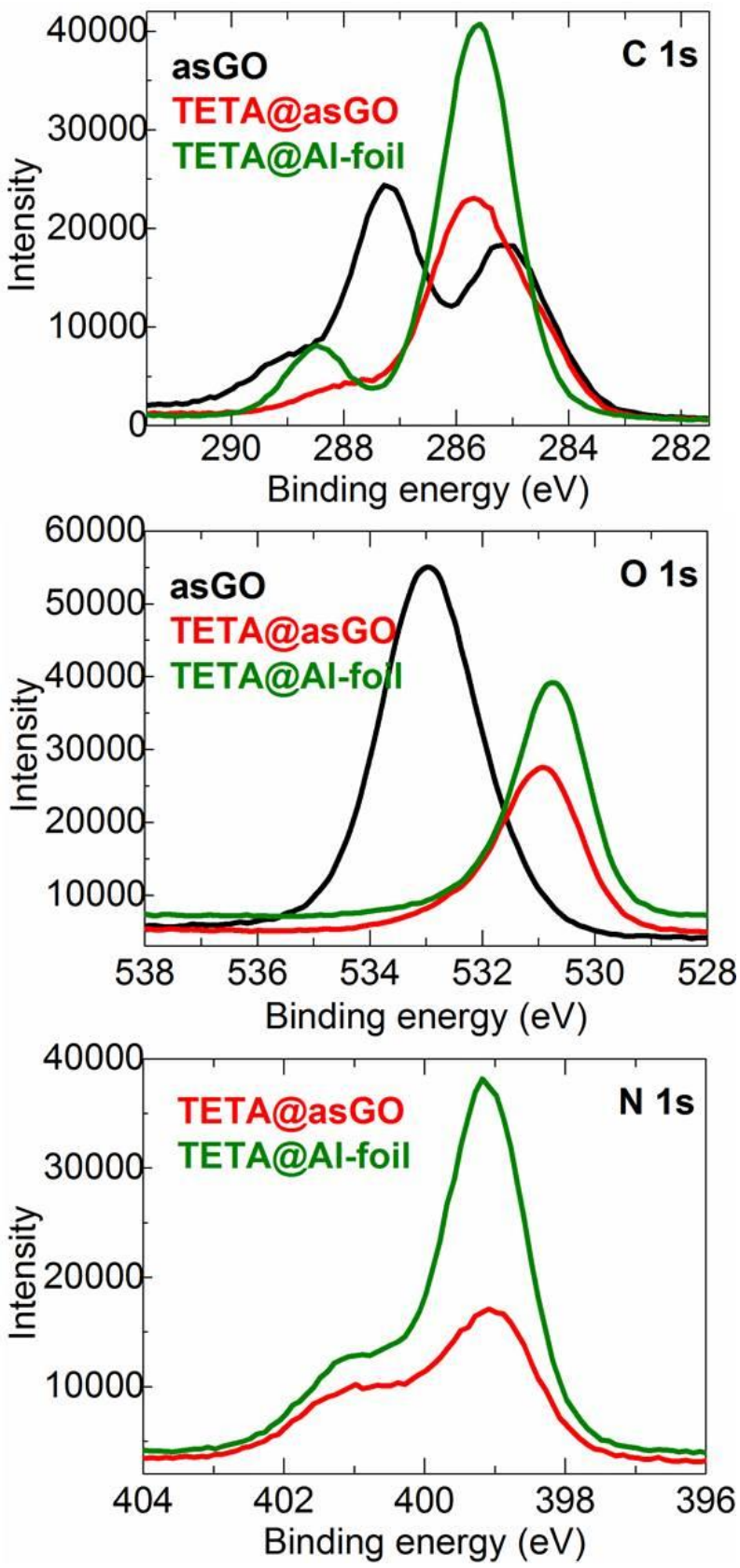

Figure S25. XPS spectra of asGO, TETA and TETA@asGO. Basically, TETA@asGO showing an identical XPS spectra of the bulk TETA. That is almost all the TETA@asGO is covered on the surface of asGO particles.

Table S6. Literature porous solid substrates (with respective SSA in $m^2\ g^{-1}$ and V_t in $cm^3\ g^{-1}$) used for solid amine impregnation (in %) and their CO_2 uptake capacities (in mmol/g) & conditions (uptake temperature, T in °C & uptake pressure or CO_2 concentration in dry & humidified mixed gas stream), the corresponding reference is also included.

S/N	Porosity of support		%Amine@solid	CO_2 uptake capacity	T	CO_2 pressure or $\%CO_2$ concentration	Ref. [Year]
	SSA	V_t					
1	272	1.08	60TEPA/Sepiolite	2.20	60	1	[134] [2015]
2	272	1.08	60TEPA/Sepiolite	3.80	60	1 & humid	
3	400	0.84	50TEPA/Silica	3.45	75	10	[135] [2015]
4	400	0.84	50TEPA/Silica	4.28	75	10 & humid	
5	927	0.9	60TEPA/Silica, MCM-41	2.45	70	15	[136] [2014]
6	-	-	50TEPA/IG-MWCNT	3.10	75	10 & humid	[137] [2014]
7	-	-	50TEPA/Silica, MCM-41	1.85	75	10 & humid	
8	316	0.77	50TEPABentonite clay	3.00	75	15	[138] [2013]
9	316	0.77	50TEPABentonite clay	4.30	75	15 & humid	
10	808	1.5	50TEPA/Silica nanotubes	3.58	75	10	[139] [2013]
11	808	1.5	50TEPA/Silica nanotubes	4.74	75	10 & humid	
12	659	2.0	70TEPA/Silica, MCF	4.57	75	10	[140] [2013]
13	198	0.88	61TEPA/Slica,TM2	4.00	75	10	[141] [2013]
14	6	0.03	55TEPA/Silica, IM15	2.45	75	10	
15	302	0.96	50TEPA/TiO_2 nanotubes	4.00	70	15	[142] [2013]
16	272	1.54	70TEPA/Silica, MSU-F	4.17	40	100	[143] [2013]
17	780	0.21	40TEPA/MOF-74	6.00	60	15	[144] [2013]
18	302	0.96	69TEPA/TiO_2 nanotubes	4.37	60	15	[145] [2013]
19	302	0.96	69TEPA/TiO_2 nanotubes	5.24	60	15 & humid	
20	500	1.2	38TEPA/Silica, Diaion™	3.90	40	15	[146] [2012]
21	300	1.15	36TEPA/Silica, Davisil	2.60	40	15	
22	263	1.24	39TEPA/Silica, Q-10	2.30	40	15	
23	663	0.43	13TEPA/Silica, Q-3	0.60	40	15	
24	900	0.97	50TEPA/Silica	3.86	75	100	[147] [2012]
25	725	0.73	83TEPA/Silica capsule	6.40	75	20	[148] [2011]
26	725	0.73	83TEPA/Silica capsule	7.93	75	10 & humid	
27	725	0.73	83PEI/Silica capsule	4.91	75	20	
28	725	0.73	83PEI/Silica capsule	5.58	75	10 & humid	
29	881	0.64	50TEPA/Silica, MSU-1	3.40	75	10	[149] [2011]
30	14	0.08	50TEPA/Silica, MSU-1	3.90	75	10	

31	-	-	50TEPA/Silica, KIT-6	2.85	60	10	[150] [2011]
32	-	-	50TEPA/Silica, KIT-6	3.20	60	10 & humid	
33	118	0.31	50TEPA/Silica, SBA-15	4.60	75	15	[151][2011]
34	118	0.31	50TEPA/Silica, SBA-15	5.00	75	15 & humid	
35	943	1.0	50TEPA/Silica, KIT-6	2.90	60	10	[152] [2010]
36	523	1.13	40TEPA/Silica monolith	3.90	75	100	[153] [2010]
37	54	0.4	50TEPA/Silica, MSFas	4.10	75	15	[154] [2010]
38	54	0.4	50TEPA/Silica, MSFas	5.30	75	15 & humid	
39	975	0.3	50TEPA/Zeolite, Y60	2.60	60	15	[155][2010]
40	975	0.3	50TEPA/Zeolite, Y60	4.30	60	15 & humid	
41	1101	0.96	50TEPA/Silica, MCM-41	0.90	25	100	[156] [2010]
42	1124	0.98	50TEPA/Silica, MCM-48	0.70	25	100	
43	712	0.68	50TEPA/Silica, SBA-15	0.70	25	100	
44	950	3.2	65TEPA/Silica monolith	5.90	75	100	[157] [2009]
45	16	0.03	50TEPA/Silica, MCM-41	4.80	75	100	[158] [2008]
46	345	0.71	70TEPA/Silica, SBA-15	3.90	75	100	[159] [2006]
47	366	0.55	50PEI/Silica	2.75	85	0.6 bar	[160] [2016]
48	1073	0.78	45PEI/Mesoporous carbon	1.97	75	1 bar	[161] [2016]
49	337	1.28	50PEI/Silica	3.14	75	1 bar	[162] [2015]
50	597	1.42	50PEI/Resin	3.63	75	1 bar	[163] [2013]
51	253	0.71	50PEI/Clay	3.22	75	1 bar	[164] [2014]
52	2070	1.43	40PEI/Porous Aromatic Framework-5	2.66	25	1 bar	[165] [2014]
53	1486	1.00	50PEI/Silica, MCM-41	2.54	75	1 bar	[166] [2003]
54	775	1.10	50PEI/Silica, SBA-15	2.05	75	1 bar	[167] [2010]
55	908	1.7	50PEI/Silica, MCF	2.30	25	1 bar	[168] [2015]
56	3355	1.89	50PEI/MOF, MIL-101(Cr)	5.00	25	1 bar	[169], [170] [2014, 2013]
57	437	1.08	60PEI/Silica	2.95	75	1 bar	[171] [2012]
58	895	1.22	50PEI/Silica, KIT-6	3.07	75	1 bar	[172] [2008]
59	1168	1.17	50PEI/Silica, MCM-48	2.70	75	1 bar	
60	753	0.94	50PEI/Silica, SBA-15	2.90	75	1 bar	
61	1042	0.85	50PEI/Silica, MCM-41	2.52	75	1 bar	
62	736	0.75	50PEI/Silica, SBA-16	2.93	75	1 bar	
63	-	-	50PEI/Silica, SBA-15	4.20	75	1 bar	[173] [2012]
64	125	0.70	50PEI/Silica, precipitated	3.93	70	1 bar	[174] [2010]
65	125	0.70	50PEHA/Silica, Precipitated	4.36	70	1 bar	
66	125	0.70	50TEPA/Silica, Precipitated	4.54	70	1 bar	
67	699	1.41	65PEI+5surfactant/Silica,	4.66	75	1 bar	[175] [2012]

68	757	3.61	65PEI+5surfactant/MCA, mesoporous carbon aerogel	4.77	75	1 bar	
69	532	1.82	50PEI/Silica, Mesocellular foam	3.45	75	15%CO_2	[176] [2011]
70	532	1.82	60PEI/Silica, Mesocellular foam	4.50	70	1 bar	[177] [2012]
71	246	2.36	50PEI/Silica, monolith	3.80	80	1 bar	[178] [2012]
72	1254	2.44	55PEI/Silica,MCM-41	4.61	75	1 bar	[179] [2011]
73	580	0.95	55 PEI/Silica, SBA-15	3.93	75	1 bar	[180] [2011]
74	Highest reported for COFs among 69 samples, summarized			5.53	0	1 bar	[181] [2016]
75	Highest reported for MOFs among best 20 summarized			5.25	40	0.15 bar	[182], [183] [2016, 2015]
76	Highest reported for MOFs among best 20 summarized			7.60	40	1.0 bar	
78	628	0.28	EDA grafted Y Zeolite	1.60	40	1 bar	[184] [2016]
79	628	0.28	EDA grafted Y Zeolite	1.90	130	15% & humidified	
80	3270	1.38	Diamine appended MOFs	3.60	75	15% & humidified	[185], [186], [187], [188] [2015, 2015, 2015, 2012]
81	3270	1.38	Diamine appended MOFs	2.50	75	390 ppm & humidified	
82	1286 L	0.54	Monodentate hydroxide	4.00	25	0.15 bar	[189] [2015]
83	1286 L	0.54	Monodentate hydroxide	7.10	25	1 bar	
84	1286 L	0.54	Monodentate hydroxide	3.00	40	15% & humidified	
85	498	2.69	PEI/Silica	4.30	60	8% & humidified	[190] [2014]
86	498	2.69	PEI/Silica	11.80	25	8% & humidified	
87	570	0.97	45TEPA/PMMA	3.96	50	10%	[191] [2016]
88	550	0.77	40TEPA/Mesoporous graphitic carbon	1.30	75	1 bar	[192] [2015]
89	582	0.85	64TEPA/Silica, KCC-1	3.52	50	15%	[193] [2016]
90	194	0.57	66PEI/Graphene (hydroxylated)	4.13	25	1 bar	[194] [2015]
91	999	3.10	55PEI(+surfactant)/Mesoporous Carbon	3.60	75	5000 ppm	[195] [2015]
92	999	3.10	55PEI(+surfactant)/Mesoporous Carbon	5.50	75	1 bar	

93	476	1.60	75PEI/Graphene-oxide	2.50	0	1 bar	[85] [2013]
94	930	0.71	PEI/ Silica sheets	4.32	75	1 bar	[196] [2013]
95	671	1.26	55PEI/PMMA	4.20	75	1 bar	[197] [2014]
96	671	1.26	55PEI/PMMA	4.90	25	1 bar	
97	329	0.91	50PEI/Silica, fumed	2.44	25	From air (400 ppm)	[198] [2014]
98	329	0.91	50PEI/Silica, fumed	1.70	25	From dry air (400 ppm)	[199] [2011]
99	1486	2.69	65PEI/Carbon black	3.50	75	1 bar	[200] [2012]
100	1352	1.40	PVA/Mesoporous Carbon, CMK-3	3.52	30	1 bar	[201] [2011]
101	452	0.95	70PEHA/Silica, SBA-15	4.58	80	1 bar	[202] [2013]
102	757	3.61	65PEI/Mesoporous Carbon	4.82	75	15%	[203] [2013]
103	882	0.95	60PEHA/Silica, MCM-41	3.75	75	1 bar	[204] [2015]
104	-	-	43PEI/Graphene-oxide	1.80	25	1 bar	[205] [2015]
105	703	0.34	DETA/PPN-125 (Porous polymer networks)	1.18	40	15%	[206] [2015]
106	688	4.17	75PEI/Silica, MCF	6.00	85	95%	[128] [2014]
107	194	0.45	PEI/Alumina	0.75	30	400 ppm, dry (air capture)	[207] [2016]
108	38	0.17	PEI/Alumina	1.71	30	400 ppm, 50% RH (simulated air capture)	[208] [2014]
109	-	-	30DAB/GO	2.00	25	0.35	[209] [2014]
110	2700	5.35	79.6TEPA/MC	5.64	75	0.15 bar	[210] [2015]
111	2700	5.35	66.7TEPA/MC	3.37	75	0.15 bar	
112	2700	5.35	85.7TEPA/MC	4.61	75	0.15 bar	
113	2700	5.35	83.3TEPA/MC	5.24	75	0.15 bar	
114	2700	5.35	78.3TEPA/MC	4.80	75	0.15 bar	
115	2700	5.35	76.7TEPA/MC	4.65	75	0.15 bar	
116	2700	5.35	77.3TEPA/MC	4.76	75	0.15 bar	
117	2700	5.35	76.2TEPA/MC	4.20	75	0.15 bar	
118	2445	1.95	64.0TEPA/AC	2.45	75	0.15 bar	

119	2445	1.95	69.3TEPA/AC	3.17	75	0.15 bar	
120	2445	1.95	81.5TEPA/AC	2.40	75	0.15 bar	
121	2445	1.95	76.7TEPA/AC	3.16	75	0.15 bar	
122	2445	1.95	83.0TEPA/MC	5.20	75	15% & Humid	
123	2445	1.95	85.7TEPA/MC	4.60	75	15% & Humid	
124	2445	1.95	81.5TEPA/AC	2.85	75	15% & Humid	
125	299	1.70	PEI/Silica	3.80	40	15% & 3% H_2O	[211] [2016]
126	299	1.70	EB-PEI/Silica	3.00	40	,,	
127	299	1.70	EB-PEI/Silica	2.2	40	‘’	
128	428	1.18	50PEI/Silica, SBA-15	3.14	45	1 bar	[212] [2013]
129	428	1.18	50TEPA/Silica, SBA-15	3.73	,,	,,	
130	428	1.18	50AP-TEPA/Silica, SBA-15	4.89	,,	,,	
131	428	1.18	50AP-TEPA/Silica, SBA-15	5.32	75	,,	
132	428	1.18	50AP-TEPA/Silica, SBA-15	5.34	45	0.15% & humid	
133	303	0.96	69TEPA/TiO_2 nanotubes	4.10	30	1 bar	[213] [2013]
134	303	0.96	49TETA/TiO_2 nanotubes	2.70	30	1 bar	
135	261	3.57	50PEI/Silica	115	75	1 bar	[214] [2015]
136	504	5.45	50PEI/Silica	151.2	75	,,	
137	504	5.45	60PEI/Silica	188.3	75	,,	
138	594	0.82	50PEI/Silica	92.9	75	,,	
139	761	0.96	50PEI/Silica	111.4	75	,,	
140	997	0.90	50TETA/Silica-gel, MCM-41	4.27	55	0.15 bar	[215] [2015]
141	997	0.90	30TEPA+30AMP/Silica, MCM-41	3.01	70	15%	[216] [2015]

142	1088	0.83	50PEI/Silica, MCM-41	96.9	45	1 bar	[217] [2015]
143	1088	0.83	50PEHA/Silica, MCM-41	88.2	45	,,	
144	1088	0.83	50TEPA/Silica, MCM-41	88.3	45	,,	
145			40TEPA/Silica, MCM-41	1.96	30	10%	[218] [2015]
146			40PEHA/Silica, MCM-41	2.34	30	,,	
147	1336	0.68	75TETA/AC, mesoporous	1.85	70	0.1 bar	[219] [2015]
148	817	1.1	75TETA/AC, mesoporous	1.30	70	0.1 bar	
149	373	0.13	40DETA/ZSM-5	55	65	1 bar	[220] [2014]
150	373	0.13	40TETA/ZSM-5	60	65	1 bar	
151	920	0.48	40DETA/Silica, SBA-15	88	65	1 bar	
152	920	0.48	40TETA/Silica, SBA-15	210	65	1 bar	
153	744	1.14	31TETA/Polymer	1.49	25	1 bar	[221] [2015]
154	744	1.14	31TEPA/Polymer	1.44	25	1 bar	
155	584	0.73	50TETA/Silica, Zr-SBA	3.50	50	5%	[222] [2015]
156	120	0.47	50TETA/Silica, Zr-SBA	4.27	50	5%	
157	120	0.47	70TETA/Silica, Zr-SBA	3.45	50	5%	
158	120	0.47	90TETA/Silica, Zr-SBA	3.30	50	5%	
159	930	0.50	50DETA/TiO_2 (C6-Ti)	2.08	75	10%	[223] [2013]
160	930	0.50	50TETA/TiO_2 (C6-Ti)	1.80	75	10%	
161	930	0.50	50TEPA/TiO_2 (C6-Ti)	1.38	75	10%	
162	1037	0.62	50DETA/TiO_2 (C8-Ti)	2.67	75	10%	
163	1037	0.62	50TETA/TiO_2 (C8-Ti)	2.24	75	10%	
164	1037	0.62	50TEPA/TiO_2 (C8-Ti)	1.75	75	10%	
165	722	0.44	50DETA/TiO_2 (C12-Ti)	1.54	75	10%	
166	722	0.44	50TETA/TiO_2 (C12-Ti)	1.47	75	10%	

167	722	0.44	50TEPA/TiO_2 (C12-Ti)	1.34	75	10%	
168	448	0.31	50DETA/TiO_2 (C18-Ti)	1.90	75	10%	
169	448	0.31	50TETA/TiO_2 (C18-Ti)	1.85	75	10%	
170	448	0.31	50TEPA/TiO_2 (C18-Ti)	1.56	75	10%	
171	670	0.60	50TETA/Silica, MCM-41	2.22	60	15%	[224] [2010]
172	670	0.60	50DETA/Silica, MCM-41	1.87	60	15%	
173	4023		Polyamine-Tethered Porous Polymer Networks (PPN)	3.0	22	0.15 bar	[225] [2012]

PV1A=Polyvinylamine; DETA=Diethylenetriamine; TEPA=Tetraethylenepentamine; PEHA=Pentaethylenehexamine; PEI=Polyethyleneamine; DAB=Amine-terminated diaminobutane; EB=1,2-epoxybutane; L=Langmuir.

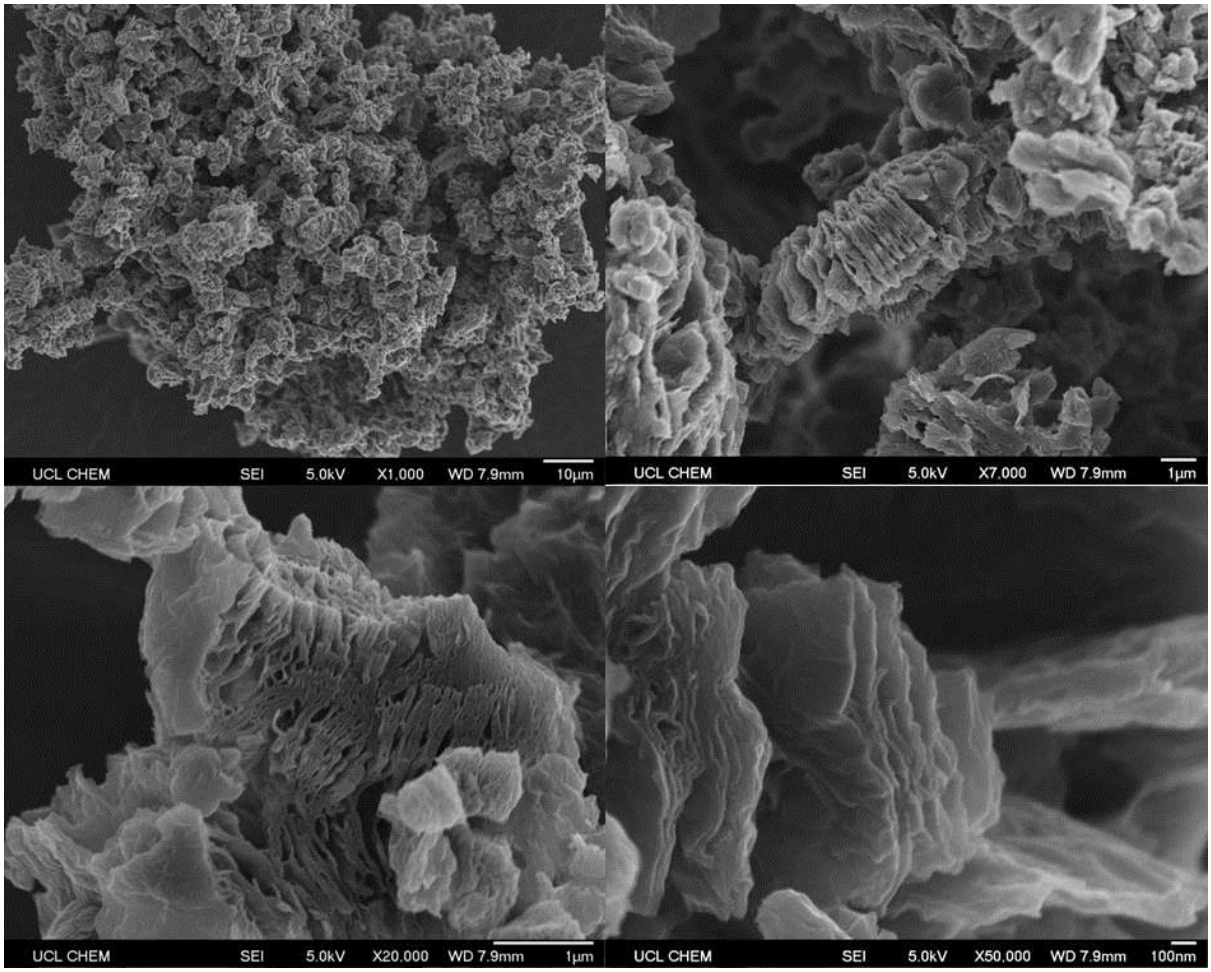

Figure S26. SEM micrographs of exfGO-D × 7.0 TETA (loading of ~7.0 mg per mg), showing a clear morphology change from its host exfGO-D (**Figure S19**). Still the macropores are not completely filled. This sample is able to accept up to 10 mg TETA per mg of exfGO sample within its exfoliated graphene networks.

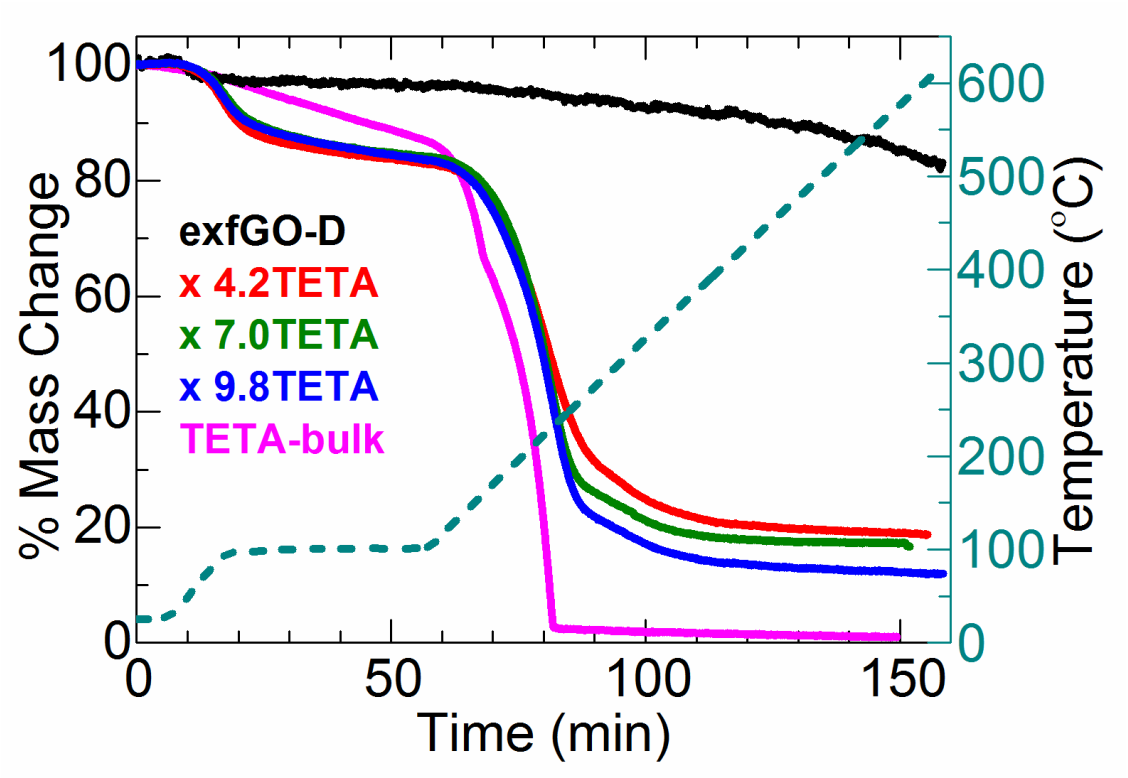

Figure S27. Thermogravimetric plots of TETA@exfGO samples. Starting exfGO substrate material and bulk TETA sample, also measured for the comparison.

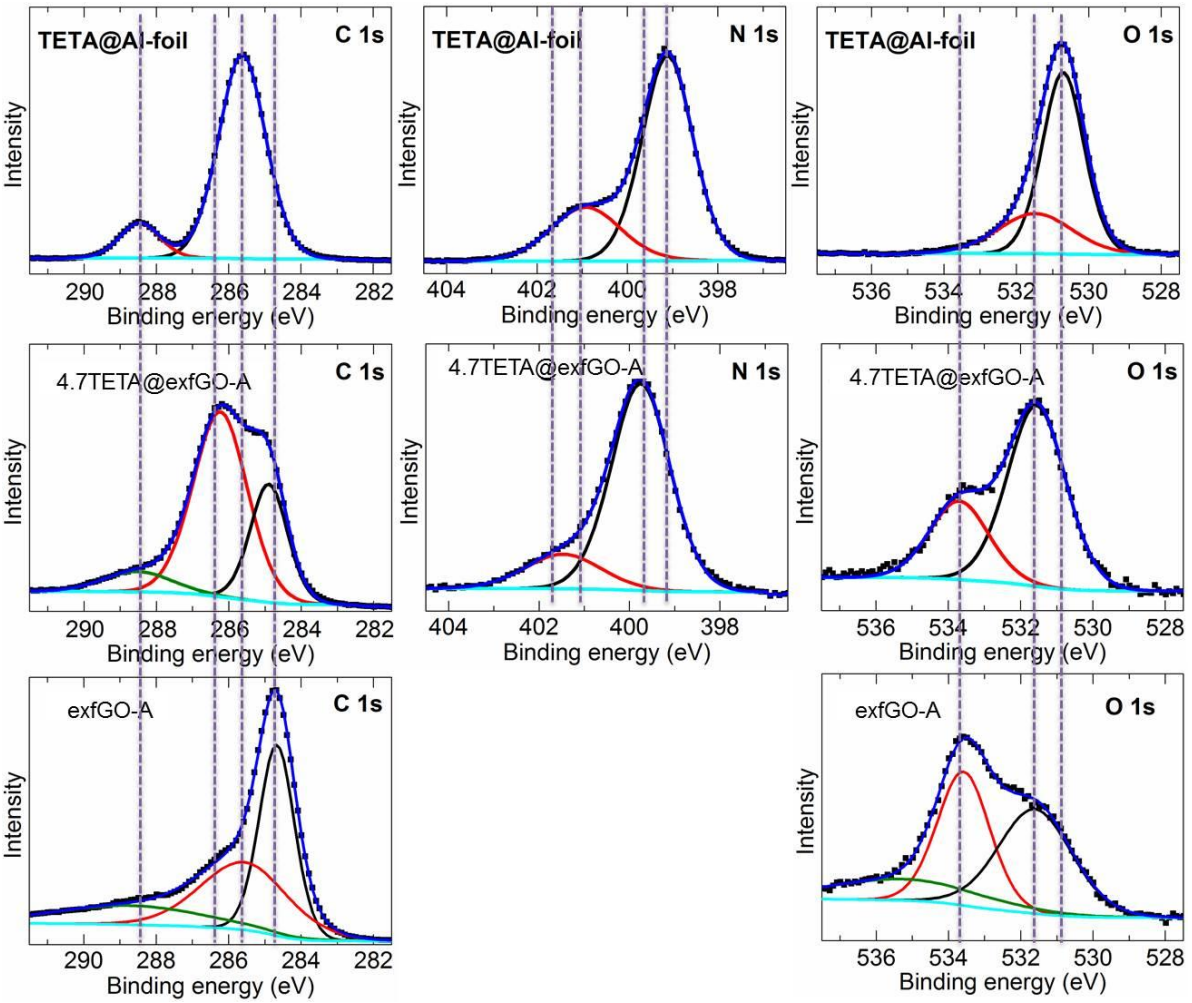

Figure S28. Comparative XPS spectra of TETA, TETA@exfGO and exfGO. Vertical guide lines show the respective peak shifts in the TETA@exfGO sample with respect to the exfGO and TETA-bulk.

C 1s, N 1s and O 1s peak deconvolution results

TEPA@Al-foil

C 1s 87.2% (at 285.6 eV, C=C) & 12.8% (at 288.46 eV, C-N)

N 1s 73.4% (at 399.12 eV, C-N) & 26.6% (at 400.92 eV, -NH_2)

O 1s 71.8% (at 530.71 eV, =O) & 28.2% (at 531.5 eV, NHC=O)

4.7 TEPA@exfGO-A

C 1s 28.0% (at 284.9 eV, C=C), 63.4% (at 286.24 eV, C-N/C-O) & 8.7% (at 288.5 eV, C=O)

N 1s 82.4% (at 399.75 eV, NH_2) & 17.6% (at 401.47 eV, protonated amine, --NH2/NH_3^+)

O 1s 69.5% (at 531.55 eV, C=O) & 30.5% (at 533.69 eV, C-OH)

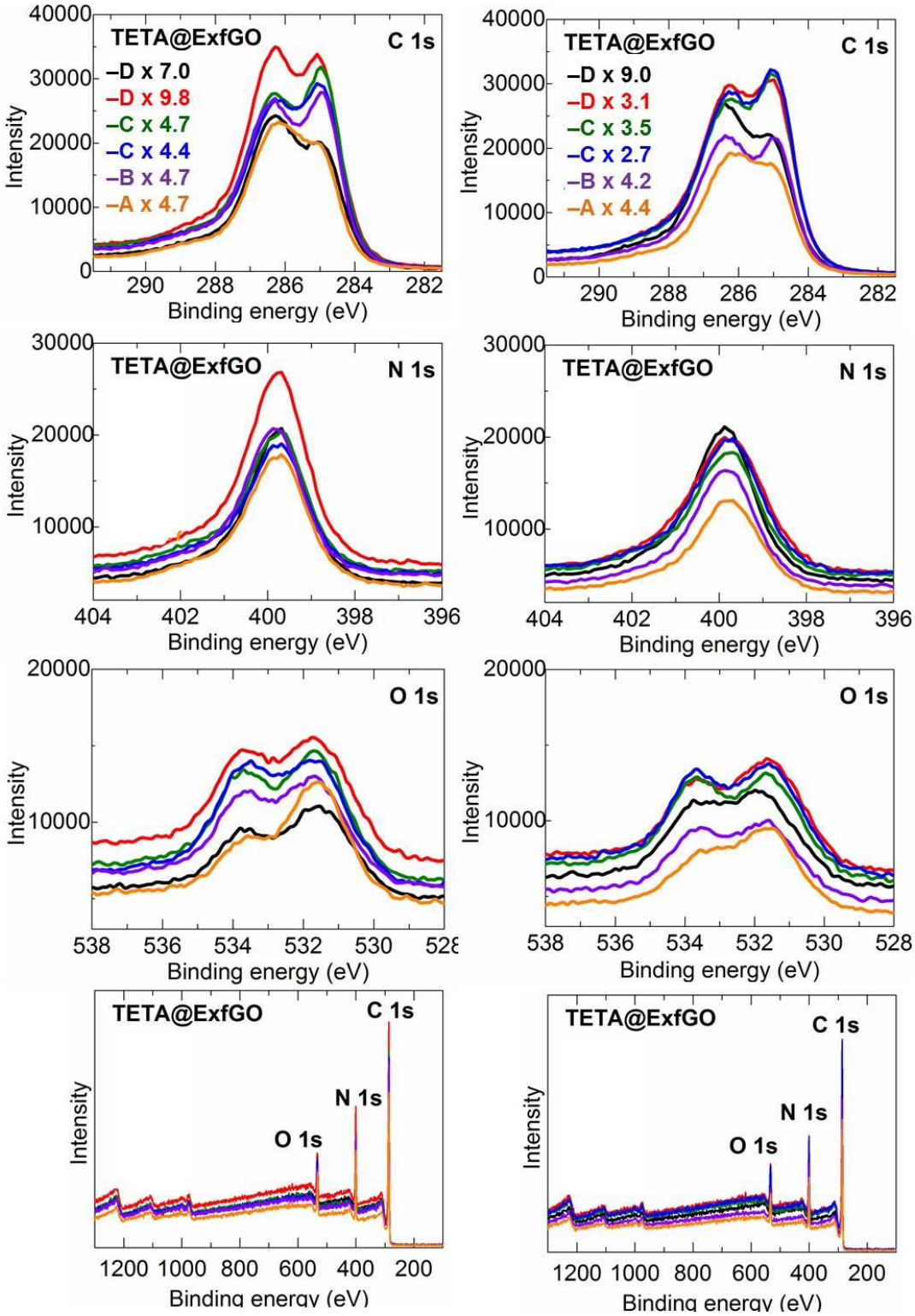

Figure S29. XPS C 1s, N 1s, O 1s and Survey spectra of the TETA@exfGO samples of different TETA loading, represented with multiplication number. See that a shift of the C 1s peak of the exfGO to 285.0 eV and a new peak at 286.5 eV for N–C bonds from the TETA (see **Fig. S28**). Change of the O 1s peak for TETA interaction with C–O/C=O of the host exfGO. These new peaks are become more prominent with increased amine loading in the structures, which is also true for less porous exfGO-A compared with highly porous exfGO-D, at a same amine loading. Left & right panels represent samples of different levels of TETA loading.

Table S7. XPS elemental analysis of TETA, TETA impregnated exfGO samples, the spectra was recorded at two different spots on each sample. The atomic percentage for C, N and O were estimated from the C 1s, N 1s and O 1s peaks in the Survey spectra.

S/N	Sample	C (at%)	N (at%)	O (at%)
1	TETA@Al foil	58.0	26.4	15.6
		59.6	26.5	14.0
2	TETA@Carbon tape	61.6	24.0	14.5
		61.9	23.4	14.6
3	asGO x1.0 TETA	61.1	21.7	17.2
		60.4	21.0	18.6
4	exfGO-A x 4.7 TETA	74.5	17.5	8.0
		74.7	16.9	8.6
5	exfGO-B x 4.7 TETA	77.3	14.5	8.2
		78.2	14.1	7.7
6	exfGO-C x 4.4 TETA	77.4	11.15	11.5
		76.6	14.0	7.7
7	exfGO-Cb2 x 4.7 TETA	77.8	14.0	8.2
		78.1	13.5	8.3
8	exfGO-D x 7.0 TETA	77.1	16.1	6.8
		76.8	16.0	7.2
9	exfGO-D x 9.8 TETA	75.0	17.0	8.0
		74.8	16.0	9.2
10	exfGO-A x 4.2 TETA	76.0	15.6	8.4
		77.0	16.5	6.5
11	exfGO-B x 4.4 TETA	77.6	15.4	7.0
		77.7	15.5	6.8
12	exfGO-C x 3.5 TETA	78.3	14.0	8.2
		78.4	13.7	7.8
13	exfGO-D x 5.7 TETA	77.6	14.4	8.0
		78.5	14.5	7.0

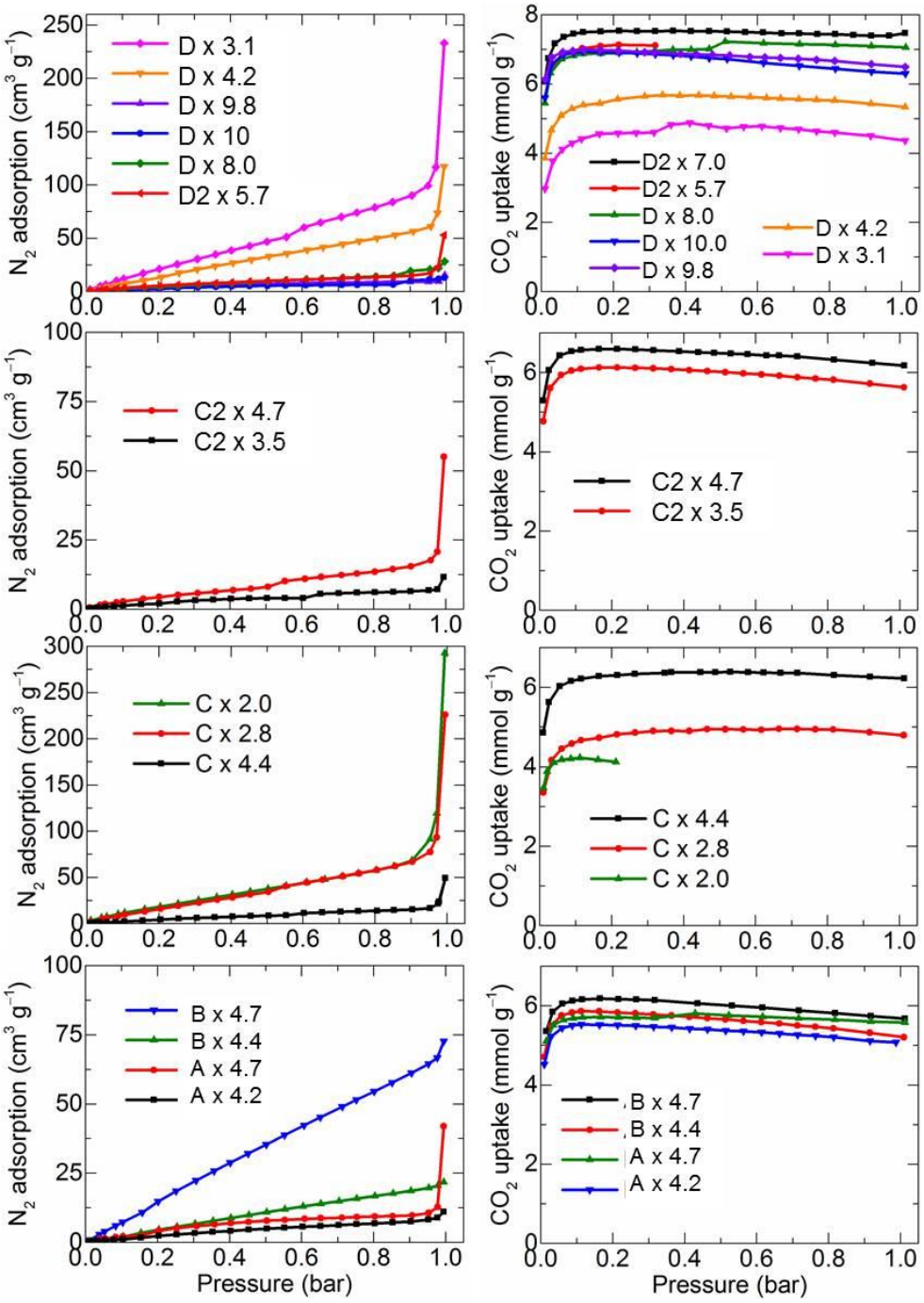

Figure S30. Porosity and volumetric CO_2 (100 % dry) uptake capacity of the TETA@exfGO samples. Left panel: 77 K N_2 uptake isotherms of the samples at different TETA loadings. Right panel: 75 °C CO_2 uptake isotherms of the samples at different TETA loadings. See that the increased amine loading leads to the greatly reduced pore volume in the exfGO samples. The CO_2 uptake is considerably enhanced with the high pore volume host substrate exfGO-D, which also hold high amount of TETA.

Note that the maximum CO_2 capture capacities are directly governed by sample porosity to facilitate high amine loading, though of course excessive amine loading, much higher than the pore volume equivalent, does not show favourable CO_2 capture properties. This is due to the complete pore filling or increased bulk amine in the large or macro-pores, and thus reduces the amine efficiency for CO_2 capture due to the smeared out active surface area for adsorption and diffusion of CO_2, inhibiting the mass transport.

Table S8. Porosity & volumetric CO_2 (100%, dry) isotherm uptake at 0.15 bar of TETA impregnated exfGO samples, measured at different temperatures, (75, 65 and 30) °C.

S/N	Sample	Total pore volume ($cm^3\ g^{-1}$)	CO_2 uptake at 0.15 bar (mmol g^{-1})	Uptake temperature (°C)
1	exfGO-A x 4.7 TETA	0.034	5.72	75
2	exfGO-A x 4.2 TETA-r2	0.112	5.53	75
3	exfGO-B x 4.7 TETA	0.017	6.18	75
4	exfGO-B x 4.4 TETA-r2	0.065	5.86	75
5	exfGO-C x 4.7 TETA	0.018	6.69	75
6	exfGO-Cb2 x 4.4 TETA	0.076	6.26	75
7	exfGO-C x 3.5 TETA-r3	0.085	6.12	75
8	exfGO-Cb2 x 2.7 TETA-r3	0.350	4.71	75
9	exfGO-Cb2 x 2.0 TETA	0.453	4.23	75
10	exfGO-D x 10.0 TETA	0.020	6.93	75
11	exfGO-D x 9.8 TETA	-	6.98	75
12	exfGO-D x 8.0 TETA	0.044	6.88	75
13	exfGO-D2 x7.0 TETA	0.024	7.52	75
14	exfGO-D2 x5.7 TETA-r4	0.082	7.13	75
15	exfGO-D x 10.0 TETA-r2	-	4.60	65
16	exfGO-D x 8.0 TETA-r2	-	5.60	65
17	exfGO-D x 4.2 TETA	0.181	5.43	75
18	exfGO-D x 3.1 TETA	0.361	4.53	75
19	exfGO-B x 4.0 TETA-r3	-	1.80	30
20	exfGO-B x 4.0 TETA-r3	-	2.06	30
21	exfGO-C x 3.3 TETA-r4	-	2.61	30
22	exfGO-Cb2 x 2.6 TETA-r3	-	1.40	30
23	exfGO-D x 8.5 TETA-r3	-	2.92	30
24	exfGO-D x 3.0 TETA-r4	-	1.19	30

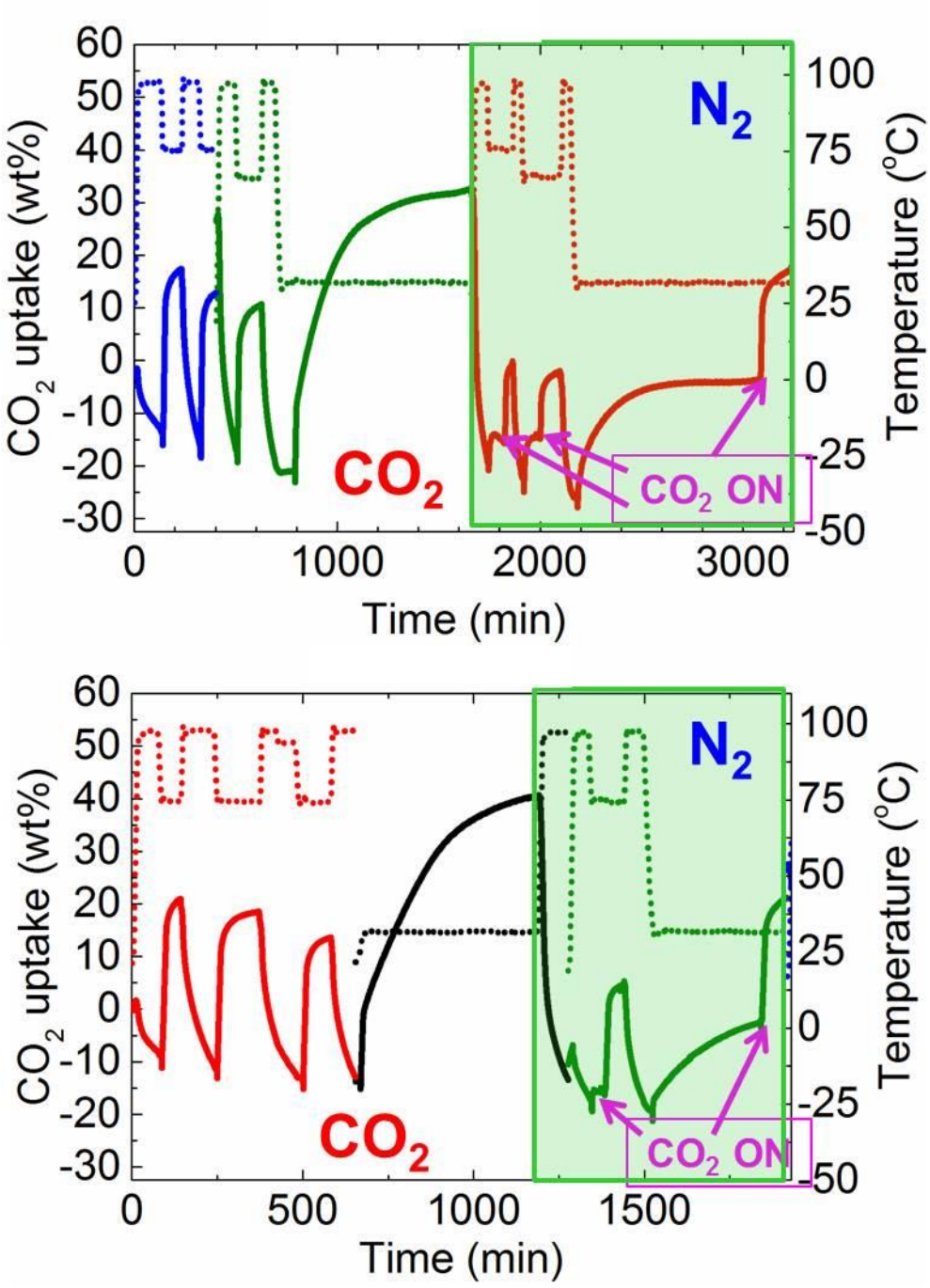

Figure S31. Gravimetric temperature swing flue-gas uptakes of exfGO-A x 4.7TETA (top) and exfGO-B x 4.7TETA (bottom) samples, measured at different temperatures on continuous cycles. The temperature is indicated on the right Y-axis and dotted line data. Note that the flue-gas uptakes were carried out with 15% CO_2 + 85% N_2 gas bubbled through water at a flow rate of 100 ml min^{-1}, and all the desorption runs were performed under flowing dry N_2 at 100 °C for 50 min. The highlighted area tests are for controlled experiment with a humidified N_2 to show the uptake difference between flue-gas CO_2 and humidified N_2. Arrow marks indicate the switching off the N_2 gas flow to CO_2 gas flow at the same temperature. This also shows a rapid uptake of the CO_2 after humidification with N_2 at 30 °C, compared to the direct flue-gas (see 30 °C uptake data)-left side of the highlighted box.

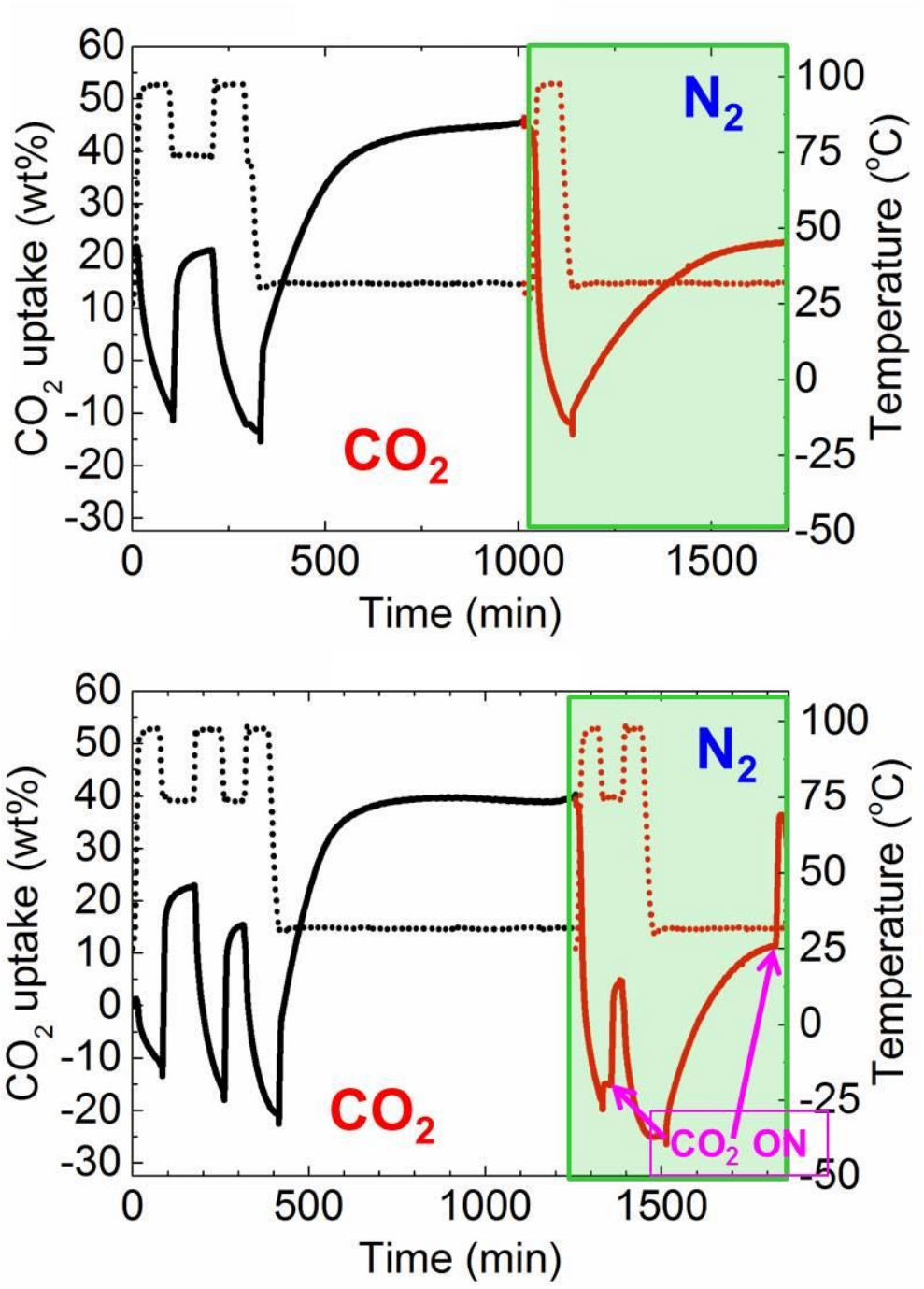

Figure S32. Gravimetric temperature swing flue-gas uptakes of exfGO-C x 4.4TETA (top) and exfGO-Cb2 x 4.7TETA (bottom) samples, measured at different temperatures on continuous cycles. The temperature is indicated on the right Y-axis and dotted line data. Note that the flue-gas uptakes were carried out with 15% CO_2 + 85% N_2 gas bubbled through water at a flow rate of 100 ml min^{-1}, and all the desorption runs were performed under flowing dry N_2 at 100 °C for 50 min. The highlighted area tests are for controlled experiment with a humidified N_2 to show the uptake difference between flue-gas CO_2 and humidified N_2. Arrow marks indicate the switching off the N_2 gas flow to CO_2 gas flow at the same temperature. This also shows a rapid uptake of the CO_2 after humidification with N_2 at 30 °C, compared to the direct flue-gas (see 30 °C uptake data)-left side of the highlighted box.

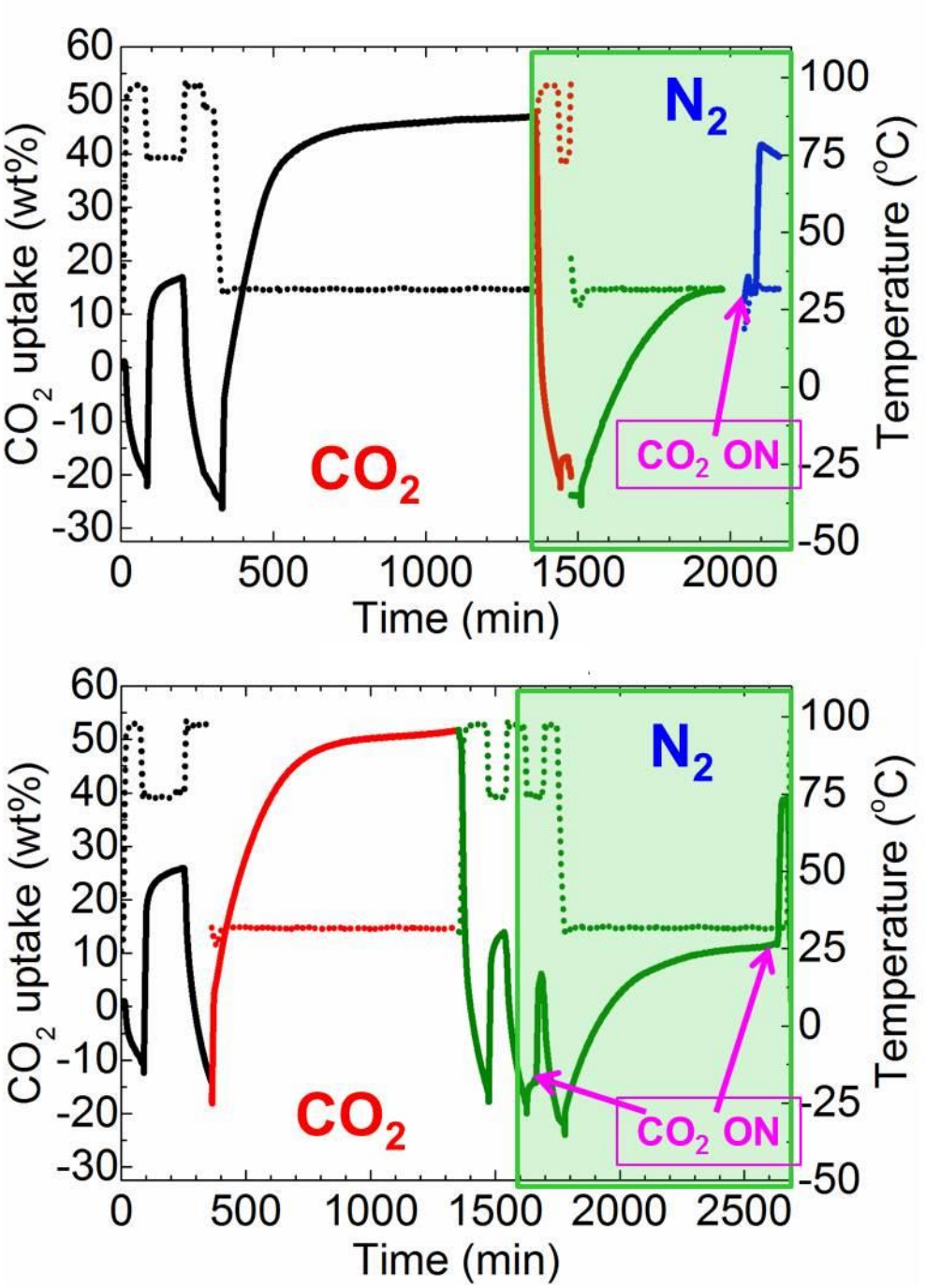

Figure S33. Gravimetric temperature swing flue-gas uptakes of exfGO-D x 7.0TETA (top) and exfGO-D x 10.0TETA (bottom) samples, measured at different temperatures on continuous cycles. The temperature is indicated on the right Y-axis and dotted line data. Note that the flue-gas uptakes were carried out with 15% CO_2 + 85% N_2 gas bubbled through water at a flow rate of 100 ml min^{-1}, and all the desorption runs were performed under flowing dry N_2 at 100 °C for 50 min. The highlighted area tests are for controlled experiment with a humidified N_2 to show the uptake difference between flue-gas CO_2 and humidified N_2. Arrow marks indicate the switching off the N_2 gas flow to CO_2 gas flow at the same temperature. This also shows a rapid uptake of the CO_2 after humidification with N_2 at 30 °C, compared to the direct flue-gas (see 30 °C uptake data)-left side of the highlighted box.

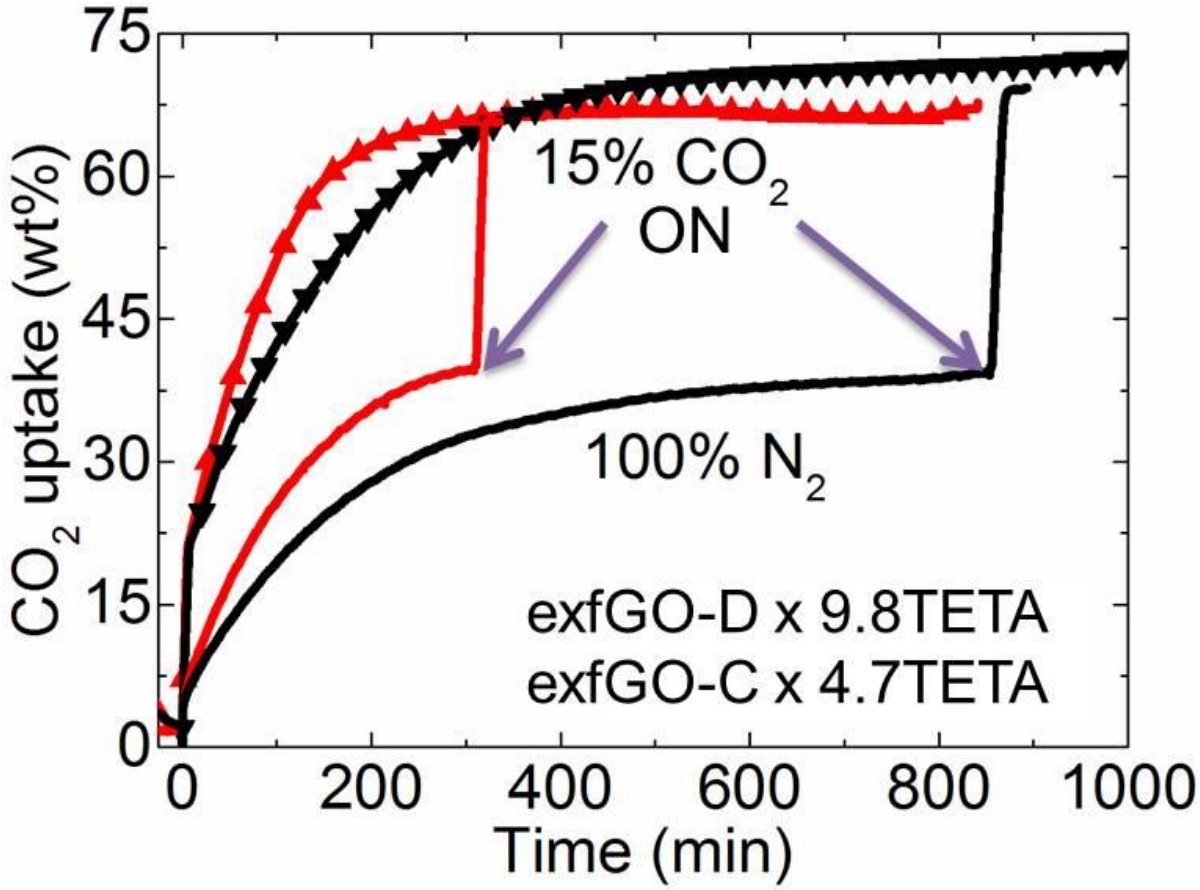

Figure S34. Gravimetric flue-gas (triangle data) and N_2 (solid-line) uptake at 30 °C in TETA@exfGO-C &-D. Note that after reaching the saturation uptake with humidified N_2, a rapid CO_2 uptake kinetics and saturation in (10–15) min, is seen (switched the gas from N_2 to CO_2 under same flow and temperature). This accounts a true CO_2 uptake value of > 30 wt%. Thus a rapid CO_2 uptake in the amine grafted solids at or near room temperature is highly possible by simply pre-humidification of the solid-amine system.

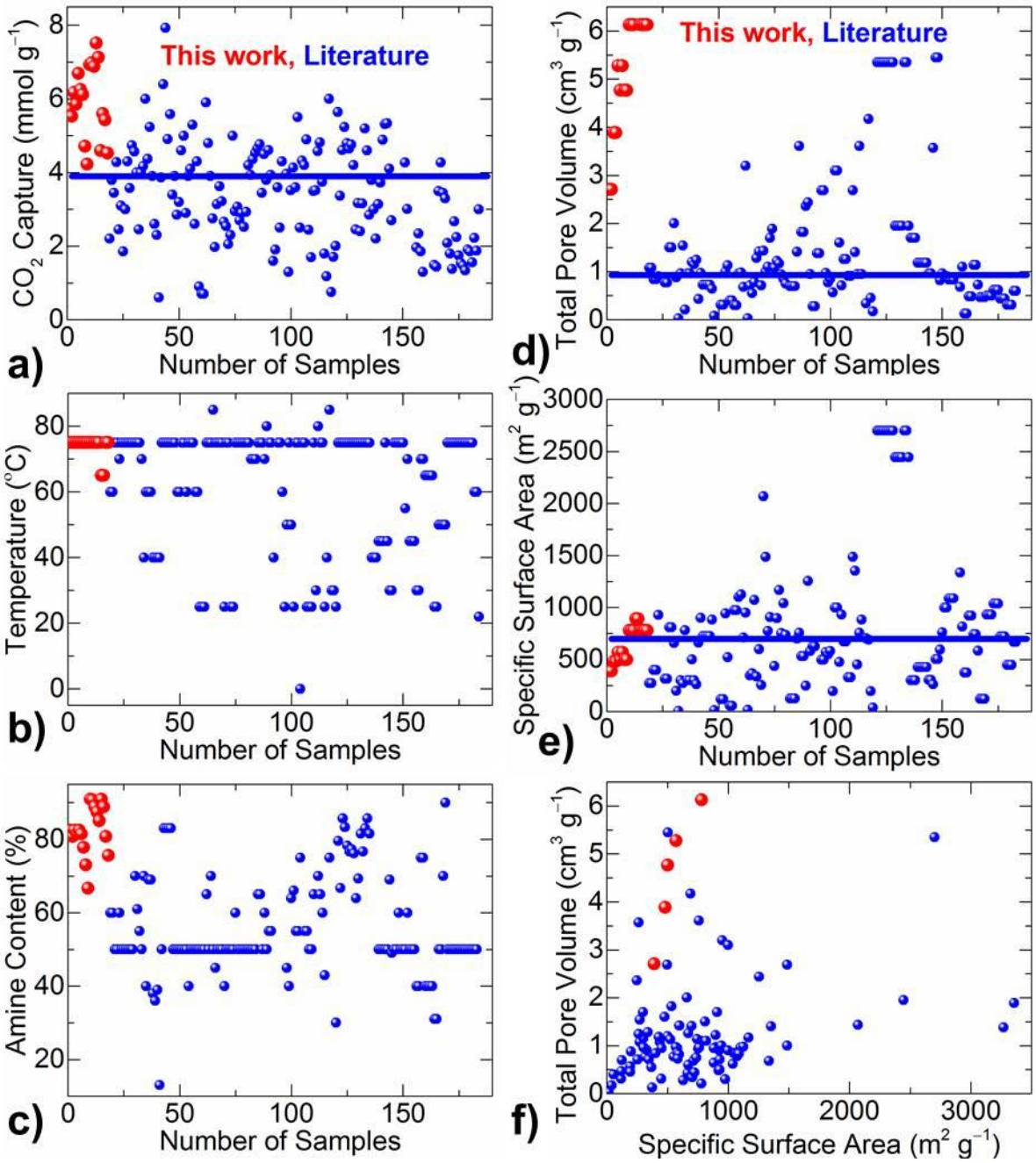

Figure S35. A comparative CO_2 uptake performance data plots of exfGO with respect to the literature amine/solid samples. Left panels show the CO_2 uptake against number of samples (a), and at a respective uptake temperature (b) and amine loading (c). Right panels show the host solid porosity, that is total pore volume (d) and SSA (e) values of the solids used for amine impregnation is showed against number of the samples (d-e). Solid substrates total pore volume against SSA is also plotted (f). All these data is obtained from the samples listed in **Table S6 & S8**.

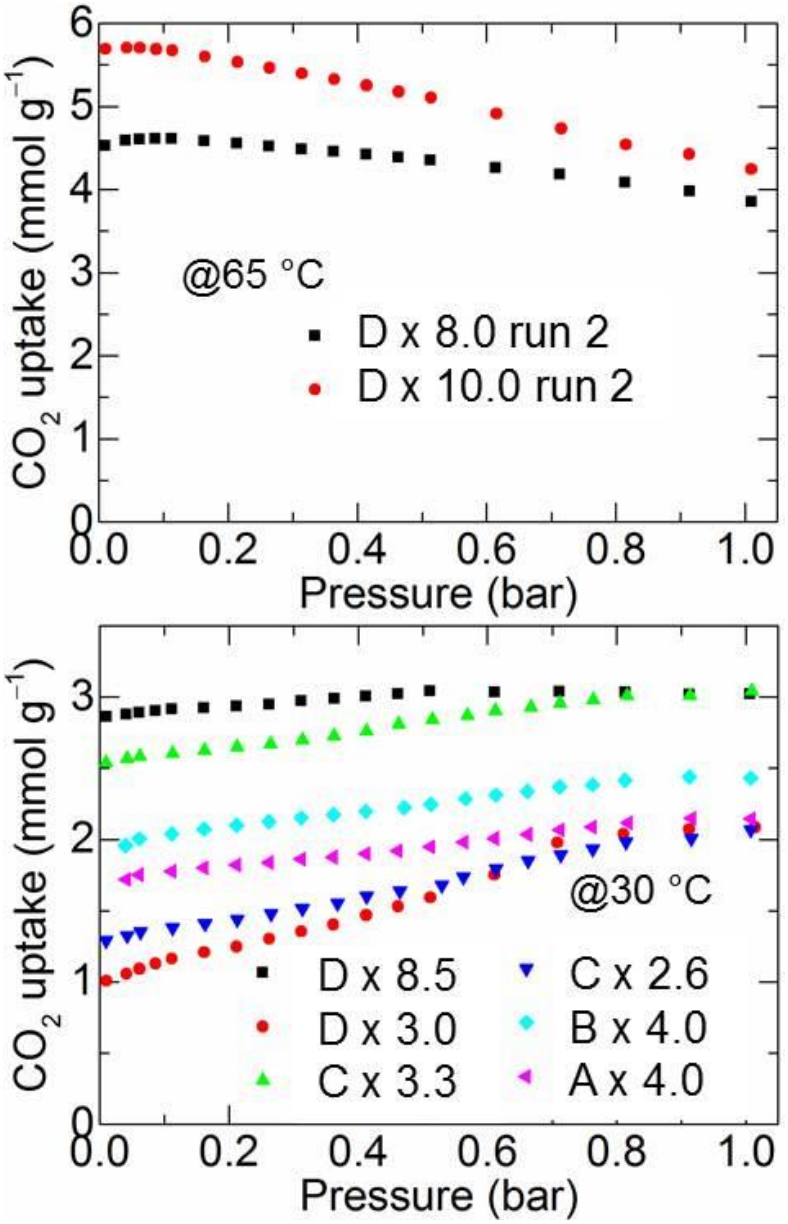

Figure S36. Volumetric CO_2 (100% & dry) uptake isotherms of the samples measured at 65 °C and 30 °C, shows reduction in the uptake at reduced temperatures, is in good agreement with the temperature enhanced kinetic diffusion of CO_2-amine interaction.

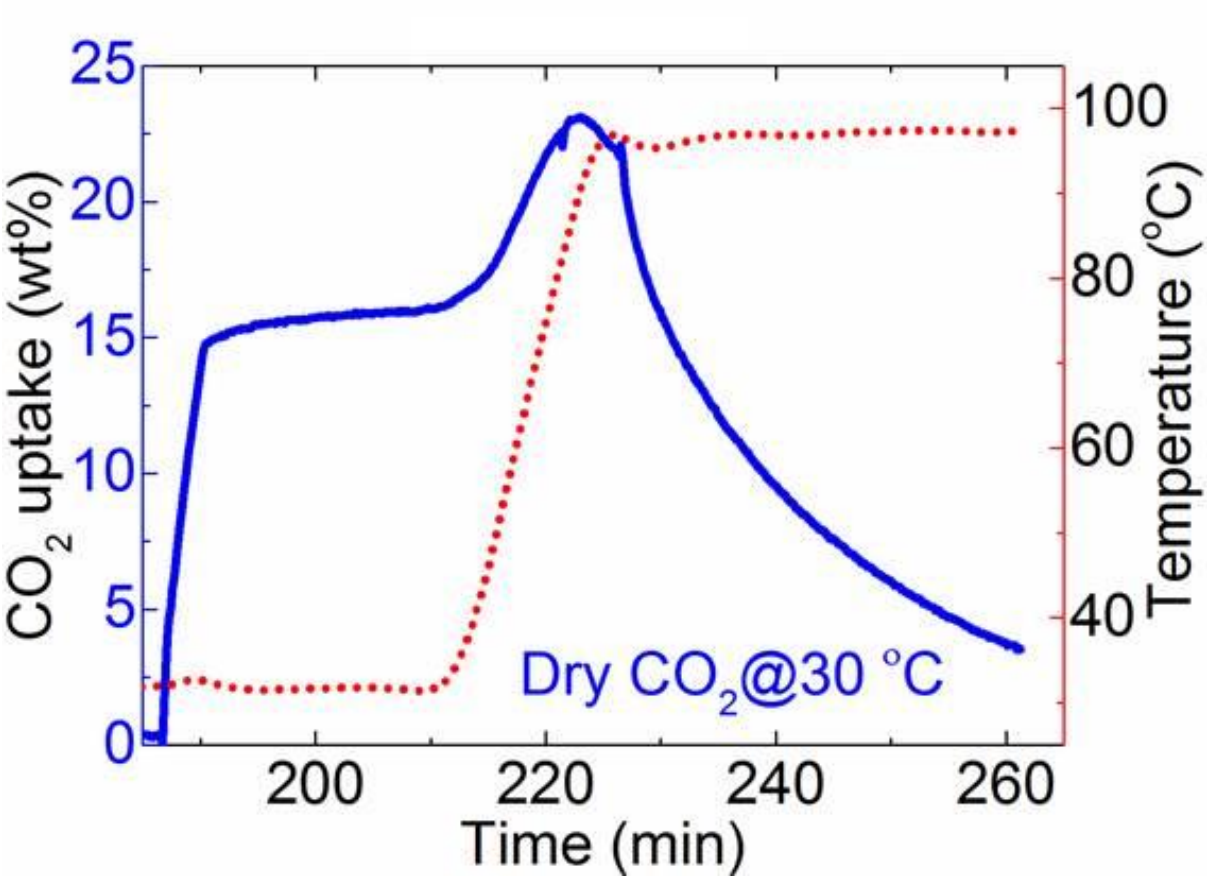

Figure S37. Gravimetric CO_2 (dry, 15% CO_2) uptake with respect to the temperature (heating rate of 5 °C per minute after maintained at 30 °C to reach the uptake saturation). The 100% dry CO_2 uptake can be increased with increasing the sample temperature up to 100 °C.

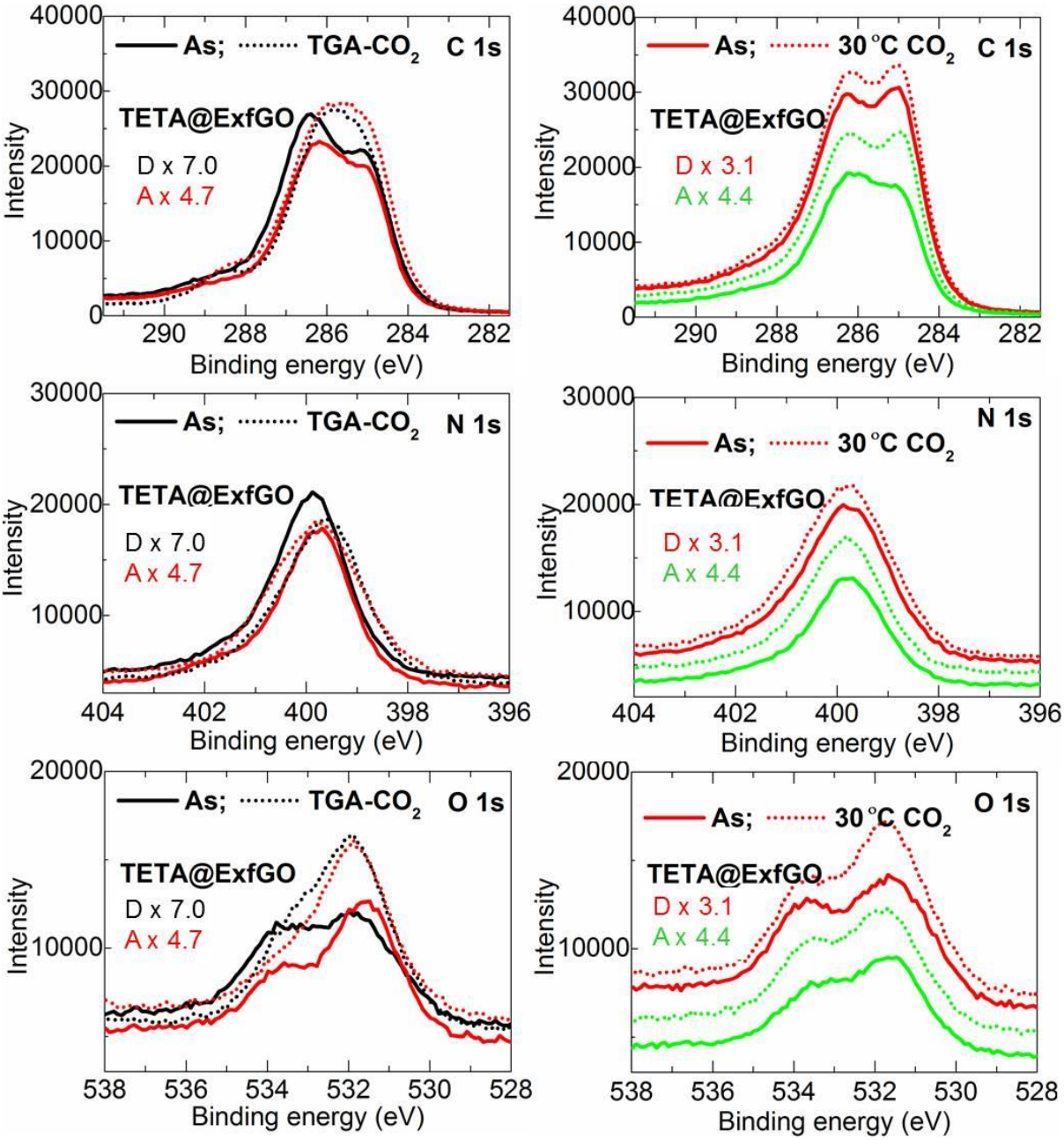

Figure S38. XPS characteristics of the TETA@exfGO samples before and after CO_2 uptake for flue-gas on TG (left panels) and after 30 °C dry CO_2 uptake isotherm runs on the volumetric rig (right panels). A clear flue-gas CO_2 absorption binding with amine is seen at C 1s, N 1s and O 1s on the laft panels. O 1s spectra show prominent amine-CO_2 peak after CO_2 absorption due to an ammonium hydrogen-carbonate ion pair or H_2CO_3 formation: $R-NH_2+CO_2+H_2O \Leftrightarrow R-NH_3^+ + HCO_3^-$. Where as on right panels, a little difference is seen on the dry CO_2 uptake due to a low absorption and a carbamic acid formation: $R-NH_2+CO_2 \Leftrightarrow R-NH-COOH$. N 1s spectra shows broadening and two peak behaviour (~399.6 eV and ~400.2 eV) due to the amide (NHC=O) groups.

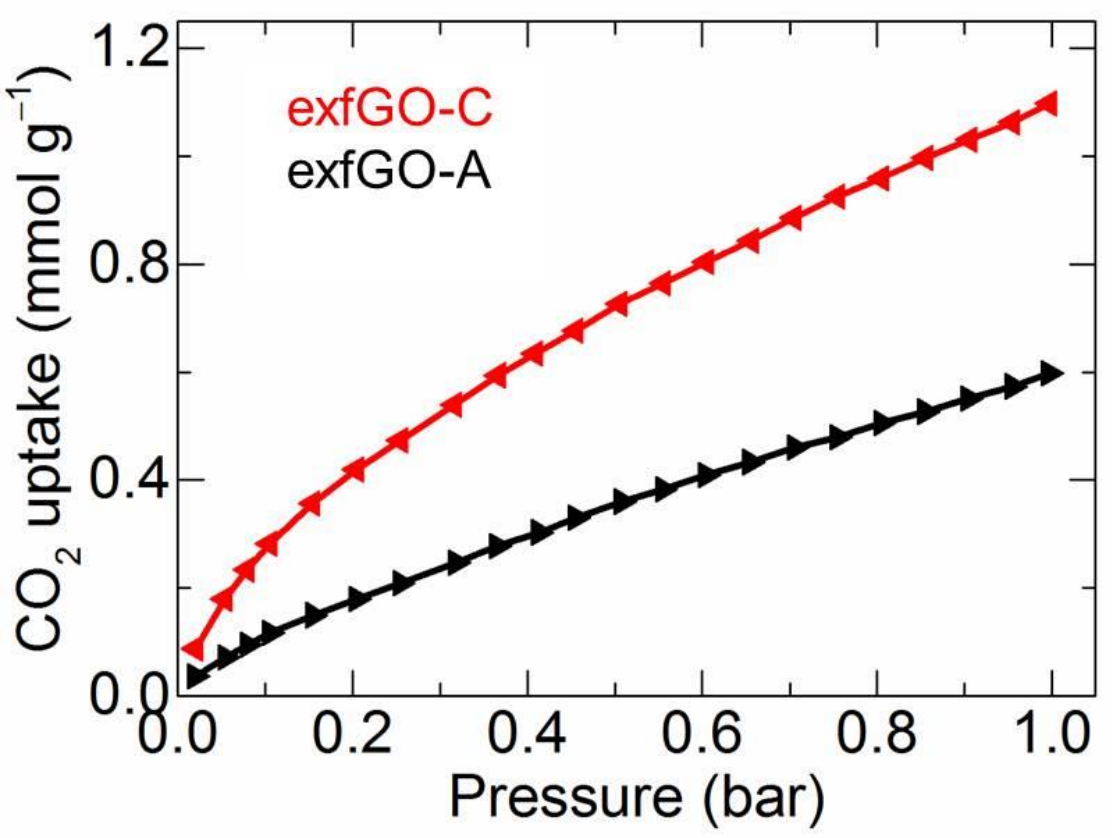

Figure S39. Volumetric CO_2 (100% & dry) uptake isotherms of exfGO samples, measured at 25 °C. A maximum uptake of < 0.4 mmol g^{-1} & ~1.1 mmol g^{-1} at 0.15 bar and 1.0 bar, respectively is observed, indicating again a high mesoporosity in the structures.

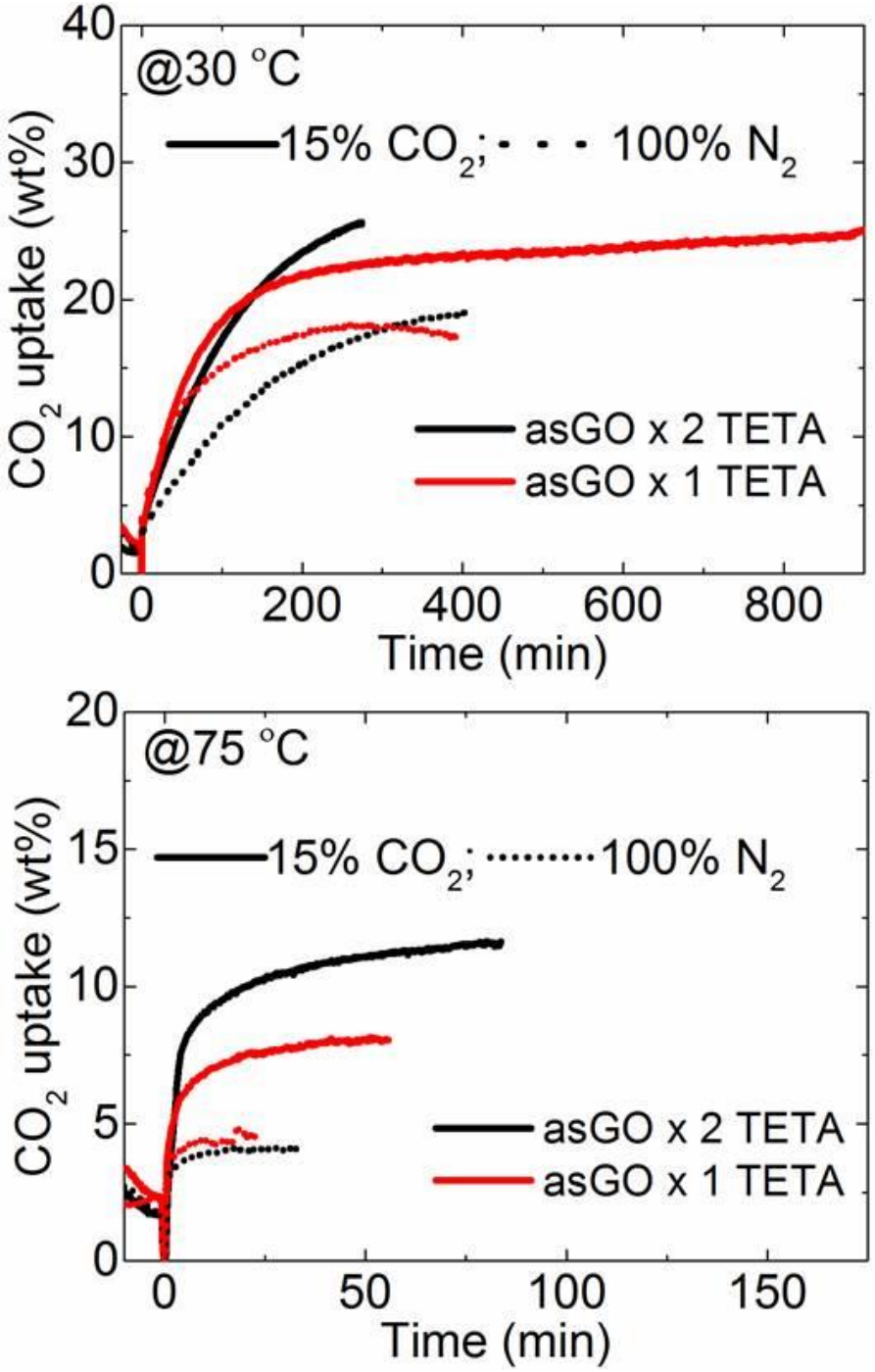

Figure S40. Gravimetric flue-gas CO_2 uptake of TETA@asGO samples, measured at 30 °C (top) and 75 °C (bottom). At room temperature, most of the flue-gas uptake is attributed to the moisture uptake. Overall flue-gas uptake of less than 10 wt% is achieved at 75 °C, considerably low compared to the exfGO samples (with over 30 wt%).

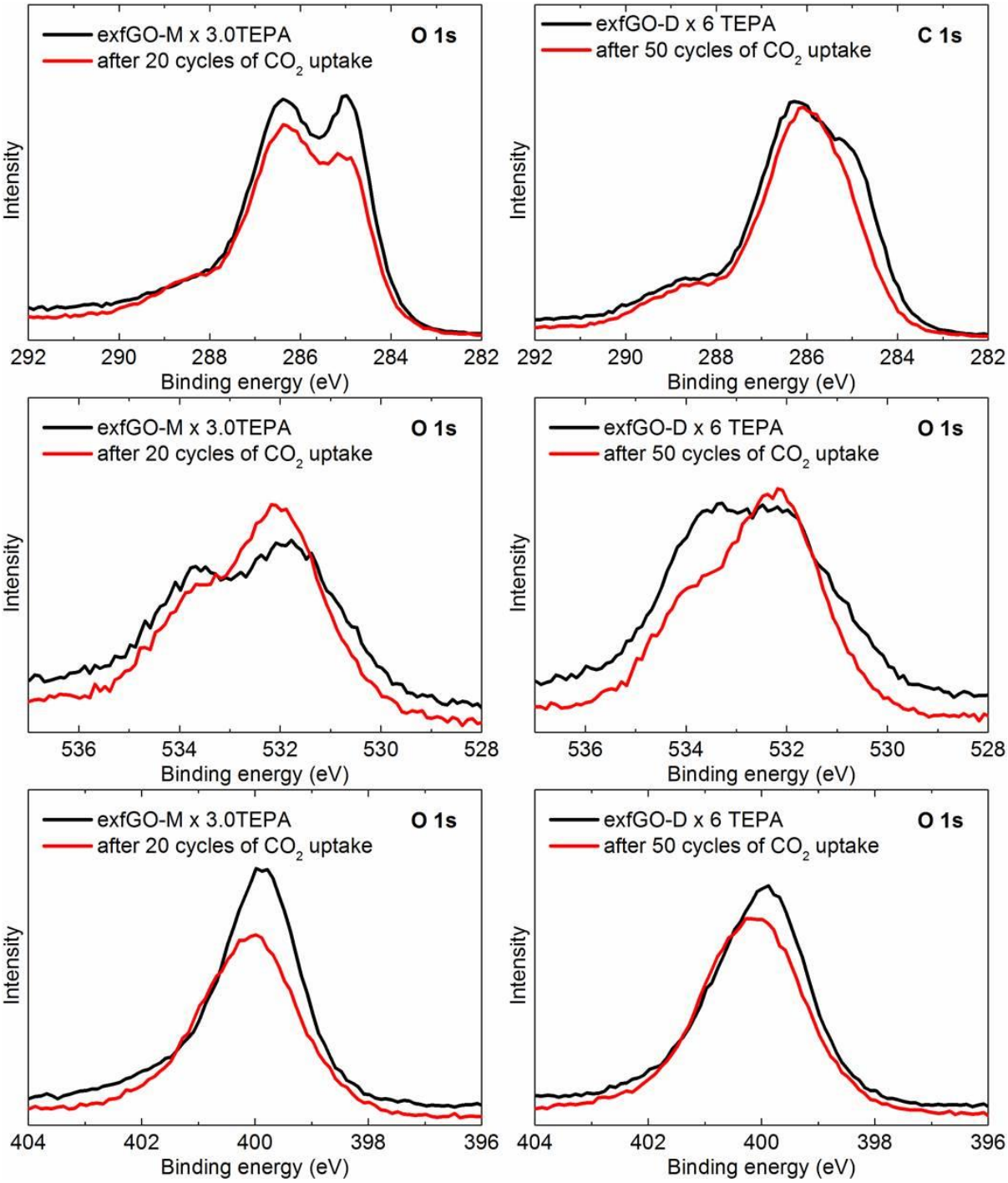

Figure S41. XPS C 1s, O1s and N 1s spectra of TEPA@exfGO samples before after CO_2 cyclic uptake runs. Shift in the C 1 s and O 1s spectra for samples after uptake cyclic tests reveal formation of C-O bonds. Shift in N 1s peak to higher binding energy is consistent with the partial oxidation of amines.[210] However, there is no clear evidence of urea formation (https://srdata.nist.gov/xps/Query_class_type_detail.aspx?ID_No=2165&Class_srch=urea).

References

1 W. Zhang, Y. Li and S. Peng, *ACS Appl. Mater. Interfaces*, 2016, **8**, 15187–15195.

2 Y. Qiu, F. Guo, R. Hurt and I. Külaots, *Carbon*, 2014, **72**, 215–223.

3 H. C. Schniepp, J. Li, M. J. Mcallister, H. Sai, M. Herrera-alonso, D. H. Adamson, R. K. Prud'homme, R. Car, D. A. Saville and I. A. Aksay, *J. Phys. Chem. B*, 2006, **2**, 8535–8539.

4 C. X. Guo, Y. Wang and C. M. Li, *ACS Sustain. Chem. Eng.*, 2013, **1**, 14–18.

5 S. Y. Lee and S. J. Park, *Carbon*, 2014, **68**, 112–117.

6 Z. Lin, G. H. Waller, Y. Liu, M. Liu and C. P. Wong, *Carbon*, 2013, **53**, 130–136.

7 Y. Zhao, C. Hu, L. Song, L. Wang, G. Shi, L. Dai and L. Qu, *Energy Environ. Sci.*, 2014, **7**, 1913–1918.

8 S. H. Park, H. K. Kim, S. B. Yoon, C. W. Lee, D. Ahn, S. I. Lee, K. C. Roh and K. B. Kim, *Chem. Mater.*, 2015, **27**, 457–465.

9 Y. Xu, C.-Y. Chen, Z. Zhao, Z. Lin, C. Lee, X. Xu, C. Wang, Y. Huang, M. I. Shakir and X. Duan, *Nano Lett.*, 2015, **15**, 4605–4610.

10 Z. Wen, X. Wang, S. Mao, Z. Bo, H. Kim, S. Cui, G. Lu, X. Feng and J. Chen, *Adv. Mater.*, 2012, **24**, 5610–5616.

11 T. Kim, G. Jung, S. Yoo, S. .S. Suh and R. S. Ruoff, *ACS Nano*, 2013, **8**, 6899–6905.

12 P. Lian, X. Zhu, S. Liang, Z. Li, W. Yang and H. Wang, *Electrochim. Acta*, 2010, **55**, 3909–3914.

13 Y. Wang, Z. Shi, Y. Huang, Y. Ma, C. Wang, M. Chen and Y. Chen, *J. Phys. Chem. C*, 2009, **113**, 13103–13107.

14 Y. Zhu, S. Murali, M. D. Stoller, A. Velamakanni, R. D. Piner and R. S. Ruoff, *Carbon*, 2010, **48**, 2118–2122.

15 J. Luo, H. D. Jang, T. Sun, L. Xiao, Z. He, A. P. Katsoulidis, M. G. Kanatzidis, J. M. Gibson and J. Huang, *ACS Nano*, 2011, **5**, 8943–8949.

16 K. Lee, D. Kim, Y. Yoon, J. Yang, H.-G. Yun, I.-K. You and H. Lee, *RSC Adv.*, 2015, **5**, 60914–60919.

17 Y. Yoon, K. Lee, C. Baik, H. Yoo, M. Min, Y. Park, S. M. Lee and H. Lee, *Adv. Mater.*, 2013, **25**, 4437–4444.

18 Z. Wu, Y. Sun, Y. Tan and S. Yang, *J. Am. Chem. Soc.*, 2012, **134**, 19532–19535.

19 Z. Jia, B. Wang, Y. Wang, T. Qi, Y. Liu and Q. Wang, *RSC Adv.*, 2016, **6**, 49497–49504.

20 Q. Du, M. Zheng, L. Zhang, Y. Wang, J. Chen, L. Xue, W. Dai, G. Ji and J. Cao, *Electrochim. Acta*, 2010, **55**, 3897–3903.

21 X. Du, P. Guo, H. Song and X. Chen, *Electrochim. Acta*, 2010, **55**, 4812–4819.

22 J. Liu, M. Zheng, X. Shi, H. Zeng and H. Xia, *Adv. Funct. Mater.*, 2015, **26**, 919–930.

23 G. Srinivas, J. Burress and T. Yildirim, *Energy Environ. Sci.*, 2012, **5**, 6453–6459.

24 L.-P. Ma, Z.-S. Wu, J. Li, E.-D. Wu, W.-C. Ren and H.-M. Cheng, *Int. J. Hydrogen Energy*, 2009, **34**, 2329–2332.

25 S. Stankovich, D. A. Dikin, R. D. Piner, K. A. Kohlhaas, A. Kleinhammes, Y. Jia, Y. Wu, S. T. Nguyen and R. S. Ruoff, *Carbon*, 2007, **45**, 1558–1565.

26 Q. Zheng, X. Ji, S. Gao and X. Wang, *Int. J. Hydrogen Energy*, 2013, **38**, 10896–10902.

27 Y. Wang, C. Guan, K. Wang, C. X. Guo and C. M. Li, *J. Chem. Eng. Data*, 2011, **56**, 642–645.

28 W. Yuan, B. Li and L. Li, *Appl. Surf. Sci.*, 2011, **257**, 10183–10187.

29 A. K. Mishra and S. Ramaprabhu, *AIP Adv.*, 2011, **1**, 032152.

30 L. Y. Meng and S. J. Park, *J. Colloid Interface Sci.*, 2012, **386**, 285–290.

31 B. H. Kim, W. G. Hong, H. Y. Yu, Y.-K. Han, S. M. Lee, S. J. Chang, H. R. Moon, Y. Jun and H. J. Kim, *Phys. Chem. Chem. Phys.*, 2012, **14**, 1480–4.

32 G. Srinivas, J. W. Burress, J. Ford and T. Yildirim, *J. Mater. Chem.*, 2011, **21**, 11323–11329.

33 H.-K. Kim, A. R. Kamali, K. C. Roh, K.-B. Kim and D. J. Fray, *Energy Environ. Sci.*, 2016, **9**, 2249–2256.

34 H. W. Park, D. U. Lee, Y. Liu, J. Wu, L. F. Nazar and Z. Chen, *J. Electrochem. Soc.*, 2013, **160**, A2244–A2250.

35 Y.-H. Hwang, S. M. Lee, Y. J. Kim, Y. H. Kahng and K. Lee, *Carbon*, 2016, **100**, 7–15.

36 Y. Xu, Z. Lin, X. Zhong, X. Huang, N. O. Weiss, Y. Huang and X. Duan, *Nat Commun*, 2014, **5**, 4554.

37 W. Lv, D. M. Tang, Y. B. He, C. H. You, Z. Q. Shi, X. C. Chen, C. M. Chen, P. X. Hou, C. Liu and Q. H. Yang, *ACS Nano*, 2009, **3**, 3730–3736.

38 X. Sun, P. Cheng, H. Wang, H. Xu, L. Dang, Z. Liu and Z. Lei, *Carbon*, 2015, **92**, 1–10.

39 K. Lee, Y. Yoon, Y. Cho, S. M. Lee, Y. Shin, H. Lee and H. Lee, *ACS Nano*, 2016, **10**, 6799–6807.

40 D. Zhang, T. Yan, L. Shi, Z. Peng, X. Wen and J. Zhang, *J. Mater. Chem.*, 2012, **22**, 14696–14704.

41 M. Boota, C. Chen, M. R. Becuwe, L. Miao and Y. Gogotsi, *Energy Environ. Sci.*, 2016, **9**, 2586–2594.

42 F. Zhang, D. Zhu, X. Chen, X. Xu, Z. Yang, C. Zou, K. Yang and S. Huang, *Phys. Chem. Chem. Phys.*, 2014, **16**, 4186–4192.

43 L. Lai, L. Chen, D. Zhan, L. Sun, J. Liu, S. H. Lim, C. K. Poh, Z. Shen and J. Lin, *Carbon*, 2011, **49**, 3250–3257.

44 Y. J. Lee, H. W. Park, G. P. Kim, J. Yi and I. K. Song, *Curr. Appl. Phys.*, 2013, **13**, 945–949.

45 D. Sun, X. Yan, J. Lang and Q. Xue, *J. Power Sources*, 2013, **222**, 52–58.

46 H.-L. Guo, P. Su, X. Kang and S.-K. Ning, *J. Mater. Chem. A*, 2013, **1**, 2248–2255.

47 Y. H. Lee, K. H. Chang and C. C. Hu, *J. Power Sources*, 2013, **227**, 300–308.

48 Y. Bai, R. B. Rakhi, W. Chen and H. N. Alshareef, *J. Power Sources*, 2013, **233**, 313–319.

49 Y. Zou, I. A. Kinloch and R. A. W. Dryfe, *J. Mater. Chem. A*, 2014, **2**, 19495–19499.

50 Z. S. Wu, A. Winter, L. Chen, Y. Sun, A. Turchanin, X. Feng and K. Müllen, *Adv. Mater.*, 2012, **24**, 5130–5135.

51 M. Li, J. Ding and J. Xue, *J. Mater. Chem. A*, 2013, **1**, 7469–7476.

52 Z. Fan, Q. Zhao, T. Li, J. Yan, Y. Ren, J. Feng and T. Wei, *Carbon*, 2012, **50**, 1699–1703.

53 J. Yan, J. Liu, Z. Fan, T. Wei and L. Zhang, *Carbon*, 2012, **50**, 2179–2188.

54 H. Sun, L. Cao and L. Lu, *Energy Environ. Sci.*, 2012, **5**, 6206–6213.

55 Y. Tao, X. Xie, W. Lv, D.-M. Tang, D. Kong, Z. Huang, H. Nishihara, T. Ishii, B. Li, D. Golberg, F. Kang, T. Kyotani and Q.-H. Yang, *Sci. Rep.*, 2013, **3**, 2975.

56 W. H. Hong, B. G. Choi, M. Yang, W. H. Hong, J. W. Choi and Y. S. Huh, *ACS Nano*, 2016, **6**, 4020–4028.

57 Z. Lei, N. Christov and X. S. Zhao, *Energy Environ. Sci.*, 2011, **4**, 1866–1873.

58 X. Zhang, Z. Sui, B. Xu, S. Yue, Y. Luo, W. Zhan and B. Liu, *J. Mater. Chem.*, 2011, **21**, 6494–6497.

59 L. Zhang and G. Shi, *J. Phys. Chem. C*, 2011, **115**, 17206–17212.

60 M. D. Stoller, S. Park, Z. Yanwu, J. An and R. S. Ruoff, *Nano Lett.*, 2008, **8**, 3498–3502.

61 J. Zhu, X. Yang, Z. Fu, J. He, C. Wang, W. Wu and L. Zhang, *Chem. - A Eur. J.*, 2016, **22**, 2515–2524.

62 C. Zhu, T. Liu, F. Qian, T. Y.-J. Han, E. B. Duoss, J. D. Kuntz, C. M. Spadaccini, M. A. Worsley and Y. Li, *Nano Lett.*, 2016, **16**, 3448–3456.

63 C. H. J. Kim, D. Zhao, G. Lee and J. Liu, *Adv. Funct. Mater.*, 2016, **26**, 4976–4983.

64 X. Zhuang, F. Zhang, D. Wu, N. Forler, H. Liang, M. Wagner, D. Gehrig, M. R. Hansen, F. Laquai and X. Feng, *Angew. Chemie - Int. Ed.*, 2013, **52**, 9668–9672.

65 G. Srinivas, Y. Zhu, R. Piner, N. Skipper, M. Ellerby and R. Ruoff, *Carbon*, 2010, **48**, 630–635.

66 J. W. Burress, S. Gadipelli, J. Ford, J. M. Simmons, W. Zhou and T. Yildirim, *Angew. Chemie - Int. Ed.*, 2010, **49**, 8902–8904.

67 E. Pourazadi, E. Haque, W. Zhang, A. T. Harris and A. I. Minett, *Chem. Commun.*, 2013, **49**, 11068–11070.

68 G. Mercier, A. Klechikov, M. Hedenström, D. Johnels, I. A. Baburin, G. Seifert, R. Mysyk and A. V. Talyzin, *J. Phys. Chem. C*, 2015, **119**, 27179–27191.

69 A. Ganesan and M. M. Shaijumon, *Microporous Mesoporous Mater.*, 2016, **220**, 21–27.

70 E. Umeshbabu, G. Rajeshkhanna, P. Justin and G. R. Rao, *J. Solid State Electrochem.*, 2016, **20**, 2725–2736.

71 K. Qiu, G. Chai, C. Jiang, M. Ling, J. Tang and Z. Guo, *ACS Catal.*, 2016, **6**, 3558–3568.

72 X. Huang, Y. Zhao, Z. Ao and G. Wang, *Sci. Rep.*, 2014, **4**, 7557.

73 X. Huang, K. Qian, J. Yang, J. Zhang, L. Li, C. Yu and D. Zhao, *Adv. Mater.*, 2012, **24**, 4419–4423.

74 H. Sun, Z. Xu and C. Gao, *Adv. Mater.*, 2013, **25**, 2554–2560.

75 Y. Zhao, C. Hu, Y. Hu, H. Cheng, G. Shi and L. Qu, *Angew. Chemie - Int. Ed.*, 2012, **51**, 11371–11375.

76 R. Li, Z. Wei and X. Gou, *ACS Catal.*, 2015, **5**, 4133–4142.

77 N. Q. Tran, B. K. Kang, M. H. Woo and D. H. Yoon, *ChemSusChem*, 2016, **9**, 2261–2268.

78 S. Yu, Y. Li and N. Pan, *RSC Adv.*, 2014, **4**, 48758–48764.

79 K. S. Subrahmanyam, S. R. C. Vivekchand, A. Govindaraj and C. N. R. Rao, *J. Mater. Chem.*, 2010, **18**, 1517–1523.

80 D. Zhou, T.-L. Zhang and B.-H. Han, *Microporous Mesoporous Mater.*, 2013, **165**, 234–239.

81 D. Zhou and B. G. Han, *Adv. Funct. Mater.*, 2010, **20**, 2717–2722.

82 Z. Jin, W. Lu, K. J. Oneill, P. A. Parilla, L. J. Simpson, C. Kittrell and J. M. Tour, *Chem. Mater.*, 2011, **23**, 923–925.

83 D. Zhou, Q. Y. Cheng, Y. Cui, T. Wang, X. Li and B. H. Han, *Carbon*, 2014, **66**, 592–598.

84 Y. Matsuo, S. Ueda, K. Konishi, J. P. Marco-Lozar, D. Lozano-Castelló and D. Cazorla-Amorós, *Int. J. Hydrogen Energy*, 2012, **37**, 10702–10708.

85 Z. Y. Sui, Y. Cui, J. H. Zhu and B. H. Han, *ACS Appl. Mater. Interfaces*, 2013, **5**, 9172–9179.

86 Z. L. Hu, M. Aizawa, Z. M. Wang, N. Yoshizawa and H. Hatori, *Langmuir*, 2010, **26**, 6681–6688.

87 C.-C. Huang, N.-W. Pu, C.-A. Wang, J.-C. Huang, Y. Sung and M.-D. Ger, *Sep. Purif. Technol.*, 2011, **82**, 210–215.

88 C. H. Chen, T. Y. Chung, C. C. Shen, M. S. Yu, C. S. Tsao, G. N. Shi, C. C. Huang, M. Der Ger and W. L. Lee, *Int. J. Hydrogen Energy*, 2013, **38**, 3681–3688.

89 Y. Wang, C. X. Guo, X. Wang, C. Guan, H. Yang, K. Wang and C. M. Li, *Energy Environ. Sci.*, 2011, **4**, 195–200.

90 L. Guardia, F. Suárez-García, J. I. Paredes, P. Solís-Fernández, R. Rozada, M. J. Fernández-Merino, A. Martínez-Alonso and J. M. D. Tascón, *Microporous Mesoporous Mater.*, 2012, **160**, 18–24.

91 S. Yang, L. Zhi, K. Tang, X. Feng, J. Maier and K. Müllen, *Adv. Funct. Mater.*, 2012, **22**, 3634–3640.

92 X. Cui, S. Yang, X. Yan, J. Leng, S. Shuang, P. M. Ajayan and Z. Zhang, *Adv. Funct. Mater.*, 2016, **26**, 5708–5717.

93 S. Li, Z. Wang, H. Jiang, L. Zhang, J. Ren, M. T. Zheng, L. Dong and L. Sun, *Chem. Commun.*, 2016, **52**, 10988–10991.

94 Q. Zhou, Z. Zhao, Y. Chen, H. Hu and J. Qiu, *J. Mater. Chem.*, 2012, **22**, 6061–6066.

95 G. Ning, Z. Fan, G. Wang, J. Gao, W. Qian and F. Wei, *Chem Commun*, 2011, **47**, 5976–5978.

96 J. Han, L. L. Zhang, S. Lee, J. Oh, K. S. Lee, J. R. Potts, J. Ji, X. Zhao, R. S. Ruoff and S. Park, *ACS Nano*, 2013, **7**, 19–26.

97 L. Niu, Z. Li, W. Hong, J. Sun, Z. Wang, L. Ma, J. Wang and S. Yang, *Electrochim. Acta*, 2013, **108**, 666–673.

98 S. Wan, H. Bi, X. Xie, S. Su, K. Du, H. Jia, T. Xu, L. He, K. Yin and L. Sun, *Sci. Rep.*, 2016, **6**, 32746.

99 Y. Y. Peng, Y. M. Liu, J. K. Chang, C. H. Wu, M. Der Ger, N. W. Pu and C. L. Chang, *Carbon*, 2015, **81**, 347–356.

100 Y. Li and D. Zhao, *Chem. Commun.*, 2014, **51**, 1–4.

101 Y. Gu, H. Wu, Z. G. Xiong, W. Al Abdulla and X. S. Zhao, *J. Mater. Chem. A*, 2014, **2**, 451–459.

102 W. Shi, H. Li, X. Cao, Z. Y. Leong, J. Zhang, T. Chen, H. Zhang and H. Y. Yang, *Sci. Rep.*, 2016, **6**, 18966.

103 Y. Wen, T. E. Rufford, D. Hulicova-Jurcakova, L. Wang and X. Zhu, *ACS Appl. Mater. Interfaces*, 2016, **8**,18051–18059.

104 L. Z. Fan, J. L. Liu, R. Ud-Din, X. Yan and X. Qu, *Carbon*, 2012, **50**, 3724–3730.

105 B. Zhao, P. Liu, Y. Jiang, D. Pan, H. Tao, J. Song, T. Fang and W. Xu, *J. Power Sources*, 2012, **198**, 423–427.

106 C. M. Chen, Q. Zhang, M. G. Yang, C. H. Huang, Y. G. Yang and M. Z. Wang, *Carbon*, 2012, **50**, 3572–3584.

107 J. Hu, Z. Kang, F. Li and X. Huang, *Carbon*, 2014, **67**, 221–229.

108 S. Chowdhury and R. Balasubramanian, *Ind. Eng. Chem. Res.*, 2016, **55**, 7906–7916.

109 H. Bi, T. Lin, F. Xu, Y. Tang, Z. Liu and F. Huang, *Nano Lett.*, 2016, **16**, 349–354.

110 Y. Chen, X. Zhang, H. Zhang, X. Sun, D. Zhang and Y. Ma, *RSC Adv.*, 2012, **2**, 7747–7753.

111 X. Li, X. Zang, Z. Li, X. Li, P. Li, P. Sun, X. Lee, R. Zhang, Z. Huang, K. Wang, D. Wu, F. Kang and H. Zhu, *Adv. Funct. Mater.*, 2013, **23**, 4862–4869.

112 D. Liu, Z. Jia and D. Wang, *Carbon*, 2016, **100**, 664–677.

113 B. Zheng, T. W. Chen, F. N. Xiao, W. J. Bao and X. H. Xia, *J. Solid State Electrochem.*, 2013, **17**, 1809–1814.

114 L. L. Zhang, X. Zhao, M. D. Stoller, Y. Zhu, H. Ji, S. Murali, Y. Wu, S. Perales, B. Clevenger and R. S. Ruoff, *Nano Lett.*, 2012, **12**, 1806–1812.

115 S. Wu, G. Chen, N. Y. Kim, K. Ni, W. Zeng, Y. Zhao, Z. Tao, H. Ji, Z. Lee and Y. Zhu, *Small*, 2016, **12**, 2376–2384.

116 L. Zhang, F. Zhang, X. Yang, G. Long, Y. Wu, T. Zhang, K. Leng, Y. Huang, Y. Ma, A. Yu and Y. Chen, *Sci Rep*, 2013, **3**, 1408.

117 S. Wang, F. Tristan, D. Minami, T. Fujimori, R. Cruz-Silva, M. Terrones, K. Takeuchi, K. Teshima, F. Rodr??guez-Reinoso, M. Endo and K. Kaneko, *Carbon*, 2014, **76**, 220–231.

118 C. Zheng, X. F. Zhou, H. L. Cao, G. H. Wang and Z. P. Liu, *J. Mater. Chem. A*, 2015, **3**, 9543–9549.

119 V. Chandra, S. U. Yu, S. H. Kim, Y. S. Yoon, D. Y. Kim, A. H. Kwon, M. Meyyappan and K. S. Kim, *Chem. Commun.*, 2012, **48**, 735–737.

120 K. C. Kemp, V. Chandra, M. Saleh and K. S. Kim, *Nanotechnology*, 2013, **24**, 235703.

121 H. Seema, K. C. Kemp, N. H. Le, S. W. Park, V. Chandra, J. W. Lee and K. S. Kim, *Carbon*, 2014, **66**, 320–326.

122 S. M. Egger, K. R. Hurley, A. Datt, G. Swindlehurst and C. L. Haynes, *Chem. Mater.*, 2015, **27**, 3193–3196.

123 H. Furukawa, K. E. Cordova, M. O'Keeffe and O. M. Yaghi, *Science*, 2013, **341**, 1230444–1230444.

124 D. Li, F. Han, S. Wang, F. Cheng, Q. Sun and W. C. Li, *ACS Appl. Mater. Interfaces*, 2013, **5**, 2208–2213.

125 J. Pampel and T.-P. Fellinger, *Adv. Energy Mater.*, 2016, **6**, 1502389.

126 J. Zhao, H. Lai, Z. Lyu, Y. Jiang, K. Xie, X. Wang, Q. Wu, L. Yang, Z. Jin, Y. Ma, J. Liu and Z. Hu, *Adv. Mater.*, 2015, **27**, 3541–3545.

127 A. Manthiram, L. Li, C. Liu, G. He and D. E. Fan, *Energy Environ. Sci.*, 2015, **8**, 3274–3282.

128 H. Zhang, A. Goeppert, M. Czaun, G. K. S. Prakash and G. Olah, *RSC Adv.*, 2014, **4**, 19403–19417.

129 G. Srinivas, V. Krungleviciute, Z.-X. Guo and T. Yildirim, *Energy Environ. Sci.*, 2014, **7**, 335–342.

130 M. A. Worsley, T. Y. Olson, J. R. I. Lee, T. M. Willey, M. H. Nielsen, S. K. Roberts, P. J. Pauzauskie, J. Biener, J. H. Satcher and T. F. Baumann, *J. Phys. Chem. Lett.*, 2011, **2**, 921–925.

131 Z. Lyu, D. Xu, L. Yang, R. Che, R. Feng, J. Zhao, Y. Li, Q. Wu, X. Wang and Z. Hu, *Nano Energy*, 2015, **12**, 657–665.

132 B. Han, E. J. Lee, W. H. Choi, W. C. Yoo and J. H. Bang, *New J. Chem.*, 2015, **39**, 6178–6185.

133 J. Xie, X. Yao, Q. Cheng, I. P. Madden, P. Dornath, C. C. Chang, W. Fan and D. Wang, *Angew. Chemie - Int. Ed.*, 2015, **54**, 4299–4303.

134 M. Irani, M. Fan, H. Ismail, A. Tuwati, B. Dutcher and A. G. Russell, *Nano Energy*, 2015, **11**, 235–246.

135 L. Wang, M. Yao, X. Hu, G. Hu, J. Lu, M. Luo and M. Fan, *Appl. Surf. Sci.*, 2015, **324**, 286–292.

136 X. Wang, L. Chen and Q. Guo, *Chem. Eng. J.*, 2014, **260**, 573–581.

137 Q. Liu, B. Xiong, J. Shi, M. Tao, Y. He and Y. Shi, *Energy & Fuels*, 2014, **28**, 6494–6501.

138 W. Wang, X. Wang, C. Song, X. Wei, J. Ding and J. Xiao, *Energy and Fuels*, 2013, **27**, 1538–1546.

139 M. Yao, Y. Dong, X. Hu, X. Feng, A. Jia, G. Xie, G. Hu, J. Lu, M. Luo and M. Fan, *Energy & Fuels*, 2013, **27**, 1538–1546.

140 X. Feng, G. Hu, X. Hu, G. Xie, Y. Xie, J. Lu and M. Luo, *Ind. Eng. Chem. Res.*, 2013, **52**, 4221–4228.

141 Y. Li, X. Wen, L. Li, F. Wang, N. Zhao, F. Xiao, W. Wei and Y. Sun, *J. Sol-Gel Sci. Technol.*, 2013, **66**, 353–362.

142 F. Song, Y. Zhao and Q. Zhong, *J. Environ. Sci.*, 2013, **25**, 554–560.

143 D. S. Dao, H. Yamada and K. Yogo, *Ind. Eng. Chem. Res.*, 2013, **52**, 13810–13817.

144 Y. Cao, F. Song, Y. Zhao and Q. Zhong, *J. Environ. Sci.*, 2013, **25**, 2081–2087.

145 F. Song, Y. Zhao, Y. Cao, J. Ding, Y. Bu and Q. Zhong, *Appl. Surf. Sci.*, 2013, **268**, 124–128.

146 R. Veneman, Z. S. Li, J. a. Hogendoorn, S. R. a. Kersten and D. W. F. Brilman, *Chem. Eng. J.*, 2012, **207**–**208**, 18–26.

147 J. Yu, Y. Le and B. Cheng, *RSC Adv.*, 2012, **2**, 6784–6791.

148 G. Qi, Y. Wang, L. Estevez, X. Duan, N. Anako, A.-H. A. Park, W. Li, C. W. Jones and E. P. Giannelis, *Energy Environ. Sci.*, 2011, **4**, 444–452.

149 X. Wang, H. Li, H. Liu and X. Hou, *Microporous Mesoporous Mater.*, 2011, **142**, 564–569.

150 Y. Liu, Q. Ye, M. Shen, J. Shi, J. Chen, H. Pan and Y. Shi, *Environ. Sci. Technol.*, 2011, **45**, 5710–5716.

151 S.-H. Liu, Y.-C. Lin, Y.-C. Chien and H.-R. Hyu, *J. Air Waste Manag. Assoc.*, 2011, **61**, 226–233.

152 Y. Liu, J. Shi, J. Chen, Q. Ye, H. Pan, Z. Shao and Y. Shi, *Microporous Mesoporous Mater.*, 2010, **134**, 16–21.

153 J. J. Wen, F. N. Gu, F. Wei, Y. Zhou, W. G. Lin, J. Yang, J. Y. Yang, Y. Wang, Z. G. Zou and J. H. Zhu, *J. Mater. Chem.*, 2010, **20**, 2840–2846.

154 S. H. Liu, C. H. Wu, H. K. Lee and S. Bin Liu, *Top. Catal.*, 2010, **53**, 210–217.

155 F. Su, C. Lu, S. C. Kuo and W. Zeng, *Energy and Fuels*, 2010, **24**, 1441–1448.

156 M. Bhagiyalakshmi, L. J. Yun, R. Anuradha and H. T. Jang, *J. Hazard. Mater.*, 2010, **175**, 928–938.

157 C. Chen, S.-T. Yang, W.-S. Ahn and R. Ryoo, *Chem. Commun.*, 2009, 3627–3629.

158 M. B. Yue, L. B. Sun, Y. Cao, Y. Wang, Z. J. Wang and J. H. Zhu, *Chem. - A Eur. J.*, 2008, **14**, 3442–3451.

159 M. B. Yue, Y. Chun, Y. Cao, X. Dong and J. H. Zhu, *Adv. Funct. Mater.*, 2006, **16**, 1717–1722.

160 M. Niu, H. Yang, X. Zhang, Y. Wang and A. Tang, *ACS Appl. Mater. Interfaces*, 2016, 8, 17312–17320.

161 S. Chai, Z. Liu, K. Huang, S. Tan and S. Dai, *Ind. Eng. Che. Res*., 2016, **55**, 7355–7361.

162 K. Li, J. Jiang, S. Tian, F. Yan and X. Chen, *J. Mater. Chem. A*, 2015, **3**, 2166–2175.

163 Z. Chen, S. Deng, H. Wei, B. Wang, J. Huang and G. Yu, *ACS Appl. Mater. Interfaces*, 2013, **5**, 6937–6945.

164 W. Wang, J. Xiao, X. Wei, J. Ding, X. Wang and C. Song, *Appl. Energy*, 2014, **113**, 334–341.

165 S. Sung and M. P. Suh, *J. Mater. Chem. A*, 2014, **2**, 13245–13249.

166 X. Xu, C. Song, J. M. Andrésen, B. G. Miller and A. W. Scaroni, *Microporous Mesoporous Mater.*, 2003, **62**, 29–45.

167 R. Sanz, G. Calleja, A. Arencibia and E. S. Sanz-Perez, *Appl. Surf. Sci.*, 2010, **256**, 5323–5328.

168 E. Vilarrasa-Garcia, E. M. O. Moya, J. A. Cecilia, C. L. Cavalcante, J. Jimenez-Jimenez, D. C. S. Azevedo and E. Rodriguez-Castellon, *Microporous Mesoporous Mater.*, 2015, **209**, 172–183.

169 Y. Lin, H. Lin, H. Wang, Y. Suo, B. Li, C. Kong and L. Chen, *J. Mater. Chem. A*, 2014, **2**, 14658–14665.

170 Y. Lin, Q. Yan, C. Kong and L. Chen, *Sci. Rep.*, 2013, **3**, 1859.

171 T. Witoon, *Mater. Chem. Phys.*, 2012, **137**, 235–245.

172 W.-J. Son, J.-S. Choi and W.-S. Ahn, *Microporous Mesoporous Mater.*, 2008, **113**, 31–40.

173 X. Wang and C. Song, *Catal. Today*, 2012, **194**, 44–52.

174 A. Goeppert, S. Meth, G. K. S. Prakash and G. Olah, *Energy Environ. Sci.*, 2010, **3**, 1949–1960.

175 J. Wang, D. Long, H. Zhou, Q. Chen, X. Liu and L. Ling, *Energy Environ. Sci.*, 2012, **5**, 5742–5749.

176 X. Yan, L. Zhang, Y. Zhang, K. Qiao, Z. Yan and S. Komarneni, *Chem. Eng. J.*, 2011, **168**, 918–924.

177 W. Yan, J. Tang, Z. Bian, J. Hu and H. Liu, *Ind. Eng. Chem. Res.*, 2012, **51**, 3653–3662.

178 T. Witoon and M. Chareonpanich, *Mater. Lett.*, 2012, **81**, 181–184.

179 A. Heydari-Gorji, Y. Belmabkhout and A. Sayari, *Langmuir*, 2011, **27**, 12411–12416.

180 A. Heydari-Gorji, Y. Yang and A. Sayari, *Energy and Fuels*, 2011, **25**, 4206–4210.

181 Y. Zeng, R. Zou and Y. Zhao, *Adv. Mater.*, 2016, 28, 2855–2873.

182 W. M. Verdegaal, K. Wang, J. P. Sculley, M. Wriedt and H. C. Zhou, *ChemSusChem*, 2016, **5810**, 636–643.

183 J. A. Mason, T. M. McDonald, T. H. Bae, J. E. Bachman, K. Sumida, J. J. Dutton, S. S. Kaye and J. R. Long, *J. Am. Chem. Soc.*, 2015, **137**, 4787–4803.

184 C. Kim, H. S. Cho, S. Chang, S. J. Cho and M. Choi, *Energy Environ. Sci.*, 2016, **9**, 1803–1811.

185 T. M. McDonald, J. A. Mason, X. Kong, E. D. Bloch, D. Gygi, A. Dani, V. Crocellà, F. Giordanino, S. O. Odoh, W. S. Drisdell, B. Vlaisavljevich, A. L. Dzubak, R. Poloni, S. K. Schnell, N. Planas, K. Lee, T. Pascal, L. F. Wan, D. Prendergast, J. B. Neaton, B. Smit, J. B. Kortright, L. Gagliardi, S. Bordiga, J. A. Reimer and J. R. Long, *Nature*, 2015, **519**, 303–308.

186 W. R. Lee, H. Jo, L.-M. Yang, H. Lee, D. W. Ryu, K. S. Lim, J. H. Song, D. Y. Min, S. S. Han, J. G. Seo, Y. K. Park, D. Moon and C. S. Hong, *Chem. Sci.*, 2015, **6**, 3697–3705.

187 J. S. Yeon, W. R. Lee, N. W. Kim, H. Jo, H. Lee, J. H. Song, K. S. Lim, D. W. Kang, J. G. Seo, D. Moon, B. Wiers and C. S. Hong, *J. Mater. Chem. A*, 2015, **3**, 19177–19185.

188 T. M. McDonald, W. R. Lee, J. A. Mason, B. M. Wiers, C. S. Hong and J. R. Long, *J. Am. Chem. Soc.*, 2012, **134**, 7056–7065.

189 P.-Q. Liao, H. Chen, D.-D. Zhou, S.-Y. Liu, C.-T. He, Z. Rui, H. Ji, J.-P. Zhang and X.-M. Chen, *Energy Environ. Sci.*, 2015, **8**, 1011–1016.

190 G. Qi, L. Fu and E. P. Giannelis, *Nat. Commun.*, 2014, **5**, 5796.

191 W. Xie, X. Ji, T. Fan, X. Feng and X. Lu, *Energy & Fuels*, 2016, **30**, 5083–5091.

192 Y. Wang, X. Bai, F. Wang, H. Qin, C. Yin, S. Kang, X. Li, Y. Zuo and L. Cui, *Sci. Rep.*, 2016, **6**, 26673.

193 B. Singh and V. Polshettiwar, *J. Mater. Chem. A*, 2016, **4**, 7005–7019.

194 F.-Q. Liu, W. Li, J. Zhao, W.-H. Li, D.-M. Chen, L.-S. Sun, L. Wang and R.-X. Li, *J. Mater. Chem. A*, 2015, **3**, 12252–12258.

195 J. Wang, H. Huang, M. Wang, L. Yao, W. Qiao, D. Long and L. Ling, *Ind. Eng. Chem. Res.*, 2015, **54**, 5319–5327.

196 S. Yang, L. Zhan, X. Xu, Y. Wang, L. Ling and X. Feng, *Adv. Mater.*, 2013, **25**, 2130–2134.

197 H. Jung, D. H. Jo, C. H. Lee, W. Chung, D. Shin and S. H. Kim, *Energy and Fuels*, 2014, **28**, 3994–4001.

198 A. Goeppert, H. Zhang, M. Czaun, R. B. May, G. K. S. Prakash, G. A. Olah and S. R. Narayanan, *ChemSusChem*, 2014, **7**, 1386–1397.

199 A. Goeppert, M. Czaun, R. B. May, G. K. S. Prakash, G. A. Olah and S. R. Narayanan, *J. Am. Chem. Soc.*, 2011, **133**, 20164–20167.

200 D. Wang, X. Ma, C. Sentorun-Shalaby and C. Song, *Ind. Eng. Chem. Res.*, 2012, **51**, 3048–3057.

201 C. C. Hwang, Z. Jin, W. Lu, Z. Sun, L. B. Alemany, J. R. Lomeda and J. M. Tour, *ACS Appl. Mater. Interfaces*, 2011, **3**, 4782–4786.

202 L. Wei, Z. Gao, Y. Jing and Y. Wang, *Ind. Eng. Chem. Res.*, 2013, **52**, 14965–14974.

203 J. Wang, H. Chen, H. Zhou, X. Liu, W. Qiao, D. Long and L. Ling, *J. Environ. Sci.*, 2013, **25**, 124–132.

204 L. Wei, Y. Jing, Z. Gao and Y. Wang, *Chinese J. Chem. Eng.*, 2015, **23**, 366–371.

205 E. P. Dillon, E. Andreoli, L. Cullum and A. R. Barron, *J. Exp. Nanosci.*, 2015, **10**, 746–768.

206 W. Lu, M. Bosch, D. Yuan and H. C. Zhou, *ChemSusChem*, 2015, **8**, 433–438.

207 M. A. Sakwa-Novak, C.-J. Yoo, S. Tan, F. Rashidi and C. W. Jones, *ChemSusChem*, 2016, **9**, 1859–1868.

208 M. A. Sakwa-Novak and C. W. Jones, *ACS Appl. Mater. Interfaces*, 2014, **6**, 9245–9255.

209 T. Tsoufis, F. Katsaros, Z. Sideratou, G. Romanos, O. Ivashenko, P. Rudolf, B. J. Kooi, S. Papageorgiou and M. A. Karakassides, *Chem. Commun.*, 2014, **64**, 10967–10970.

210 S. Gadipelli, H. A. Patel and Z. Guo, *Adv. Mater.*, 2015, **27**, 4903–4909.

211 W. Choi, K. Min, C. Kim, Y. S. Ko, J. W. Jeon, H. Seo, Y.-K. Park and M. Choi, *Nat. Commun.*, 2016, **7**, 12640.

212 R. Sanz, G. Calleja, A. Arencibia and E. S. Sanz-Perez, *J. Mater. Chem. A*, 2013, **1**, 1956–1962.

213 F. Song, Y. Zhao, H. Ding, Y. Cao, J. Ding, Y. Bu and Q. Zhong, *Environ. Technol.*, 2012, **34**, 1405–1410.

214 Y. Han, G. Hwang, H. Kim, B. Z. Haznedaroglu and B. Lee, *Chem. Eng. J.*, 2015, **259**, 653–662.

215 X. Wang, Q. Guo and T. Kong, *Chem. Eng. J.*, 2015, **273**, 472–480.

216 X. Wang, Q. Guo, J. Zhao and L. Chen, *Int. J. Greenh. Gas Control*, 2015, **37**, 90–98.

217 R. Sanz, G. Calleja, A. Arencibia and E. S. Sanz-P??rez, *Microporous Mesoporous Mater.*, 2015, **209**, 165–171.

218 Z. Liu, Y. Teng, K. Zhang and H. Chen, *J. Energy Chem.*, 2015, **24**, 322–330.

219 J. A. A. Gibson, A. V Gromov, S. Brandani and E. E. B. Campbell, *Microporous Mesoporous Mater.*, 2015, **208,** 129–139.

220 D. Aruldoss, R. Saigoanker, J. Das Savarimuthu and J. Jagannathan, *Ceram. Int.*, 2014, **40**, 7583–7587.

221 D. Lee, C. Zhang and H. Gao, *Macromol. Chem. Phys.*, 2015, **216**, 489–494.

222 F. Yang, A. Y. Liu, A. L. Chen and A. C. Au, *Aust. J. Chem.*, 2015, **68**, 1427–1433.

223 L. Ma, R. Bai, G. Hu, R. Chen, X. Hu, W. Dai, H. F. M. Dacosta and M. Fan, *Energy & Fuels*, 2013, **27**, 5433–5439.

224 J. Wei, L. Liao, Y. Xiao, P. Zhang and Y. Shi, *J. Environ. Sci.*, 2010, **22**, 1558–1563.

225 W. Lu, J. P. Sculley, D. Yuan, R. Krishna, Z. Wei and H. C. Zhou, *Angew. Chemie - Int. Ed.*, 2012, **51**, 7480–7484.